

Direct lineage programming - a tool to generate and analyze human cortical layer specific neurons

Dissertation

zur Erlangung des Doktorgrades (Dr. rer. nat.)
der
Mathematisch-Naturwissenschaftlichen
Fakultät
der
Rheinischen Friedrich-Wilhelms-Universität Bonn

Vorgelegt von

Kevin Weynans

Aus Viersen-Dülken

Bonn, Oktober 2019

Anfertigung mit Genehmigung der Mathematisch-Naturwissenschaftlichen Fakultät
der Rheinischen Friedrich-Wilhelms-Universität Bonn

1. Gutachter: Prof. Dr. Philipp Koch

2. Gutachter: Prof. Dr. Hubert Schorle

Tag der Promotion: 16.03.2020

Erscheinungsjahr: 2020

“Man kann so klug sein wie die Klugen dieser Welt und geht doch jederzeit in die nächste Minute wie ein Kind ins Dunkle.”

*Otto von Bismarck (1815-1898)
preußisch-deutscher Staatsmann, 1. deutscher Reichskanzler*

Table of contents

1. INTRODUCTION	1
1.1 THE HUMAN CORTEX AND ITS NEURONAL DIVERSITY	1
1.1.1 The role of transcription factors in directing the generation of projection neurons in the cerebral cortex	3
1.1.2 The role of microRNAs in regulating cortical development	5
1.1.3 Human cortical malformations – perturbed cortical layer formation	8
1.2 HOW TO MAKE A HUMAN NEURON IN VITRO	10
1.2.1 Guided differentiation of pluripotent stem cells (PSC) into telencephalic progenitors and neurons	10
1.2.2 TF based cell programming of PSC	12
1.2.3 Direct conversion of fibroblasts into functional neurons	13
1.2.4 Enhancing direct conversion efficiencies	15
1.2.5 Direct conversion of fibroblasts into defined neuronal subtypes	16
1.2.6 Direct conversion – a tool for disease modeling	17
1.3 AIM OF THIS STUDY	19
2. MATERIALS	20
2.1 TECHNICAL EQUIPMENT	20
2.2 CELL CULTURE AND MOLECULAR BIOLOGY CONSUMABLES	22
2.3 CHEMICALS	23
2.4 CELL CULTURE	25
2.4.1 Cell culture media	25
2.4.2 Cell culture solutions	28
2.4.3 Cell culture additives	29
2.4.4 Cell lines	29
2.5 MOLECULAR BIOLOGY	30
2.5.1 Reagents	30
2.5.2 Enzymes	31
2.5.3 Plasmids	32
2.5.4 Restriction endonucleases	32
2.5.5 Bacterial solutions	32
2.5.6 Kits	33
2.5.7 Primer	33
2.5.8 Oligonucleotides	35
2.5.9 Antibodies	36
2.6 SOFTWARE	36

3. METHODS	38
3.1 CULTIVATION OF HUMAN FIBROBLASTS	38
3.2 CULTIVATION OF HUMAN INDUCED PLURIPOTENT STEM CELLS (hiPSCs).....	38
3.3 DESIGN OF LENTIVIRAL VECTORS	38
3.4 PRODUCTION AND CONCENTRATION OF LENTIVIRAL PARTICLES	39
3.5 LENTIVIRAL TRANSDUCTION OF HUMAN FIBROBLASTS	40
3.6 LENTIVIRAL TRANSGENESIS OF hiPSCs	40
3.7 TRANSCRIPTION FACTOR BASED DIRECT CONVERSION OF HUMAN FIBROBLASTS INTO INDUCED NEURONS (iN).....	40
3.8 DIRECTED DIFFERENTIATION OF hiPSC.....	41
3.9 RNA EXTRACTION	41
3.10 RNA PURIFICATION	42
3.11 cDNA SYNTHESIS	42
3.12 QUANTITATIVE RT-PCR	43
3.13 IMMUNOCYTOCHEMICAL ANALYSIS	43
3.14 BRANCHING ASSAY	44
3.15 MOTILITY ASSAY	44
3.16 STATISTICAL ANALYSIS	44
4. RESULTS	46
4.1 IN VITRO GENERATION OF CORTICAL LAYER SPECIFIC HUMAN NEURONS.....	46
4.1.1 Directed differentiation of human pluripotent stem cells to into cortical progenitors and neurons	46
4.1.2 Transcription factor-based induction of PSC into corticofugal neurons.....	47
4.1.2.1 Generation of transgene inducible PSC lines.....	48
4.1.2.2 Differentiation of PSCs into corticofugal neurons.....	49
4.1.3 Transcription factor based direct conversion of human fibroblasts into corticofugal neurons	52
4.1.3.1 Generation and validation of human fibroblasts carrying tet-on controllable Ascl1, Ngn2 and Fezf2 constructs.....	52
4.1.3.2 Direct conversion of human FAN-fibroblasts into corticofugal neurons.....	53
4.2 CiNs TO MODEL MALFORMATIONS OF CORTICAL DEVELOPMENT (CDM).....	56
4.2.1 Generation of CiNs derived from Miller-Dieker-Syndrome patient fibroblasts.....	56
4.2.2 Phenotypic characterization of MDS patient-derived CiNs.....	58
4.2.2.1 Characterization of lissencephaly patient-derived CiNs migration behavior	58
4.2.2.2 Morphological phenotyping of MDS-derived CiNs.....	59
4.2.3 Mechanistic principles underlying the phenotypic changes in MDS-derived CiNs	61

4.2.3.1 Generation of CiNs with a gain- and loss-of-function of microRNA-22 and microRNA-132.....	63
4.2.3.2 microRNA-22 and microRNA-132 impact CiN migration.....	65
4.2.3.3 MicroRNA-22 and microRNA-132 impact CiN morphology.....	67
4.2.4 microRNA-22 impacts CiN morphology via the PTEN / PDK1 signaling pathway	69
4.2.5 microRNA-132 impacts CiN morphology via p250GAP / Rac1-signaling.....	72
5. DISCUSSION.....	74
5.1 FEZF2 INDUCES DEEP CORTICAL LAYER IDENTITY	74
5.1.1 Differentiation of hiPSCs into human cortical layer specific neurons	74
5.1.2 Direct conversion of human fibroblasts into human cortical layer specific neurons	76
5.1.3 Direct conversion of somatic cells versus differentiation of PSCs.....	77
5.2 TRANSCRIPTION FACTOR BASED DIRECT CONVERSION AS A POWERFUL TOOL TO STUDY CORTICAL DEVELOPMENT MALFORMATIONS	79
5.3 IMPAIRED NEURONAL MORPHOLOGY AND BEHAVIOR IN MDS	80
5.4 MICRORNAs: IMPORTANT REGULATORS BESIDES LIS1 AND YWHAE	82
5.5 IMPAIRED AXONAL OUTGROWTH IN MDS PATIENTS	84
5.6 PERTURBED ACTIN FIBER FORMATION IN MDS.....	86
5.8 CONCLUSIONS	88
6. ABBREVIATIONS	89
7. ABSTRACT	94
8. ZUSAMMENFASSUNG.....	95
9. REFERENCES.....	97
10. DANKSAGUNG	115
11. ERKLÄRUNG	116

1. Introduction

1.1 The human cortex and its neuronal diversity

The human cerebral cortex represents roughly three quarters of the human brain and functions as an organizing center of afferent and efferent signals (Mountcastle 1998). It is a distinct six-layered structure subserving critical functions. Those six layers are populated by cortical neurons. During embryogenesis cortical neurons are generated within the ventricular zone (VZ; Molyneaux *et al.*, 2007) (Figure 1). At an early stage of development, this zone consists of a single layer of rapidly dividing cells, which is the germinal neuroepithelium. The massive proliferation drastically enlarges the neuroepithelium. During the course of neurogenesis, a second proliferative layer develops upstream of the VZ. This layer is termed as subventricular zone (SVZ; Bayer and Altman 1991). The VZ and SVZ comprise neural progenitors including radial glia cells (RGC), intermediate progenitors (IP) and outer RGCs, which will give rise to glutamatergic projection neurons of the six neocortical layers (Molyneaux *et al.*, 2007). Those glutamatergic projection neurons migrate radially toward the pial surface to end up in the cortical plate (CP; Kassai *et al.*, 2008). In human, the development of the cortical plate is initiated during the seventh week of gestation, when a layer of pioneering neurons initiates the so-called preplate (Marin-Padilla 1978; Marin-Padilla 1992). Between the seventh and the eighth week of gestation the preplate splits into the subplate and the marginal zone (Derer and Nakanishi, 1983; Goffinet and Lyon, 1979; Goffinet 1979; Nichols and Olson, 2010; Sheppard and Pearlman, 1997). In between the marginal zone and the subplate, the cortical plate, which is the destination of the migrating neurons, will develop (Figure 1). The marginal zone, which will be on top of the future cortical plate, contains Cajal-Retzius cells. Those cells secrete the chemotropic factor Reelin, which is necessary for the correct positioning of migrating neurons within the CP (D’Arcangelo *et al.*, 1995; Hoerder-Suabedissen and Molnar, 2013; Osheroﬀ and Hatten, 2009).

After exiting the cell cycle, the immature neurons, which are born in the VZ, migrate with a multipolar morphology through an intermediate zone between the SVZ and the subplate (Noctor *et al.*, 2004; Tabata and Nakajima, 2003). When they reach the subplate, they change their morphology from multipolar to bipolar and they attach to the fibers of the radial glia (Jossin and Cooper, 2011). Radial glia cells assist the radial migration of projection neurons. They span through the neuroepithelium while

keeping attached to the pial surface and the luminal side of the neural tube (Bystron *et al.*, 2006; Howard *et al.*, 2008; Lui *et al.*, 2011; Taverna *et al.*, 2014) (Figure 1). Thus they serve as guiding tracks for immature neurons, which migrate along the RGCs to the pial side, where they settle as postmitotic neurons and build the cortical plate (Olson 2014; Rakic 1988; Rakic 2007). The cortical plate is formed in an inside out pattern, which means that early born neurons establish the deep layers of the future structure and later born neurons pass the early born neurons to form the upper layers (Angevine and Sidman, 1961; Mountcastle 1998; Rakic 1974). It is believed that early born neurons originate from apical radial glia cells in the ventricular zone, whereas the neurons of the upper layers derive from secondary progenitors in the subventricular zone (Lui *et al.*, 2011). At this neural migration stage, integration of many different molecules including reelin (RELN), are required for the formation of a complete neocortex. Reelin plays an important role in the formation of the cortical plate. It is an extracellular matrix protein, which is synthesized and secreted by the Cajal-Retzius cells of the marginal zone (Curran and D'Arcangelo, 1998; Jossin *et al.*, 2003).

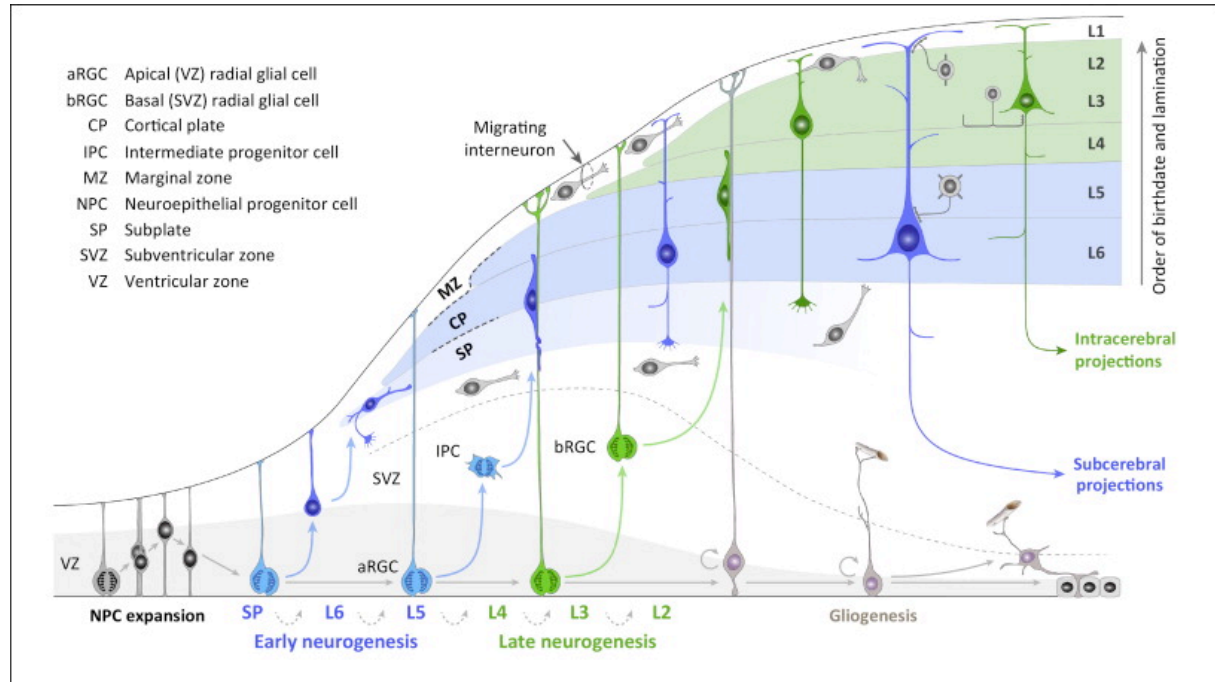


Figure 1 Development of the cerebral cortex. After an initial expansion phase, neuroepithelial progenitor cells differentiate and migrate along radial glial cells towards the cortical plate. During early neurogenesis, deep layers of the cortical plate (blue) are generated. During the course of neurogenesis, the later born neurons migrate through the early born neurons to compose the upper layers of the cortical plate (green). In upper layers intracerebral projection neurons are located, which project within the brain. The deep layers consist of subcerebral neurons, which can project up to the spinal cord. Adopted from Shibata *et al.*, 2015.

At the end of cortical development, mammalian brains commonly show a six-layer neocortex, whereupon each layer possesses a specific function by producing complex synaptic connections. The different functionalities of layers are accomplished by different neuronal subtypes. There are three classes of cortical projection neurons within the human neocortex, defined as associative, commissural and corticofugal projection neurons. The upper layers of the cortical plate (layers II/III) consist predominantly of callosal projection neurons, which belong to the group of commissural neurons. Their name derives from the way of their axonal projections, because they extend their axons across the corpus callosum. These neurons never project axons outside the telencephalon. Underneath these layers, mostly corticofugal projection neurons form the deep layers of the cortex (layers V/VI). This group of neurons is further subdivided into corticothalamic neurons and subcerebral projection neurons. The corticothalamic neurons are primarily located within layer VI and are known to project subcortically to the thalamus. The superficial layer V consists mostly of subcerebral projection neurons, which are pyramidal neurons of the largest size. They possess long-range projections to the brainstem and the spinal cord (Molyneaux *et al.*, 2007).

Within the cerebral cortex another type of neuron exists, namely inhibitory interneurons, which are generated in the ventral telencephalon and have to migrate tangentially into the cortex to integrate into local networks (Hansen *et al.*, 2013; Ma *et al.*, 2013). These interneurons play an essential role in modulating brain activity by making synaptic connections with excitatory neurons or other interneurons (Gelman and Marin 2010).

1.1.1 The role of transcription factors in directing the generation of projection neurons in the cerebral cortex

During the cortical development, transcription factors (TF) are important for the specification of these different types of projection neurons within the human cortex. TF are key regulators of gene transcription, which are composed of at least one DNA-binding domain. Alone or together with other co-factors they promote or block the recruitment of the RNA-polymerase to the DNA strand. By that, TF can induce or repress the transcription of specific genes.

The generation and specification of the different neuronal subtypes requires the expression of various key transcription factors.

For the production of corticothalamic neurons the T-box transcription factor Tbr1 acts as a key TF (Han *et al.*, 2011; Hevner *et al.*, 2001; McKenna *et al.*, 2011) (Figure 2). It promotes the corticothalamic identity through a repression of the expression of the TF Fezf2 by binding a conserved consensus site (Han *et al.*, 2011). Fezf2 is a zinc finger TF, which promotes the specification of corticofugal neurons (Chen *et al.*, 2008; Molyneaux *et al.*, 2005; Shim *et al.*, 2012). Through the decrease of Fezf2 expression via Tbr1, this facilitation is decreased and the developing neurons adopt a corticothalamic identity.

For the specification of corticofugal neurons there are two more important TF besides Fezf2. Those TF are Ctip2 and Satb2 (Figure 2). Ctip2 is a COUP TF1-interacting protein, which is essential for the axonal outgrowth of corticofugal neurons (Arlotta *et al.*, 2005). The chromatin remodeling protein Satb2 acts usually as a major regulator of callosal neurons but is also involved in the specification of corticofugal neurons. It was shown that Satb2 promotes the identities of corticofugal and callosal neurons in a cell context-dependent manner (Leone *et al.*, 2015; McKenna *et al.*, 2015). Satb2 induces the expression of corticofugal genes, which are essential for the fate specification (e.g. Fezf2) and represses also other corticofugal genes, which are necessary for the axonal development of corticofugal neurons (e.g. Ctip2) (McKenna *et al.*, 2015). The resulting high levels of Fezf2 in turn repress the Satb2 expression leading to a decreased expression. The reduced Satb2 expression ensures high expression levels of corticofugal genes like Ctip2, which further promote the corticofugal identity (McKenna *et al.*, 2015).

During the specification of callosal neurons, Satb2 does not activate Fezf2 and remains highly expressed (McKenna *et al.*, 2015). The high levels of Satb2 promote the expression of upper layer genes, which are important for the development of callosal neurons (McKenna *et al.*, 2015). The repression of corticofugal genes is still present. It represses for example Ctip2 by binding to regulatory regions (MAR sequences) in the Ctip2 locus (Alcamo *et al.*, 2008). Recently it was described that the protooncogene Ski is coexpressed with Satb2 in superficial layers (Leone *et al.*, 2015). It is not involved in the interaction between Satb2 and the MAR sequences, but it is required for the recruitment of HDAC1, which leads to an assembly of the NuRD complex resulting in the repression of Ctip2 (Leone *et al.*, 2015). In order to

al., 2009). This regulation is usually in a negative manner by binding to the 3'UTR of a messenger RNA (mRNA) (Carthew and Sontheimer, 2009; Kim *et al.*, 2009).

As part of the non-coding RNAs, they were first neglected, but in the last couple of years it was shown that those miRNAs could act as key players in different biological processes such as developmental processes or in signaling pathways (Ambros 2004; Bartel 2004). In particular it was revealed that they are involved in the regulation of processes in the central nervous system (CNS) like neurite outgrowth and neuronal function (Mc Neill and Van Vactor, 2012). A few miRNAs were found, which can also activate the translation of target genes (Schwartz *et al.*, 2008; Vasudevan *et al.*, 2007).

The biogenesis of miRNAs consists of different steps. Primarily, miRNAs are transcribed by the RNA polymerase II (Cai *et al.*, 2004; Lee *et al.*, 2004). However, meanwhile various miRNAs were reported to be transcribed by RNA polymerase III (Borchert *et al.*, 2006; Ozsolak *et al.*, 2008). The transcription results in an immature nuclear precursor, which is referred as pri-miRNA. The pri-miRNA contains a stem loop after transcription and it is further processed by the type III-like ribonuclease Drosha (Krol *et al.*, 2010; Miyoshi *et al.*, 2010). Afterwards, the pri-miRNA is cleaved and persists as a 60-100 nucleotides long hairpin-containing intermediate precursor. This precursor is called pre-miRNA (Krol *et al.*, 2010; Miyoshi *et al.*, 2010). Via Exportin5, the pre-miRNA is exported out of the nucleus into the cytoplasm and there processed again by the RNase III-like ribonuclease protein dicer. The dicer cleaves the pre-miRNA into an 18-22 nucleotides long duplex, which is the mature miRNA (Krol *et al.*, 2010; Miyoshi *et al.*, 2010). Afterwards, one strand of the duplex is loaded into the RNA-induced silencing complex (RISC complex). The RISC complex comprises RNA binding proteins of the Argonaute family, which are important for the future binding to a mRNA (Meister 2013). For the binding, there is a complementarity between 2-8 nucleotides of the miRNA and a region within the 3'UTR of the mRNA (Brennecke *et al.*, 2005). miRNAs are regulating the expression of genes usually via an induction of a post-transcriptional silencing through an inhibition of the target translation as well as through a destabilization of the mRNA (Schwartz *et al.*, 2008; Vasudevan *et al.*, 2007) (Figure 3).

As regulators of gene expression, microRNAs play an important role in a variety of cellular processes. Amongst others they have a central role in many processes during the cortical development like cell type specification, migration, differentiation,

apoptosis, maturation and synaptogenesis (Davis *et al.*, 2008; De Pietri Tonelli *et al.*, 2008; Kawase-Koga *et al.*, 2009; Nowakowski *et al.*, 2013).

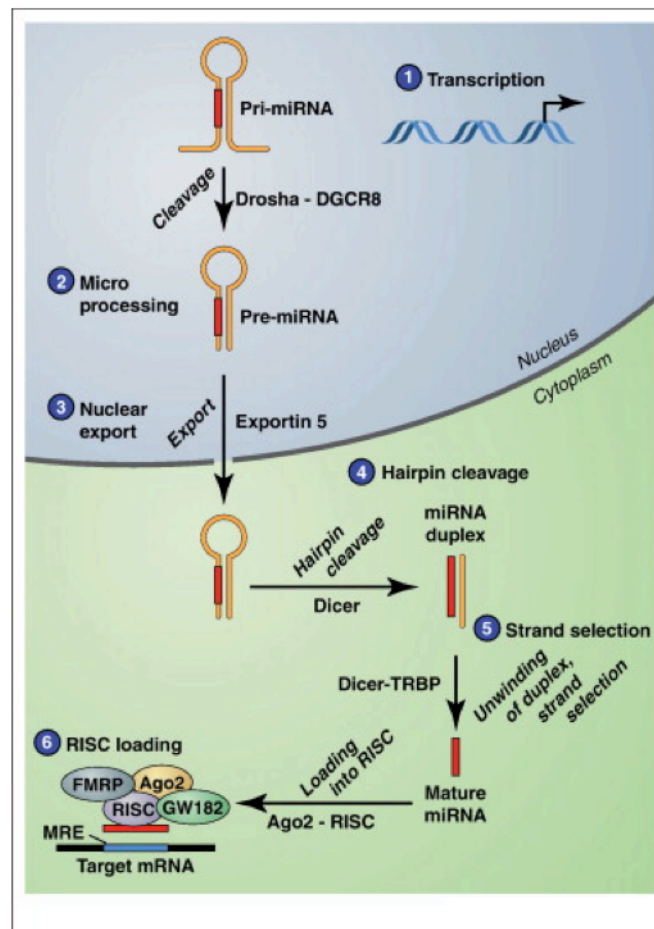


Figure 3 Biogenesis of microRNAs (miRs). After transcription, the miR consists of a hairpin structure (1). It is processed via a cleavage with Drosha (2) and subsequently exported from the nucleus into the cytoplasm (3). In the cytoplasm, the miR is further processed by a hairpin cleavage (4). Afterwards the Dicer unwinds the miR duplex structure and one strand of the duplex is loaded into the RISC-complex. The RISC-miR combination then binds at the specific target messenger RNA (mRNA) and inhibits their expression. (Adopted from Im and Kenny 2012).

Small alterations of their expression were associated with numerous of brain disorders (Abelson *et al.*, 2005; Kim *et al.*, 2007; Stark *et al.*, 2008; Wang *et al.*, 2009). In this regard, one well-studied microRNA is microRNA-124, which is highly specific to postmitotic neurons and has been reported to promote neurogenesis by targeting polypyrimidine tract-binding protein 1 (PTBP1) (Makeyev *et al.*, 2007). Another microRNA, which is broadly expressed within the developing cortex, is microRNA-9. microRNA-9 is known to target the TF Foxg1 and Gsx2, which results in a regulation of developmental patterning and neuronal migration (Clovis *et al.*, 2012; Shibata *et al.*, 2011).

In this context, two additional microRNAs, namely microRNA-22 and microRNA-132, were described to be involved in cortical development. microRNA-22 is a widely expressed microRNA, which was shown to be involved in many different cellular processes in mammalian systems (Landgraf *et al.*, 2007). In regard to cortical development, Volvert and colleagues described the role of microRNA-22 in neuronal polarization and migration during the development of the cortex through targeting CoREST and thereby influencing the intracellular Doublecortin (Dcx) level (Volvert *et al.*, 2014). Furthermore, several studies pointed out that microRNA-22 has an anti-apoptotic effect and thus linked to different kinds of cancer or Huntington Disease (Berenguer *et al.*, 2013; Jovicic *et al.*, 2013).

microRNA-132 is like many other microRNAs connected to a variety of cellular processes including apoptosis or signaling pathways like the Notch signaling pathway (Salta *et al.*, 2014; Wong *et al.*, 2013). With respect to cortical development it is involved in the neuronal development itself, by regulating axonal outgrowth and the neuritogenesis (Hancock *et al.*, 2014; Remenyi *et al.*, 2013; Vo *et al.*, 2005). Altered expression of microRNA-132 was reported to have a massive implication of dendritic complexity and spine density (Edbauer *et al.*, 2010; Magill *et al.*, 2010).

1.1.3 Human cortical malformations – perturbed cortical layer formation

Human cortical malformations associated with defects in neuronal migration result in severe developmental consequences including epilepsy and intellectual disability.

Prominent disorders due to an abnormal neuronal migration and a subsequent disrupted cortical layer formation are periventricular heterotopia, subcortical band heterotopia and lissencephaly (Pang *et al.*, 2008). Periventricular heterotopia is caused by an arrest of neuronal migration along the radial glial fibers, which results in linearly distributed, heterotopic neurons. The subcortical band heterotopia is characterized by an additional band of subcortical neurons between the ventricles and the cerebral cortex (Gleeson *et al.*, 1999). The brain of lissencephalic patients exhibits abnormal gyri (pachygyria) or no gyri (agyria; Barkovich *et al.*, 2012; Francis *et al.*, 2006) (Figure 4). Although several of the genes responsible for human congenital disorders have been identified, the pathophysiological mechanisms causing such malformations are not entirely understood. In regard to lissencephaly it is the widespread notion that heterozygous deletion or mutations of *LIS1* causes

lissencephaly in humans (Kato and Dobyns, 2003). LIS1 is a member of an intracellular multiprotein complex together with NDEL1 and 14.3.3 ϵ . It functions as a regulator of cytoplasmatic dynein, microtubule dynamics and centrosomal protein localization (Reiner and Sapir, 2013; Wynshaw-Boris, 2007). The disruption of this multiprotein complex has influences in neuronal migration and proliferation of radial glia cells (Bi *et al.*, 2009; Tsai *et al.*, 2005; Yingling *et al.*, 2008).

The Miller Dieker Syndrome (MDS) is a severe form of lissencephaly leading to enlarged ventricles and an abnormally thick cerebral cortex with a disorganized cortical plate (Dobyns *et al.*, 1983; Francis *et al.*, 2006). Furthermore, the cortex is simplified without any (agyria) or abnormal cortical convolutions (pachygyria; Barkovich *et al.*, 2012; Francis *et al.*, 2006). Although the cortical plate is enlarged, it consists of only four layers instead of six (Ferrer and Fernandez-Alvarez, 1977). Moreover, the existing four layers of the cerebral cortex are disorganized. The molecular layer I is closely located to the pial surface. The underlying layer II consists of pyramidal neurons in the upper part and granular cells in the lower part. Layer III persists of either multipolar neurons or neurons harboring a round cell soma instead of a pyramidal. Beneath this layer pleiomorphic neuronal cells and misoriented pyramidal neurons were found to build the fourth layer (Romero *et al.*, 2018). MDS is linked with a haploinsufficiency on chromosome 17p13.3, harbouring a lot of different genes including *PAFAH1B1 (LIS1)* and *YWHAE*, which are encoding for Lis1 and 14.3.3 ϵ respectively (Cardoso *et al.*, 2003; Chong *et al.*, 1997; Dobyns *et al.*, 1983; Hattori *et al.*, 1994; Reiner *et al.*, 1993; Schwartz *et al.*, 1988). Lis1 and 14.3.3 ϵ form together with NDEL1 an intracellular multicomplex, which is important for the regulation of microtubule dynamics and the cytoplasmic dynein (Wynshaw-Boris 2007). Recently it was shown that the causes for a disruption in the cortical niche are alterations within the microtubules network of radial glia cells (Iefremova *et al.*, 2017). Moreover, cell divisional changes were also identified in outer radial glia cells (Bershteyn *et al.*, 2017). Besides the lissencephalic brain, MDS is associated with craniofacial dysmorphisms, mental and motor impairment as well as epilepsy (Dobyns *et al.*, 1983; Nagamani *et al.*, 2009; Yingling *et al.*, 2003). Furthermore, MDS patients have a reduced lifespan. If there are born at all, patients usually die during their first couple of years of life (Yingling *et al.*, 2003).

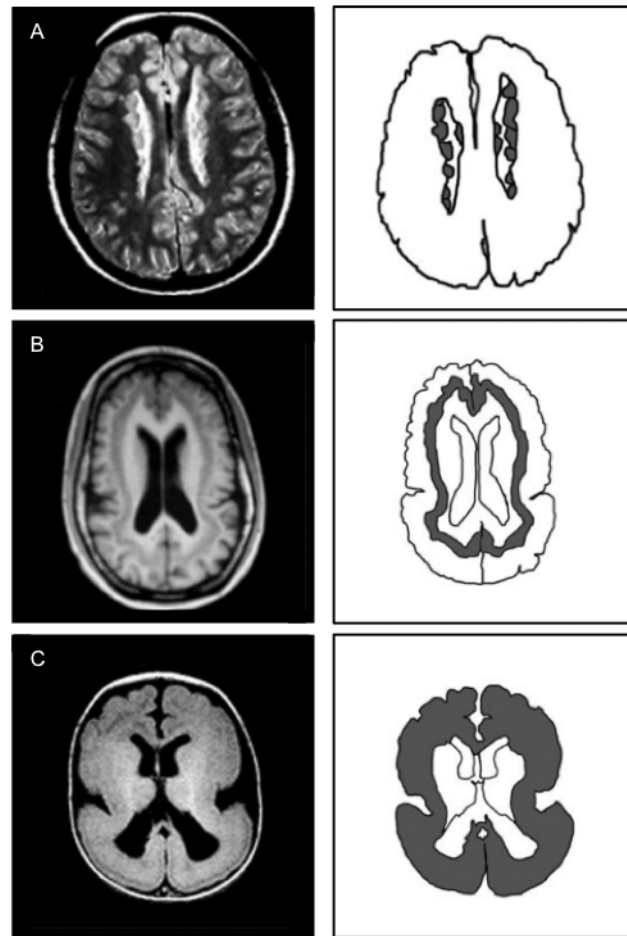


Figure 4 Cortical malformations in neurological diseases. Examples for different cortical malformations. A: MRI and scheme of a brain with periventricular heterotopia. A migration arrest results in an accumulation of heterotypic neurons. B: MRI and scheme of a brain with subcortical band heterotopia. Neurons build an additional band between the ventricles and the cerebral cortex. C: MRI and scheme of a brain with lissencephaly. The brain is malformed due to agyria and pachygyria. Modified from Pang *et al.*, 2008.

1.2 How to make a human neuron *in vitro*

1.2.1 Guided differentiation of pluripotent stem cells (PSC) into telencephalic progenitors and neurons

For a long time, the major limitation in experimental human brain research was the lack of available model systems. With the advent of induced pluripotent stem cells (iPS cells) and defined protocols for the guided differentiation of these cells into specific somatic cell fates, cells of the human brain has become freely available for biomedical research and disease modeling. In fact, iPS cell research has

revolutionized the study of human brain development and disease (Takahashi and Yamanaka, 2006). Major advances in our understanding of developmental programs and the improvement of *in vitro* protocols eventually cumulated in the generation of guided differentiation protocols. To guide the differentiation of PSCs for the generation of neural progenitor cells (NPCs) and functional neurons, developmental signals, which resemble those signals that instruct the respective cell identity during *in vivo* development, were used. *In vivo*, the determination of the neuronal fate is initiated with the positional identities of NPCs instructed by morphogens and mitogens (Fasano *et al.*, 2010; Kriks *et al.*, 2011; Pasca *et al.*, 2011). Different morphogens form gradients along the dorsal-ventral and anterior-posterior axis, which specify the identity of NPCs. For example sonic hedgehog (SHH) is secreted from ventral regions, whereas the dorsal regions secrete bone morphogenetic protein (BMP) and WNT proteins (Ciani and Salinas, 2005; Fuccillo *et al.*, 2006; Liu and Niswander, 2005). The positioning along the anterior-posterior axis is defined by signaling cues downstream of fibroblast growth factors (FGFs) and retinoic acid (RA) (Maden 2007; Mason 2007).

In an elegant study, Gaspard *et al.* cultured mouse PSCs in a default differentiation medium. As a result, the cells naturally adopted a telencephalic identity with the majority expressing ventral progenitor cell markers due to an induced SHH expression during neuronal conversion. In response to that, they showed that an application of a SHH antagonist, here cyclopamine, prevented the ventralization and led to the induction of excitatory cortical neurons, derived from the dorsal telencephalon (Gaspard *et al.*, 2008).

In a different study, an inhibition of the WNT pathway combined with an inhibition of SMAD signaling showed to promote a forebrain identity in human PSC-derived NPCs. Therefore the culture conditions were modified by implementing BMP and Activin/Nodal inhibitors, which prevents the transcriptional activity of SMAD in the end (Chambers *et al.*, 2009). A further differentiation to forebrain neurons was not reported. Based on this finding different studies demonstrated the generation of cortical neurons by inhibiting the SMAD signaling pathway (Li *et al.*, 2009; Pasca *et al.*, 2011). Shi *et al.* showed that the combination of retinoid signaling with an inhibition of SMAD signaling promoted the neural induction and led to a directed differentiation of human PSCs to cerebral cortex stem and progenitor cells. This differentiation was followed by an extended period of cortical neurogenesis

accompanied by a terminal differentiation to cortical neurons with equal amounts of deep layer neurons and upper layer neurons (Shi *et al.*, 2012). Excitatory cortical neurons could also be generated from human PSCs without the addition of morphogens. Only SMAD signaling was inhibited. In contrast to Shi *et al.*, the majority of the generated neurons had a deep layer identity (Espuny-Camacho *et al.*, 2013).

1.2.2 TF based cell programming of PSC

The guided differentiation by using developmental signals appeared to be successful but also time-consuming. The neural differentiation usually takes 4-6 weeks and the maturation to functional neurons could last months depending of the desired neuronal subtype (Tao and Zhang, 2016; Xie *et al.*, 2013). Furthermore, the guided differentiation was accompanied by variability with low purities of the desired neuronal subtype. In addition, different PSCs from different donors showed strong differences in their differentiation potential (Bock *et al.*, 2011; Hu *et al.*, 2010; Wu *et al.*, 2007). As explained in chapter 1.1.1, cell fates are determined by an interplay of transcription factors during embryonic development. In a first approach, TF based reprogramming was shown to induce PSCs from fibroblasts (Takahashi and Yamanaka, 2006). Similarly, TFs were identified, which led to the rapid and homogenous induction of specific cell types. For example, Ngn2 was shown to efficiently direct the differentiation of mouse and human PSC to a generation of pure excitatory neurons. Thereby it was possible to induce these neurons in less than two weeks (Thoma *et al.*, 2012; Zhang *et al.*, 2013). The generated neurons exhibited neuronal transcription profiles, had the ability to form synapses and could produce action potentials (Zhang *et al.*, 2013). Additionally, these neurons showed a functional integration and active electrophysiological properties after transplantation into a mouse brain (Zhang *et al.*, 2013). Besides Ngn2, Zhang *et al.* further described NeuroD1 as another transcription factor, which was able to direct the differentiation of human PSCs to an excitatory cortical identity in response to overexpression (Zhang *et al.*, 2013). Another transcription factor, which was reported to drive the neuronal differentiation of human PSCs, is Ascl1 (Chanda *et al.*, 2014; Pang *et al.*, 2011; Yamamizu *et al.*, 2013). The expression of Ascl1 alone was described to be sufficient for the neuronal differentiation. But in contrast to the differentiation with Ngn2 or

NeuroD1, the expression of *Ascl1* had to be combined with *Brn2* and *Myt1l* to increase neuronal maturation and complexity (Pang *et al.*, 2011).

The power of transcription factors is also underlined by the ability to generate more types of neurons by ectopically expressing different transcription factors. Andersson and colleagues were one of the first, who performed a successful generation of neurons by applying a subset of transcription factors. They used the homeodomain transcription factors *Lmx1a* and *Msx1*, which are expressed in midbrain dopamine progenitor cells. Overexpression of those two TF resulted in a directed differentiation of ESCs into functional dopaminergic neurons of the midbrain (Andersson *et al.*, 2006). In a similar manner it was possible to generate serotonergic neurons from ESCs. Therefore only the transcription factors were changed to *Ascl1*, *Gata2* and *FoxA2* (Nefzger *et al.*, 2011). All these results led to the conclusion that specific combinations of transcription factors are linked to the instruction of specific neuronal identities.

1.2.3 Direct conversion of fibroblasts into functional neurons

The accomplishments in PSC programming raised the question whether a differentiated somatic cell can be directly converted into a different cell type without bypassing a pluripotent state.

The idea of converting one differentiated cell into another differentiated cell was not new. First indications were already shown several years ago by forced expression of lineage-specific genes in somatic cells such as *MyoD*. *MyoD* encodes for a transcription factor, which is crucial for the specification of skeletal muscle cells. Expression of *MyoD* was shown to be sufficient for a successful conversion of fibroblasts into contracting muscle cells (Choi *et al.*, 1990; Davis *et al.*, 1987; Weintraub *et al.*, 1989). In addition, exogenous expression of interleukin (IL)-2 and granulocyte-macrophage colony-stimulating factor receptors resulted in a myeloid conversion of committed lymphoid progenitors (Kondo *et al.*, 2000). Furthermore, it was reported in other studies that *Cebpa* in B cells or *Pu.1* in combination with *Cebpa* in fibroblasts is sufficient to induce characteristics of macrophages (Feng *et al.*, 2008; Xie *et al.*, 2004). Also *in vivo* studies confirmed the possibility of direct reprogramming between divergent lineages. For example, the expression of neurogenin 3 in combination with *Pdx1* and *Mafa* led to the conversion of pancreatic

exocrine cells into functional β -cells *in vivo* (Zhou *et al.*, 2008).

Groundbreaking work was done by Vierbuchen and colleagues, who efficiently converted mouse fibroblasts into functional neurons, which they termed induced neurons (iN) (Vierbuchen *et al.*, 2010). In their work, they started with 19 TF, which were either specifically expressed in neural cell types or they had a role in reprogramming to pluripotency. After testing different combinations of TF they narrowed it down to the three TF *Ascl1*, *Brn2* and *Myt1l* (Vierbuchen *et al.*, 2010). Out of these transcription factors, *Ascl1* was found to be crucial for the conversion process. *Ascl1* is an evolutionary conserved transcription factor, which was first identified in *Drosophila melanogaster*, and is known for its proneural activity (Masserdotti *et al.*, 2016). In the course of mammalian development it directs stem cells within the brain to neuronal identities (Casarosa *et al.*, 1999). To increase the transdifferentiation efficiency and maturation of the iNs, as well as to promote the generation of more complex neural phenotypes, the transcription factors *Brn2* and *Myt1l* were used (Vierbuchen *et al.*, 2010). Both factors were previously known for their roles in normal neurogenesis. More recently, *Myt1l* has emerged as a repressor of non-neuronal fates in developing cells, thereby improving the efficiency of reprogramming and the functional maturity of the iN (Mall *et al.*, 2017). On the basis of that work it was reported that an addition of *NeuroD1*, another basic helix–loop–helix transcription factor, to three combined TF was sufficient to convert also human fibroblasts into functional neurons (Pang *et al.*, 2011). More recently, the role of *Ascl1* as a key factor for direct reprogramming was underlined by demonstrating that *Ascl1* expression alone is sufficient to convert human fibroblasts into glutamatergic neurons (Chanda *et al.*, 2014). However, the importance of *Brn2* and *Myt1l* for neuronal generation was once again pointed out by the finding that *Ascl1* alone is sufficient to induce the neuronal feature of non-CG methylation, but the expression of the other two TFs is required to create a methylation pattern, which is more alike to mature neurons (Luo *et al.*, 2019). Other studies combined *Ascl1* expression with the expression of *Ngn2* to convert fibroblasts into neurons (Liu *et al.*, 2013; Son *et al.*, 2011).

In contrast to these studies, it was recently demonstrated that neurons could be chemically induced without the application of transcription factors by using small molecules. Mouse and human fibroblasts were directly converted by using forskolin, ISX9, CHIR99021, SB431542 and I-BET15125 or with a mixture of valproic acid,

CHIR99021, Repsox, forskolin, SP600125, GO6983 and Y-27632 (Hu *et al.*, 2015; Li *et al.*, 2015).

Besides small molecules, also microRNAs became targets in regard to direct transdifferentiation. It was shown that an overexpression of microRNA-124 and microRNA-9 is sufficient to reprogram human fibroblasts into neurons via a regulation of the REST complex (Victor *et al.*, 2014; Xue *et al.*, 2013). In combination with this crosstalk, another regulatory pathway, which includes miRNA-9, nPTB and Brn2, was found in the course of human fibroblasts conversion (Xue *et al.*, 2016).

1.2.4 Enhancing direct conversion efficiencies

Although the reported transdifferentiations were successful in instructing a specific cell fate, the conversion efficiencies were rather low (Broccoli *et al.*, 2011). Different approaches were executed to increase the conversion efficiency by using small molecules and microRNAs.

In a first report Ladewig *et al.* demonstrated that the combination of a set of small molecules with the expression of the transcription factors *Ascl1* and *Ngn2* resulted in an increase of the conversion efficiency with yields up to 200% and neuronal purities up to 80% (Ladewig *et al.*, 2012). The set of small molecules consisted SB-431542, noggin and CHIR99021. Noggin was already identified in the frog as a BMP inhibitor and thereby as a neural inducing factor in the Spemann organizer. Together with SB-431542, which is known to inhibit the Lefty/Activin/TGF β pathways by blocking the phosphorylation of ALK4, ALK5, ALK7 receptors, it was demonstrated that his combination is sufficient to induce the neural conversion of human ESCs by instructing a dual inhibition of SMAD signaling (Chambers *et al.*, 2009). In addition to the dual SMAD inhibition, WNT signaling was activated by using the GSK-3 β inhibitor CHIR99021 (Ladewig *et al.*, 2012). Another study reached an efficient conversion of human fibroblasts into neurons by combining the TF *Ngn2* with two small molecules. Forskolin, an activator of cAMP signaling, and dorsomorphin, an inhibitor of bone morphogenetic protein signaling, showed to enable *Ngn2* for the generation of cholinergic neurons (Liu *et al.*, 2013). Additionally, it was found that the combination of GSK-3 β inhibition and cAMP signaling activation led to a strong increase of conversion efficiencies. Together with this combination, additional regulators like a HDAC inhibitor, a Scr kinase inhibitor or a SIRT1 activator increased also the

neuronal purity of the generated cell population (Pfisterer *et al.*, 2016).

In addition to small molecules it was also demonstrated that microRNAs are capable of enhancing the efficiency of the neuronal conversion. MicroRNA-9/9* and microRNA-124 were previously known to control several genes, which regulate neuronal differentiation and function (Cheng *et al.*, 2009; Makeyev *et al.*, 2007; Packer *et al.*, 2008; Visvanathan *et al.*, 2007; Yoo *et al.*, 2009). Instruction of its expressions showed to enhance the efficiency of the neuronal conversion from human fibroblasts (Yoo *et al.*, 2011).

1.2.5 Direct conversion of fibroblasts into defined neuronal subtypes

The achievements in directly converting fibroblasts into functional neurons by using a cocktail of 3-4 TFs raised the question, whether this cocktail could be integrated with lineage-specific transcription factors in order to generate defined neuronal subtypes from fibroblasts.

To look into this issue, it was screened for transcription factors, which instruct the developmental generation of distinct neuronal subtypes. The identified TF were then overexpressed for the subsequent conversion. As one of the first, dopaminergic neurons were generated by integrating Lmx1a and FoxA2 into the cocktail of the three transcription factors (Pfisterer *et al.*, 2011). In a similar approach, spinal motor neurons were generated. Therefore Ngn2, Lhx3, Isl1 and Hb9 were added to the mixture (Son *et al.*, 2011). In contrast to these works, it was demonstrated that neurons could be successfully generated with complete different mixtures of transcription factors. The generation of dopaminergic neurons was also reached by using Ascl1, Nurr1 and Lmx1a (Caiazzo *et al.*, 2011) or the addition of Foxa2, Pitx3 and EN1 to the previous combination (Kim *et al.*, 2011). Furthermore, the application of the lineage specific TF FoxA2, Lmx1b and FEV together with Ascl1 resulted in the generation of serotonergic neurons (Xu *et al.*, 2016). Besides the neurons of the midbrain or brainstem, different types of neurons from the cerebral cortex were also directly generated from fibroblasts by using a distinct combination of transcription factors. The combination of Ascl1, Foxg1, Sox2, Dlx5 and Lhx6 for instance convert mouse fibroblasts into GABAergic interneurons (Colasante *et al.*, 2015).

1.2.6 Direct conversion – a tool for disease modeling

The possibility to generate specific neuronal subtypes from fibroblasts holds also great promises for the regenerative medicine. Such induced neurons of a specific subtype derived from human somatic cells could be beneficial for disease modeling due to the possibility to use patient-derived fibroblasts for the conversion. Then fibroblasts from patients with the disease, which should be modeled, can be converted into the specific cell type, which is connected to this disease. The induced neurons display the genotypic and phenotypic pattern of the distinct disease and can be utilized for analyses. How it can be applied was recently shown. Hu *et al.* reported the successful conversion of human fibroblasts from patients with the Alzheimer's disease (AD). In this report, they induced neurons, which shared typical characteristics of AD diseased cells like an abnormal A β production (Hu *et al.*, 2015). In another report, motor neurons from ALS (amyotrophic lateral sclerosis) patients were generated via direct conversion. Also these neurons showed the pathophysiology of the respective disease (Liu *et al.*, 2015).

Another issue, which makes the direct conversion beneficial for disease modeling, is aging. In contrast to iPSC-derived cells, cells generated via direct conversion retain some characteristics of their starting cells, like their epigenetic status and age signature. In this regard, Mertens *et al.* showed that directly induced neurons exhibit an age-dependent regulation of genes, which were associated with aging. They found that RanBP17, a receptor, which is usually decreasing with aging, showed also a decrease in response to the age of the induced neurons. This decrease of RanBP17 could not be found in iPSCs (Mertens *et al.*, 2015). Furthermore it was demonstrated that directly induced neurons keep the age of the donor cells at the epigenetic level through their microRNA expression profile (Huh *et al.*, 2016). Since there are many diseases, which develop sporadically in old age, the retention of the age signature from the donor cell is very advantageous for a successful modeling.

Another advantage of direct conversion in regard to disease modeling is that this method is less expensive and time consuming. The generation of neurons from fibroblasts via iPSCs requires roughly 4-6 month including 2 months of the generation and validation of the iPSC clones and 2-6 weeks for the subsequent directed differentiation to functional neurons (Nicholas *et al.*, 2013). In contrast to iPSC differentiation, direct conversion is rather fast. Here, human induced neurons

can be generated within 1-3 weeks with an addition of a respective maturation time (Pang *et al.*, 2011; Liu *et al.*, 2013).

In addition to disease modeling, it was attempted to use directly induced cells for cell replacement studies. In one of the first approaches, directly induced dopaminergic neurons were shown to survive *in vivo* in mice (Caiazzo *et al.*, 2011). The neurons were induced by using the three TFs Ascl1, Nurr1 as well as Lmx1a and before the transplantation they showed several characteristics of functional dopaminergic neurons *in vitro*. In parallel, dopaminergic neurons were induced in another study with a combination of the six TFs Lmx1a, Nurr1, Ascl1, Foxa2, EN1 and Pitx3 (Kim *et al.*, 2011). In both studies it was demonstrated that a transplantation of induced dopaminergic neurons results in an engraftment of the neurons into the neural circuit and it also improved the symptoms in the mouse model of Parkinson's disease.

1.3 Aim of this study

The aim of this study was to investigate whether it is possible to specifically generate deep-layer corticofugal projection neurons by ectopic expression of the transcription factor *Fezf2* and whether the generated neurons can be used for modeling aspects of early cortical developmental malformations. This study should examine two different approaches to generate the desired population of cells. First, guided differentiation of PSC into telencephalic progenitors and corticofugal neurons should be combined with ectopic expression of the TFs *Fezf2* and *Ngn2*. Second, it should be tested whether subcerebral projection neurons can be directly induced from human fibroblasts using the TFs *Fezf2*, *Ascl1* and *Ngn2*. Derived neurons should be further characterized by immunocytochemical-, PCR- and morphological analyses in regard to their identity.

Furthermore, it should be investigated whether the generated cortical layer specific neurons can be utilized for modeling the early cortical malformation MDS, which represents a severe form of lissencephaly due to a deletion along chromosome 17 involving beside others the well-studied genes *LIS1* and *YWHAE* (*LIS1* and *YWHAE* are both part of the *LIS1/NDEL1/14.3.3ε* complex which is essential for the regulation of cytoplasmic dynein, centrosomal protein localization and microtubule dynamics). In MDS it was reported that neurons of the deep cortical layers exhibit immature morphologies. Corticofugal neurons induced by ectopic expression of the TFs *Fezf2*, *Ascl1* and *Ngn2* from control and MDS derived cells should be utilized to investigate whether the described phenotypic changes *in vivo* can be recapitulated in the developed *in vitro* cell culture system. Moreover, it should be examined whether additional genes located on the deletion side might contribute to the disease phenotype. More specifically, the role of two microRNA should be deciphered in detail. To that end, gain- and loss-of-function studies should give a deeper understanding on the molecular mechanisms leading to the disease specific alterations of the corticofugal neurons.

By that, this study should contribute to the field of direct lineage reprogramming by demonstrating the generation of a specific neuronal subtype *in vitro* and provide a valuable approach for modeling early cortical developmental malformations.

2. Materials

2.1 Technical equipment

Appliance	Name	Manufacturer	Registered office
Autoclave	D-150	Systec	Wettenberg, Germany
Block heater	Thermomixer	Eppendorf	Hamburg, Germany
Centrifuge (Cell culture)	Megafuge 1.0R	Sorvall	Hanau, Germany
Centrifuge (table top)	5415D	Eppendorf	Hamburg, Germany
Counting chamber	Fuchs-Rosenthal	Faust	Halle, Germany
Digital camera	C 5050 Zoom	Olympus Optical	Hamburg, Germany
Nucleofector	Nucleofector 2b	Lonza	Basel, Switzerland
Fluorescence lamp	HAL100	Carl Zeiss	Jena, Germany
Fluorescence Microscope	Axioskop 2	Carl Zeiss	Jena, Germany
Freezer -80°C	HERAfreeze	Kendro	Hanau, Germany
Gel electrophoresis chamber	Agagel	Biometra	Göttingen, Germany
Imaging system	Chemidoc 2000	Bio-Rad	München, Germany
Imaging system	Geldoc EZ	Bio-Rad	München, Germany
Incubator	HERAcell	Kendro	Hanau, Germany
Inverse light microscope	Axiovert 25	Carl Zeiss	Jena, Germany
LED light source	Colibri 2	Carl Zeiss	Jena, Germany
Liquid nitrogen store	MVE 611	Chart Industries	Burnsville, USA
Microscope	Axiovert 40 CFL	Carl Zeiss	Jena, Germany
Microscope	Axiovert 200M	Carl Zeiss	Jena, Germany
Microscope	Axio Imager Z1	Carl Zeiss	Jena, Germany
Microscope	DMI6000 B	Leica Microsystems	Wetzlar, Germany

Appliance	Name	Manufacturer	Registered office
Microscope camera	Axiocam MRM	Carl Zeiss	Jena, Germany
Micro-Spectrophotometer	Nanodrop ND-1000	Thermo Fisher Scientific	Wilmington, USA
PCR cycler	T3000 Thermocycler	Biometra	Göttingen, Germany
pH-meter	CG840	Schott	Mainz, Germany
Pipette-boy	Accu-Jet	Brand	Wertheim, Germany
Power supply for electrophoresis	Standard Power Pack P25	Biometra	Göttingen, Germany
Real-time qPCR machine	Mastercycler realplex	Eppendorf	Hamburg, Germany
Refrigerators 4°C /-20°C	G 2013 Comfort	Liebherr	Lindau, Germany
Secure horizontal flow hood	HERAsecure	Kendro	Hanau, Germany
Shaker	Bühler KS15	Johanna Otto	Hechingen, Germany
Sterile laminar flow hood	HERAsafe	Kendro	Hanau, Germany
Stereo microscope	STEMI 2000-C	Carl Zeiss	Göttingen, Germany
Table centrifuge	Centrifuge 5415R	Eppendorf	Hamburg, Germany
Thermocycler	T3 Thermocycler	Biometra	Göttingen, Germany
Ultracentrifuge	Sorvall	Discovery 90 SE	Hanau, Germany
Vacuum pump	Vacuubrand	Brand	Wertheim, Germany
Vortexer	Vortex Genie 2	Scientific Industries	New York, USA
Water bath	1008	GFL	Burgwedel, Germany

2.2 Cell culture and molecular biology consumables

Consumables	Manufacturer	Registered Office
4-well culture dishes	Thermo Fisher Scientific	Wilmington, USA
6-well culture dishes	Corning	Corning, USA
12-well culture dishes	Corning	Corning, USA
24-well culture dishes	Corning	Corning, USA
Cell Strainer 40 µm Nylon	Corning	Corning, USA
Coverslips	Menzel Gläser	Braunschweig, Germany
Cryovials 1 ml	Nunc	Wiesbaden, Germany
Cryovials 1.8 ml	Nunc	Wiesbaden, Germany
PCR strip tubes 0.2 ml	peqLab	Erlangen, Germany
Petri dishes Ø 10 cm	PAA	Pasching, Austria
Serological pipettes 1 ml	Sarstedt	Nümbrecht, Germany
Serological pipettes 2ml	Sarstedt	Nümbrecht, Germany
Serological pipettes 5ml	Costar, Corning	Corning, USA
Serological pipettes 10ml	Greiner Bio-One	Kremsmünster, Austria
Serological pipettes 25ml	Costar, Corning	Corning, USA
Syringes 50 ml	BD Biosciences	Heidelberg, Germany
Syringe filter 0.2 µm	PALL	Dreieich, Germany
TC dishes Ø 3.5 cm	FALCON, Corning	Corning, USA
TC dishes Ø 6 cm	FALCON, Corning	Corning, USA
TC dishes Ø 10 cm	FALCON, Corning	Corning, USA
Tubes 0.5 ml	Axygen, Corning	Corning, USA
Tubes 1.5 ml	Axygen, CorningBio-One	Corning, USA
Tubes 2 ml	Axygen, CorningBio-One	Corning, USA, Germany
Tubes 15 ml	FALCON, Corning	Corning, USA
Tubes 50 ml	FALCON, Corning	Corning, USA
qPCR plates	4titude	Wotton, UK
qPCR seals	4titude	Wotton, UK

2.3 Chemicals

Chemicals	Manufacturer	Registered office
Agar	Sigma-Aldrich	Deisenhofen, Germany
Agarose	PeqLab	Erlangen, Germany
Ampiciline	Sigma-Aldrich	Deisenhofen, Germany
B-27 supplement	Gibco by Life Technologies	Waltham, USA
Bromphenol blue	Sigma-Aldrich	Deisenhofen, Germany
CaCl ₂	Sigma Aldrich	Deisenhofen, Germany
Chloroform	Carl Roth	Karlsruhe, Germany
Chloroquin	Sigma Aldrich	Deisenhofen, Germany
DAPI	Sigma Aldrich	Deisenhofen, Germany
DMEM	Gibco by Life Technologies	Waltham, USA
DMEM/F12 (1:1)	Gibco by Life Technologies	Waltham, USA
DMSO	Sigma Aldrich	Deisenhofen, Germany
DNA ladder (100bp/1kbp)	PeqLab	Erlangen, Germany
dNTPs	PeqLab	Erlangen, Germany
Doxycycline	Sigma Aldrich	Deisenhofen, Germany
EDTA	Sigma Aldrich	Deisenhofen, Germany
EGF	R&D Systems	Minneapolis, USA
Ethanol	Sigma Aldrich	Deisenhofen, Germany
Ethidium bromide	Sigma-Aldrich	Deisenhofen, Germany
FCS	Invitrogen	Karlsruhe, Germany
FCS, tetracycline free	Takara (Clontech)	Kusatsu, Japan
FGF2	R&D Systems	Minneapolis, USA
G418 solution	Carl Roth	Karlsruhe, Germany
Geltrex	Gibco by Life Technologies	Waltham, USA
Glucose	Sigma-Aldrich	Deisenhofen, Germany
Glycerol	Sigma-Aldrich	Deisenhofen, Germany
HCl	Sigma Aldrich	Deisenhofen, Germany
Isopropanol	Sigma Aldrich	Deisenhofen, Germany

Chemicals	Manufacturer	Registered office
Laminin	Invitrogen	Karlsruhe, Germany
LB-Medium powder	Carl Roth	Karlsruhe, Germany
L-glutamine (100x)	Gibco by Life Technologies	Waltham, USA
Methanol ROTIPURAN	Carl Roth	Karlsruhe, Germany
Mowiol	Carl Roth	Karlsruhe, Germany
N2 supplement (100x)	Gibco by Life Technologies	Waltham, USA
Neurobasal medium	Gibco by Life Technologies	Waltham, USA
Non-essential amino acids (100x)	Gibco by Life Technologies	Waltham, USA
DPBS	Gibco by Life Technologies	Waltham, USA
PFA	Sigma Aldrich	Deisenhofen, Germany
Penicillin-Streptomycin	Gibco by Life Technologies	Waltham, USA
Poly-L-lysine hydrobromide	Sigma Aldrich	Deisenhofen, Germany
Poly-L-ornithine	Sigma-Aldrich	Deisenhofen, Germany
Puromycin	PAA	Pasching, Austria
Sodium pyruvate (100x)	Invitrogen	Karlsruhe, Germany
TriFast peqGOLD	PeqLab	Erlangen, Germany
Triton-X-100	Sigma Aldrich	Deisenhofen, Germany
Trypane Blue	Invitrogen	Karlsruhe, Germany
Trypsin-EDTA (10x)	Gibco by Life Technologies	Waltham, USA
TrypLE Express	Gibco by Life Technologies	Waltham, USA

2.4 Cell culture

2.4.1 Cell culture media

All cell culture reagents were prepared under sterile conditions and stored at 4°C; % = v/v.

MEF (mouse embryonic feeder)	
86%	DMEM-high-glucose
10%	FCS
1x	Sodium pyruvate
1x	L-Glutamine
1x	Non-essential amino acids
1x	Pen / Strep

Tetracycline free MEF (mouse embryonic feeder)	
86%	DMEM-high-glucose
10%	FCS, tetracycline free
1x	Sodium pyruvate
1x	L-Glutamine
1x	Non-essential amino acids
1x	Pen / Strep

Neuron conversion (NC) medium	
98%	DMEM/F12
0,5x	N2 Supplement
0,5x	B27 Supplement
1 mg/ml	Doxycyclin
10 µM	Forskolin
3 µM	CHIR99021
250 µg/ml	Dibutyryl-cAMP
0,5 µM	LDN
0,5 µM	A83

Neural maturation (NM) medium	
98%	DMEM/F12
0,5x	N2 Supplement
0,5x	B27 Supplement
1 mg/ml	Doxycyclin
20 ng/ml	BDNF
250 µg/ml	Dibutyryl-cAMP
20 ng/ml	GDNF
1 µg/ml	Laminin

Neural stem cell (N2) medium	
98%	DMEM/F12
0,5x	N2 Supplement
0,5x	B27 Supplement
1x	Penicillin/Streptomycin
0.8mg/ml	D-Glucose solution
0,15 µg/ml	cAMP

Neural induction medium	
96.8%	DMEM/F12
0.5x	N2 Supplement
0.5x	B27 supplement
1x	Non-essential amino acids
1x	Penicillin/Streptomycin
0.8mg/ml	D-Glucose
0,15 µg/ml	cAMP
0,5 µg/ml	LDN
0,2 µg/ml	A83
2 µM	XAV939

Neuronal generation (NGMC) medium	
96.8%	DMEM/F12
0.5x	N2 Supplement
0.5x	B27 supplement
1x	Non-essential amino acids
1x	Penicillin/Streptomycin
0.8mg/ml	D-Glucose
0,15 µg/ml	cAMP

E8 medium	
100%	DMEM/F12
64 µg/ml	LAAP
14 ng/ml	Sodium-selenit
10 µg/ml	Holo-transferin
2 ng/ml	TGFβ1
100 ng/ml	bFGF

WASH medium	
100%	DMEM-high-glucose
1x	Pen/Strep

Freezing medium for progenitors	
70%	KOSR
20%	Cytobuffer
10%	DMSO

Freezing medium for fibroblasts	
90%	Tetracycline free MEF
10%	DMSO

2.4.2 Cell culture solutions

1xTrypsin/EDTA (TE)	
90%	PBS
10%	Trypsin/EDTA (TE) 10x

Poly-L-ornithine (PO)	
100%	H ₂ O
1.5 mg/ml	Poly-L-ornithine (PO) mixed, sterile-filtered and stored at 4°C

Laminin (Ln) coating solution	
100%	H ₂ O
1 µg/ml	Laminin (Ln) in PBS

Geltrex (GT) LDEV-free coating solution	
98%	DMEM/F12
2%	Geltrex

2x HBS buffer	
8 g	NaCl
0.38 g	KCl
0.1 g	Na ₂ HPO ₄
5 g	Hepes
1 g	Glucose
H ₂ O was added to 500 ml, the pH was adjusted to 7.05, the mixture was sterile-filtered and stored at -20°C	

2.4.3 Cell culture additives

Reagent	Concentration	Solvent
A83	0,5 µg/ml	EtOH
B27 supplement	50x	Supplement mix
CHIR99021	3 µM	DMSO
BDNF	20 ng/ml	PBS + 0.1% BSA
Chloroquine	50 mM	H ₂ O
Doxycycline	1 mg/ml	H ₂ O
Dibutyryl-cAMP	250 µg/ml	H ₂ O
FGF2	10 µg/ml	PBS + 0.1% BSA
Forskolin	10 µM	DMSO
GDNF	20 ng/ml	PBS + 0.1% BSA
G418	50 mg/ml	H ₂ O
Laminin	1 µg/ml	Supplement
LDN (direct conversion)	0,5 µg/ml	DMSO
LDN (iPSC)	0,2 µg/ml	DMSO
N2 supplement	100x	Supplement
Puromycin	1 mg/ml	H ₂ O
ROCK inhibitor Y-27632	5mM	H ₂ O
XAV939	2 µM	DMSO

2.4.4 Cell lines

Cell line	Source
E. coli DH5a	Invitrogen, Deisenhofen, Germany
GM06097	Coriell Institute for Medical Research
GM06047	Coriell Institute for Medical Research
GM00696	Coriell Institute for Medical Research
HEK-293FT	Leiden, Netherlands, Dr. Alex Van der Eb
iPSC	Bonn, Germany (Iefremova <i>et al.</i> , 2017)

2.5 Molecular biology

2.5.1 Reagents

PFA fixation solution (4%)	
40 g	PFA
1000 ml	H ₂ O
The solution was heated until PFA dissolved completely, pH adjusted to 7.4 and sterile filtered.	

6x DNA loading buffer	
2 ml	EDTA (0.5M; pH 8.5)
6 g	Sucrose
0,2 ml	2% Bromphenol-blue-solution
0,2 ml	2% Xylene-cyanol-solution
0,2 g	Ficoll
3,8 ml	Aqua bidest.
The solution was mixed well, prepared in 1 ml aliquots and stored at 4°C	

Immuno-blocking solution	
89.9%	PBS
10%	FCS
0.1%	Triton X100 (only for intracellular epitopes)

Moviol / DABCO	
12 ml	Tris solution (0.2 M; pH 8.5)
6 ml	H ₂ O
6 g	Glycerol
2.6 g	Moviol
0.1 g	DABCO

PCR master mix (10 ml)	
1 ml	10x reaction buffer
600 µl	MgCl ₂ (50 mM)
40 µl each	dNTPs
8.24 ml	Ampuwa H ₂ O

qPCR master mix (5 ml)	
2000 µl	GoTaq® Flix buffer
1000 µl	MgCl ₂ (25 mM)
20 µl each	dNTPs
7.5 µl	1000x SYBR-green
1 µl	Fluorescin
400 µl	DMSO
1511.5 µl	Ampuwa H ₂ O

2.5.2 Enzymes

Enzyme name	Manufacturer	Registered office
DnaseI (molecular biology)	Invitrogen	Karlsruhe, Germany
Phusion High Fidelity DNA Polymerase	New England Biolabs	Frankfurt, Germany
T4 DNA Ligase	New England Biolabs	Frankfurt, Germany
Taq DNA Polymerase, recombinant	Invitrogen	Karlsruhe, Germany
Antarctic phosphatase	New England Biolabs	Frankfurt, Germany

2.5.3 Plasmids

Plasmid name	Source or parent DNA sequence
pMD2.G	Gift from Dider Trono, Lausanne, Switzerland
psPAX2	Gift from Dider Trono, Lausanne, Switzerland
pLVX-EtO	Modified from pLVX-Tet-ON-Advanced (Clontech)
pLVXTP	Equivalent to pLVX-Tight-Puro (Clontech)
pLVXTP-N2AA Ngn2 Ascl1	Modified from pLVX-Tet-ON-Advanced (Clontech)
pLVXTP-Fezf2	Modified from pLVX-Tet-ON-Advanced (Clontech)
pLVXTP-Ngn2	Modified from pLVX-Tet-ON-Advanced (Clontech)
pLVXTP-miR-22 sponge	Modified from pLVX-Tet-ON-Advanced (Clontech)
pLVXTP-miR-132 sponge	Modified from pLVX-Tet-ON-Advanced (Clontech)
pLVXTP-miR-22	Modified from pLVX-Tet-ON-Advanced (Clontech)
pLVXTP-miR-132	Modified from pLVX-Tet-ON-Advanced (Clontech)

2.5.4 Restriction endonucleases

Enzyme name	Restriction site	Manufacturer	Registered office
BamHI	5'...G [^] GATCC...3' 3'...CCTAG [^] G...5'	New England Biolabs	Frankfurt, Germany
EcoRI	5'...G [^] AATTC...3' 3'...CTTAA [^] G...5'	New England Biolabs	Frankfurt, Germany
MluI	5'...A [^] CGCGT...3' 3'...TGCGC [^] A...5'	New England Biolabs	Frankfurt, Germany

2.5.5 Bacterial solutions

LB agar	
20 g	LB-Medium powder (Roth)
15 g	Agar
H ₂ O was added to 1 l, the mixture was autoclaved and stored at 4 °C	

LB medium	
40 g	LB-Medium powder (Roth)
H ₂ O was added to 2 l, the mixture was autoclaved and stored at 4 °C	

2.5.6 Kits

Name	Producer	Office
DNeasy Blood & Tissue Kit	Qiagen	Hilden, Germany
iScript cDNA Synthesis Kit	Bio-Rad	München, Germany
miScript II RT Kit	Qiagen	Hilden, Germany
miScript SYBR Green PCR Kit	Qiagen	Hilden, Germany
Nucleofector™	Lonza	Basel, Switzerland
peqGOLD Gel Extraction Kit	Peqlab Biotechnologie	Erlangen, Germany
peqGOLD Plasmid Miniprep Kit	Peqlab Biotechnologie	Erlangen, Germany
PureLink™ HiPure Plasmid Maxiprep Kit	Thermo Fisher Scientific	Waltham, USA

2.5.7 Primer

Cloning primer*	
Name	Primer sequence (5'-3')
miR-22_BamHI_F	CAGCGAGGTTAACAGCTTCC
miR-22_EcoRI_R	CTCCTCAATCCAGCCAGTGT
miR-132_BamHI_F	GGATCCTCGAGGATCCAGGGGCGGT
miR-132_EcoRI_R	GAATTCTCGAGCTAGCCCTCCTGCCA

Sequencing primer	
Name	Primer sequence (5'-3')
pTRE_F	TAAGCAGAGCTCGTTTAGTG
Puro_R	TGTA CTGGTCATGGTAAGC

qPCR primer	
Name	Primer sequence (5'-3')
Clim1_F	CAGTGCTTCAAAGCCACAA
Clim1_R	GTGCTCCAAGTCAACTGCAA
CRYM_F	GAAGCTGTGCTGTACGTGGA
CRYM_R	TTGGCTGCAACTGTGTCTTC
Cux1_F	GCTCTCATCGGCCAATCACT
Cux1_R	TCTATGGCCTGCTCCACGT
Ctip2_F	AGAACTGCAGCAACTTGACG
Ctip2_R	GTACACCTCCTTGCCGATCT
Dkk3_F	TATGTGTGCAAGCCGACCTT
Dkk3_R	CTCCTCCATGAAGCTGCCAA
ER81_F	TACCCCATGGACCACAGATT
ER81_R	CACTGGGTCGTGGTACTCCT
miR-22-3p	AAGCTGCCAGTTGAAGAACTGT
miR-132-3p	TAACAGTCTACAGCCATGGTCG
p250GAP_F	AGCGGGGAATCTTGAAAGAGA
p250GAP_R	GATATTGGAGGCAACACCAGAAA
Pdk1_F	GCAAATCACCAGGACAGCC
Pdk1_R	ACCCAGCGTGACATGAACTT
PTEN_F	TTTGAAGACCATAACCCACCAC
PTEN_R	ATTACACCAGTTCGTCCCTTTC
Rac1_F	CACTGTCCCAACTCCCAT
Rac1_R	GCCGAGCACTCCAGGTATTT
RNU5	GTGGAGAGGAACA ACTCTGAGTC
Tbr1_F	TCTCGACCACTGACAACCTG
Tbr1_R	CCGTCCAAGACAGGAGAGAG
Tle4_F	CCCAGCATTTATCACATGGACA
Tle4_R	GCACTGCTACCGATGGGTG

qPCR primer	
Name	Primer sequence (5'-3')
Wnt7b_F	CCAACTACTGCGAGGAGGAC
Wnt7b_R	TGGTGTACTGGTGGGTGTTG

PCR primer	Primer sequence (5'-3')
Ascl1 transgenic/endogenous_F	CTACTCCAACGACTTGA ACTCCA
Ascl1 transgenic_R	ATTCACGCGTCTATCAGAACCA
Fezf2 transgenic/endogenous_F	GCCTTCCACCAGGTCTACAA
Fezf2 transgenic_R	TTCACGCGTTCATCAGCTCT
Ngn2 transgenic/endogenous_F	AATTCCACCTCCCCCTACAG
Ngn2 transgenic_R	GGTAGCAGAAATGGCAGCTC

2.5.8 Oligonucleotides

Cloning oligonucleotides name	Oligonucleotide sequence (5'-3')
miR-132 sponge_MluI_F	GCAGCAACGCGTCGACCATGGACAAGACTGTAAATT CGACCATGGACAAGACTGTAAACGCGTTGCTGC
miR-132 sponge_MluI_R	GCAGCAACGCGTTAACAGTCTTGTCCATGGTCGAATTT AACAGTCTTGTCCATGGTTCGACGCGTTGCTGC
miR-22 sponge_MluI_F	GCAGCAACGCGTACAGTTCTTCCGTGGCAGCTTAATT ACAGTTCTTCCGTGGCAGCTTACGCGTTGCTGC
miR-22 sponge_MluI_R	GCAGCAACGCGTAAGCTGCCACGGAAGAACTGTAATT AAGCTGCCACGGAAGAACTGTACGCGTTGCTGC

2.5.9 Antibodies

Primary antibody	Dilution	Source
β III-tubulin (ms)	1:1000	BioLegend
β III-tubulin (rb)	1:5000	BioLegend
Ctip2 (rat)	1:1000	Abcam
Cux1 (rb)	1:300	Santa Cruz Biotechnology
Dach1 (rb)	1:100	ProteinTech
Dcx (rb)	1:500	NEB
Map2AB (ms)	1:250	Sigma-Aldrich
Otx2 (gt)	1:500	R&D Systems
Pax6 (rb)	1:500	DSHB
Tbr1 (rb)	1:500	Abcam
Satb2 (rb)	1:400	Sigma-Aldrich
Sox2 (ms)	1:300	R&D Systems

Secondary antibody	Dilution	Source
Alexa488 gt-anti-ms	1:1000	Life technologies
Alexa488 gt-anti-rb	1:1000	Life technologies
Alexa555gt-anti-ms	1:1000	Life technologies
Alexa555gt-anti-rb	1:1000	Life technologies
Alexa555gt-anti-rat	1:1000	Life technologies

ms = mouse; rb = rabbit; gt = goat

2.6 Software

Name	Application	Producer
ApE – A plasmid Editor v2.0.47	Cloning strategies	M. Wayne Davis
AxioVision 40 4.5.0.0	Fluorescence microscopy	Carl Zeiss
Excel 2008	Data analysis	Microsoft
Image J 1.42q	Quantifications	NIH
Illustrator CS3	Figures	Adobe

Name	Application	Producer
LAS X	Fluorescence microscopy/ Live Cell Imaging	Leica
Microsoft Office 2008	Figures and text processing	Microsoft
Photoshop CS3	Figures processing	Adobe
Power Point 2008	Graphic illustration	Microsoft
Primer3 v0.4.0	Primer picking	Rozen and Skaletsky (2000)
Prism 6	Data analysis and statistics	GraphPad
Quantity One 4.6.8	Electrophoresis gel documentation	Bio Rad
Word 2008	Writing documents	Microsoft

3. Methods

3.1 Cultivation of human fibroblasts

Fibroblasts were commercially received from Coriell Institute for Medical Research. The cells were cultured on 6-well tissue culture dishes (Falcon) coated with 1x gelatine. The culture medium consisted of DMEM (Gibco) with 10% tetfree FCS, 1x Sodium pyruvate, 1x non-essential amino acids, 1x penicillin-streptomycin and 1x L-glutamine. The medium was changed every 3 days. Cells were usually split 1:2 once a week. For splitting, the culture medium was removed, the cells were washed two times with PBS followed by a digestion into single cells with Trypsin-EDTA for 3-6 min at 37°C. To stop the digestion, double of the amount of culture medium was added on the TE and the cells were collected in a tube. Afterwards the cells were centrifuged for 3 min at 800xg. The resulting cell pellet was resuspended in fresh culture medium and plated on 1x gelatin coated cell culture dishes.

3.2 Cultivation of human induced pluripotent stem cells (hiPSCs)

Pluripotent stem cells were cultured on 6-well tissue culture dishes (Falcon) coated with GelTrex. The cell expansion medium consisted of Pluripro® medium (Cell Guidance) and E8 Medium (50:50). The medium was changed every day. The cells were usually split 1:3 every 2-3 days. For splitting, cells were digested with TrypLE Express for 5-9 min at 37°C. The same amount WASH medium was added to stop the digestion and the cells were collected in a tube. Thereafter, the cells were centrifuged for 4 min at 1200xg. The cell pellet was resuspended in fresh culture medium and plated on Geltrex coated cell culture dishes.

3.3 Design of lentiviral vectors

As a conditional expression system, a modified variant of the Lenti-XTM Tet-On Advanced system (Clontech) was used. The modification was due to an exchange of the CMV promoter by an EF1 α promoter in the plasmid to regulate the expression of the rtTAAAdv protein. For the overexpression of Fezf2, Ascl1, Ngn2, microRNA-22,

microRNA-132, as well as for the sponges of microRNA-22 and microRNA-132, the pLVX-Tight-Puro vector was used.

PCR products were unravelled by agarose gel electrophoresis. The desired bands were manually pruned under UV light. The cut PCR products were isolated by gel purification (peqGOLD™ Gel Extraction Kit, Peqlab). Afterwards they were digested with the appropriate restriction enzymes (listed in chapter 2). At the end, they were ligated (T4 DNA Ligase, NEB) into a pLVX-Tight-Puro vector, which was previously linearized and dephosphorylated (FastAP™, Fermentas). This vector was under the control of the inducible TREtight promoter. For selection, a puromycin resistance cassette was located on the vector. All generated vectors are listed in chapter 2.5.3.

3.4 Production and concentration of lentiviral particles

To produce lentiviral particles, HEK293-FT cells were cultured on a polyornithine (1x)-coated 10 cm dish in MEF medium. When cells showed a 60-70% confluence, they were co-transfected with lentiviral plasmids of the second generation by calcium-phosphate precipitation as described before (Kutner *et al*, 2009). 0,1x Tris EDTA was mixed with 3,5 µg of the envelope plasmid pMD2.G, 7 µg of the packaging plasmid psPAX2 and 10 µg of the transfer vector. The mixture was filled up to 500 µl with H₂O. 50 µl of 2,5M CaCl₂ was added to the suspension and mixed until no flowmarks were visible anymore. Then the suspension was slowly mixed with 500 µl of 2x HBS (pH=7), followed by an incubation of 30 min at RT. After this, it was added dropwise to the HEK293-FT cells, which were pre-incubated with 25 µM chloroquine (30 min, 37°C in MEF). On the second and third day, the medium of the dishes was changed and the supernatants were collected and pooled. The pooled supernatants were filtered through a 0,45 µm filter and concentrated by using a membrane based anion exchange chromatography using polyethylene glycol 6000 (PEG 6000) (Kutner *et al*, 2009). This mixture was incubated for 1,5 h at 4°C, while it was inverted every 30 min. For the concentration of the particles, the mixture was centrifuged (4700 xg; 4°C, 30 min). Viral particles were resuspended in virus freezing medium, aliquoted and for long term storage transferred to -80°C.

3.5 Lentiviral transduction of human fibroblasts

For generating fibroblast cell lines for the transcription factor based direct conversion, lines were first transduced with lentiviral particles containing the EF1 α regulated rtTAAAdv protein. Lentiviral particles were added to the usual culture medium. The cell lines were always transduced for 24 h. After transduction, cells were chemoselected with G418 (100 μ g/ml) for five days. Afterwards, the cells were transduced with the pLVXTP-Ascl1-Ngn2 virus to obtain an inducible system for the direct conversion and with pLVXTP-Fezf2 for the later differentiation to subcortical neurons. After this transduction, the cells were chemoselected with puromycin (1 μ g/ml) for three days. To generate overexpression- and knockdown-lines of the respective microRNA, cells were additionally transduced with the respective pLVXTP construct.

3.6 Lentiviral transgenesis of hiPSCs

For generating hiPSC lines for the transcription factor based direct differentiation, lines were first transduced with lentiviral particles containing the EF1 α regulated rtTAAAdv protein. Lentiviral particles were added to conditional KOSR medium. The cell lines were always transduced for 24 h. After transduction, cells were chemoselected with G418 (100 μ g/ml) for five days. Afterwards, the cells were transduced with pLVXTP-Fezf2 for the later differentiation to subcortical neurons. Additionally cells were transduced with pLVXTP-Ngn2. After this transduction, the cells were chemoselected with puromycin (1 μ g/ml) for three days.

3.7 Transcription factor based direct conversion of human fibroblasts into induced neurons (iN)

Transduced fibroblasts were cultured in tetracycline free MEF medium and expanded. For the conversion into iNs fibroblasts were cultivated to a high density and Doxycycline (1 mg/ml) was added to the medium to induce the expression of transgenes for the conversion. After 2 days, the medium was changed to neuron conversion medium (NC). NC was supplemented by: Doxycycline (1 mg/ml) for the proper induction of transgenes, CHIR99021 (3 μ M), which inhibits GSK3 and

activates the Wnt-signaling pathway, Forskolin (10 μ M) a cAMP activator, dibutyryl-cAMP (250 μ g/ml), which is an PKA activator, and for a dual SMAD inhibition, LDN (0,5 μ g/ml) and A83 (0,5 μ g/ml) were added. The cells were cultivated in NC for 10 days, while the medium was changed every second day. After 10 days, the medium was switched to neural maturation medium (NM) for further maturation of the iNs. The NM contained Doxycycline (1 mg/ml) and dibutyryl-cAMP (250 μ g/ml) like the NC medium. In addition, it was supplemented with the growth factors BDNF (20 ng/ml) and GDNF (20 ng/ml) as well as with Laminin (1 μ g/ml). iNs were cultivated in NM until they were fixed or harvested for experiments.

3.8 Directed differentiation of hiPSC

Pluripotent stem cells were cultured to a high density. Subsequently the medium was switched to neural induction medium. Thereby dual SMAD inhibition and inhibition of the Wnt-signalling pathway was applied to the cells (Shi *et al.*, 2012). Furthermore doxycycline was added to the media to ensure the induction of transgene expression. The medium was changed every other day. During the first ten days with neural induction media, the cells were not split. In this induction phase, the pluripotent stem cells differentiated into cortical progenitors, which are more specified than the stem cells. In contrast the cortical progenitors are rather unipotent than pluripotent and differentiate further into one specific cell type. After ten days the cells were split for the first time in a 1:2 ratio. From this split on, cortical progenitors were split every two or three days until the first neurons could be observed. When the first neurons came up, the medium was switched to neuronal generation medium (NGMC). NGMC was changed as soon as the phenol red inside the medium on the cells showed a color change to yellow. The neurons were further cultured until they were fixed or harvested for experiments.

3.9 RNA extraction

Fibroblasts or neurons were harvested at different time points. Therefore the cells were washed one time with PBS, scratched off the plate with a cell scraper and collected in PBS in a 1.5 ml tube. Subsequently the cell suspension was centrifuged

for 4 min at 1200 xg. Following the centrifugation the pellet was lysed with 500 μ l Trifast and homogenized. Thereupon, 200 μ l chlorophorm were added to the suspension and the tubes were inverted for 30 s at RT. Afterwards, the mixture was incubated for 12-15 min at RT, followed by a centrifugation (10 min, 12000 xg). After centrifugation, the mixture is unravelled into three different phases. The upper one contains RNA, the intermediate DNA and the lower one proteins. The upper phase was transferred to a new 1.5 ml tube. Next, the RNA was precipitated. For the precipitation, 250 μ l isopropanol were added, the mixture was then inverted for 15 s and incubated on ice for up to three hours. The precipitation was followed by a centrifugation (10 min, 12000 xg, 4°C). After the centrifugation, a gel-like RNA-precipitate was observable. In the following, this precipitate was washed with 800 μ l of 75% EtOH-Diethyl pyrocarbonate (DEPC) water. Every wash step was followed by a centrifugation (10 min, 12000 xg, 4°C). After washing, the precipitate was air-dried for 30-60 min at RT. After that, the precipitate was redissolved in 20 μ l DEPC water and shaken for 30 min at RT.

3.10 RNA purification

The extracted RNA was purified with DNaseI (Invitrogen) by digesting the single- and double stranded DNA. Therefore 2,5 μ l of 10x DNaseI reaction buffer and 2,5 μ l of DNaseI were added to every RNA samples and incubated for 15 min at RT. Afterwards, the DNaseI was inactivated by adding 2,5 μ l EDTA (25 mM) and a following incubation for 10 min at 65°C. At last, the RNA concentration was measured using a micro-spectrophotometer (Nanodrop ND-1000).

3.11 cDNA synthesis

Total RNA was extracted from cell pellets by using a Trifast-chloroform-extraction (see chapter 3.9) and mRNA was purified with a DNaseI treatment (see chapter 3.10). For cDNA synthesis, 1 μ g of RNA was utilized and reversely transcribed into cDNA by using the qScript cDNA Synthesis Kit (Quanta) in correspondence to the manufacturer's protocol. In a last step the cDNA concentration was measured using a micro-spectrophotometer (Nanodrop ND-1000).

3.12 Quantitative RT-PCR

The quantitative RT-PCR was processed on a Biorad-iCycler realplex mastercycler. The reactions were done in triplicates by using a Taq DNA polymerase and the SYBR-green detection method. The evaluation of the PCR products were performed by using a dissociation curve analysis (iCycler iQTM Real-Time PCR Detection System). To assure comparable gene expression levels, the GOI expression levels were normalized to 18s mRNA expression levels (Quantitative RT-PCR primers listed). For the subsequent analyses, the $\Delta\Delta C_t$ -value method was used.

Step	Temperature	Time
Initial denaturation	95°C	2 min
40 cycles:		
Denaturation	95°C	15 s
Annealing	60°C	15 s
Elongation	72°C	20 s

3.13 Immunocytochemical analysis

First, the cells were fixed by using 4% PFA for 10 min at RT. Then, the cells were washed two times with PBS, followed by a blocking step with 10% FCS and 0,1% Triton-X-100 in PBS for 1 h at RT. Thereafter, primary antibodies (listed in materials) were dispensed ON at 4°C. After this incubation, the primary antibodies (in blocking solution) were removed and the cells were washed at least two times with PBS. The last washing step was performed for 5 min. After washing, secondary antibodies (in blocking solution) were applied to the cells for 1 h at RT in the dark. After 1 h, secondary antibodies were washed away and DAPI was put on the cells for 5 min at RT in the dark. At the end, the cells were washed again with PBS and covered with Moviol and a coverslip. Stainings were kept at 4°C.

3.14 Branching Assay

For analysis of the neuronal outgrowth of iNs, a so-called branching assay was developed. Therefore iNs were generated as described in chapter 3.7. The iNs were fixed after 23 d and 28 d. As described in Chapter 3.7, the fixed iNs were stained for β III-tubulin. On the basis of the stainings the neuronal outgrowth was quantified. For this quantification every branchpoint of every neuron was counted. Neurons without any branchpoints were counted as zero. In the end the mean of all branchpoints was calculated by dividing the total number of counted branchpoints through the total number of counted neurons. Thereby value for each line was calculated, which is easily to compare between different lines.

3.15 Motility Assay

For the motility assays iNs were generated as described in Chapter 3.7. After 23 days, the iNs were digested with TrypLE Express for 5-9 min at 37°C. The same amount WASH medium was added to stop the digestion and the cells were collected in a tube. Thereafter, the cells were centrifuged for 4 min at 1200 xg. After centrifugation, the pellet was resuspended gently avoiding single cell formation. The cell suspension was subsequently replated. The new plate was covered with poly-L-lysine for 60 min at RT and PBS/Laminin (1:200) for 2 h at 37°C. After replating, the iNs were cultured in NM for additional 12 d. After 35 days, live cell imaging was performed with the Live Cell microscope (37°C; 5% CO₂). Neurons were imaged for every 30 min for 2 days. Analysis was conducted by using the ImageJ software.

3.16 Statistical analysis

For quantification of the different cell lines, data was generated in biological duplicates and ≥ 3 technical replicates. Aberrations are mentioned in due course. Results represented in a bar chart show means + standard deviation (SD). Means and standard deviations were calculated using GraphPad Prism 6 software and Microsoft Excel 2008. To determine a significance difference between groups,

student's t-test was conducted by using GraphPad Prism 6 software (* $p \leq 0,05$; ** $p \leq 0,01$; *** $p \leq 0,001$; **** $p \leq 0,0001$).

4. Results

4.1 In vitro generation of cortical layer specific human neurons

4.1.1 Directed differentiation of human pluripotent stem cells to into cortical progenitors and neurons

Significant progress has been made in the controlled and guided differentiation of PSCs into cortical progenitors, neural rosettes and cortical layer-specific neuronal subtypes that appear with a remarkably preserved temporal order (Gaspard *et al.*, 2008; Shi *et al.*, 2012). We applied the protocol described by Shi *et al.*, 2012 to differentiate PSC into cortical progenitors and neurons with several adaptations (see chapter 3.8). In brief, PSC were cultured as a monolayer of single cells. Neural induction was initiated in 95% confluent cultures by an inhibition of dual SMAD signaling to block mesoderm and endoderm formation and the Wnt-signaling to prevent a ventralization of the cells. Following telencephalic specification, terminal differentiation was initiated by a withdrawal of the applied inhibitors (see schematic overview Figure 5 A).

Efficient and homogenous neural induction was investigated 12 days following neural induction by immunocytochemical analyses (Figure 5 B-C). PSC-derived neural progenitors homogeneously express the neural stem cell marker SOX2, the neuroepithelial marker Dach1 (Figure 5 C) as well as the dorsal marker Pax6 and the forebrain marker OTX2 (Figure 5 B) suggesting a dorsotelencephalic cellular identity. Cortical progenitors were further differentiated into glutamatergic cortical neurons, which stain positive for the neuronal marker β III-tubulin and the glutamate transporter vGlut indicating homogenous differentiation into glutamatergic neurons (Figure 5 D). The differentiation pattern of the dorsal cortical progenitors showed a preserved temporal order with sequential generation of neurons of the deep (Ctip2+, Figure 5 E) and upper cortical layers (Satb2+, Figure 5 F) (Gaspard *et al* 2008; Shi *et al* 2012). By that, our data confirm the efficient and homogenous differentiation of PSC into progenitors and neurons exhibiting a dorsal cortical identities.

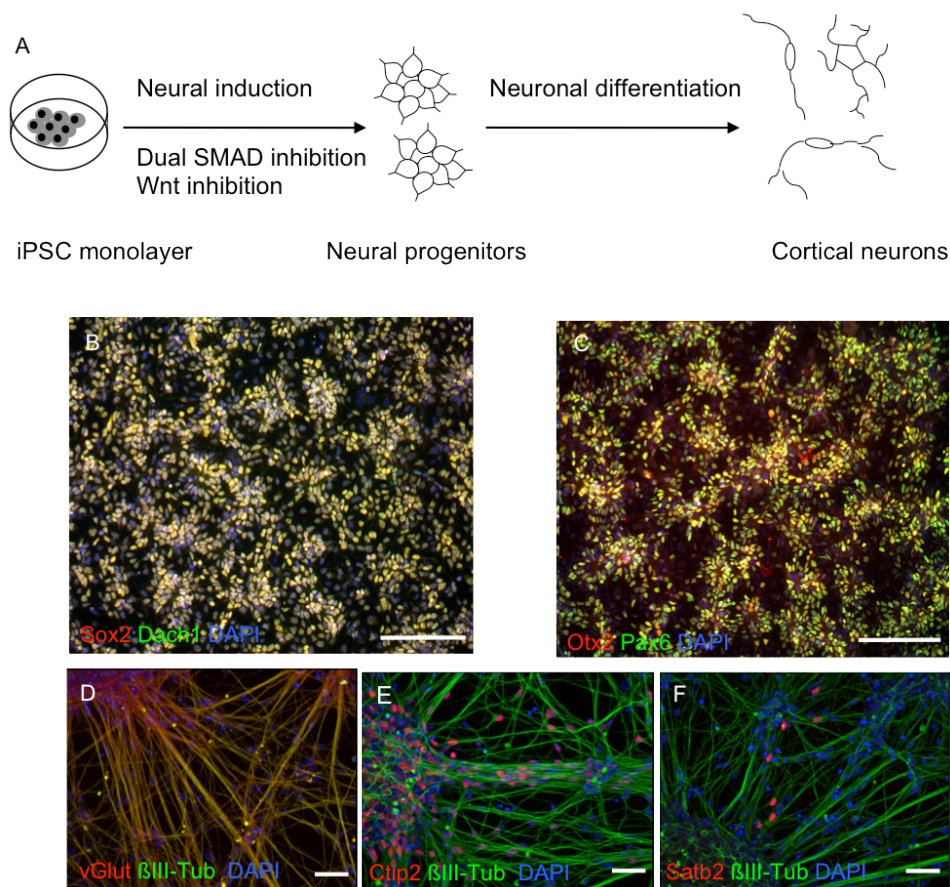


Figure 5 Differentiation of PSCs into dorsal cortical progenitors and excitatory cortical neurons. A: Schematic overview of the differentiation protocol. B-C: Progenitors express the NSC marker Sox2, the NESC marker Dach1, the forebrain marker Otx2 and the dorsal marker Pax6. D-F: Differentiated neurons (β III-Tubulin) are positive for the glutamate transporter vGlut and cortical layer-specific transcription factors Ctip2 and Satb2. Scale bars 100 μ m. NSC: neural stem cell; NESC: neuroepithelial-like stem cell. Experiments were performed together with Julia Ladewig.

4.1.2 Transcription factor-based induction of PSC into corticofugal neurons

Next, we asked if it is possible to direct the differentiation of PSCs into corticofugal neurons. Corticofugal neurons project their axons to subcortical targets such as the thalamus and subcerebral targets like the midbrain and spinal cord. They are predominantly located inside cortical layer V (subcerebral neurons), but build also a population within layer VI (corticothalamic neurons) (Leone *et al.*, 2015; Molyneaux *et al.*, 2007). During cortical development, the TF Fezf2 plays a central role for the specification of corticofugal neurons inside cortical layer V (Chen *et al.*, 2008; Molyneaux *et al.*, 2005; Shim *et al.*, 2012).

4.1.2.1 Generation of transgene inducible PSC lines

To test whether *Fezf2* represents a potent transcription factor to direct the differentiation of PSC into a homogenous population of corticofugal neurons, we transfected PSCs with a lentiviral vector carrying the TF *Fezf2* (F). *Fezf2* was described to act as a master regulator for instructing the corticofugal fate of cortical neurons (Arlotta *et al.*, 2005; Inoue *et al.*, 2005; for a detailed description of the vector design see chapter 3.3). In addition, we applied the pro-neural TF *Ngn2* (N), which was described to rapidly induce functional neurons from human PSCs in less than two weeks with a yield and purity of almost 100% (Zhang *et al.*, 2013). The generated PSC were termed hPSC-FN. As a control, we also generated a PSC line carrying *Ngn2*, only (termed: hPSC-N). Transgenes were encoded by doxycycline-inducible (tet-on) lentiviral vectors. Thereby the expression of transgenes was regulated by adding doxycycline to the media. Furthermore, lentiviral vectors possessed a puromycin resistance cassette providing the transfected cells with a resistance for puromycin. Following transfection, cells were selected via puromycin treatment. Expression of the transgene(s) was verified by PCR analyses following four days of doxycycline treatment using transgene specific primers. In accordance to the introduced construct the PCR analyses showed that treatment with doxycycline evoked the expression of the transgenes *Ngn2* and *Fezf2* in the hPSC-FN line, while the hPSC-N line only exhibit a transgenic expression of *Ngn2* (Figure 6). A sample of the hPSC-FN line, which was not treated with doxycycline, served as negative control and confirmed that transgene expression is tightly controlled by the application of doxycycline (Figure 6).

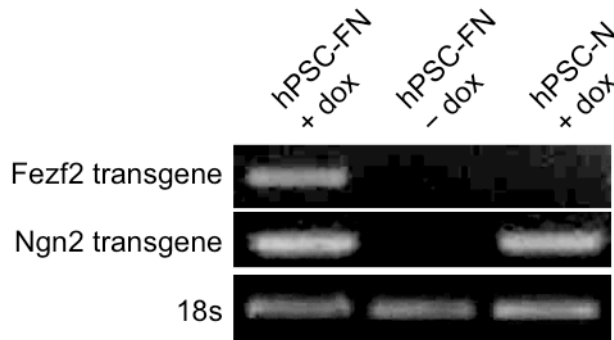


Figure 6 Validation of transgene inducible PSC lines. Transduced iPSC lines were characterized via PCR analyses. Expression of Fezf2 could be detected in the hPSC-FN line, while expression of Ngn2 was visible in the hPSC-FN and the hPSC-N line. The hPSC-FN line not treated with doxycycline did not exhibit a transgene expression. Induced N+F-PSC line shows expression of Fezf2 and Ngn2, whereas there is no signal observable without induction with doxycycline. The N-PSC line shows only Ngn2 expression. *Performed together with Julia Ladewig.*

4.1.2.2 Differentiation of PSCs into corticofugal neurons

The hPSC-FN line as well as the hPSC-N line were differentiated along the in chapter 3.8 described and validated differentiation protocol into cortical progenitors and neurons. The transgene expression was induced by doxycycline addition at day 3 of the differentiation protocol. Generated neurons were analyzed by immunocytochemical analyses 8 weeks following differentiation for the expression of the cortical layer specific markers Tbr1 (layer VI), Ctip2 (layer V), Cux1 (layers II-IV) and Satb2 (layers II/III). A sample of the hPSC-FN line, which was not induced with doxycycline, served as control.

We found that control-derived β III-tubulin positive neurons, which were not induced with doxycycline, exhibited a prominent expression for the layer VI marker Tbr1 while Ctip2 positive layer V neurons were found to a lesser extent. The expression of the layer II/III Satb2 was only occasionally detectable and Cux1 positive neurons (representing cortical layer II-IV) were not detectable (Figure 7 A upper panel). In contrast, ectopic expression of Fezf2 and Ngn2 led to neuronal cultures in which the

majority of the β III-tubulin positive neurons co-expressed the cortical layer V marker Ctip2, whereas expression of markers for upper cortical layers (Satb2 and Cux1) could not be observed (Figure 7 A middle panel). The ectopic expression of the pro-neural transcription factor Ngn2 alone led to neuronal cultures exhibiting a strong and homogenous expression of Cux1. Since neurons expressing markers for other cortical layers were largely absent from these cultures, our data indicate a predominant generation of neurons from upper cortical layer in response to the exclusive expression of Ngn2 (Figure 7 A lower panel).

To further investigate the differentiation pattern of the different PSC lines, we analyzed expression of the cortical layer specific markers Tbr1, Ctip2 and Cux1 by PCR. To that end, neuronal cultures derived from the hPSC-FN and hPSC-N line were differentiated for 6 or 8 weeks. After that, RNA was harvested and cDNA was obtained. Following PCR analyses, we found that the control neurons, which were not induced with doxycycline, exhibited no expression of Cux1. The expression of Ctip2 was strong at both time points (Figure 7 B). The ectopic induction of Fezf2 and Ngn2 within the hPSC-FN line led to a strong Ctip2 expression following 6 weeks of differentiation, which was even increasing following 8 weeks of differentiation. The expression levels of Tbr1 were weak compared to neurons, which had no transgene induction (Figure 7 B). Expression of Cux1 was hardly detectable following 6 weeks of differentiation but showed increased expression after 8 weeks of differentiation (Figure 7 B). The ectopic induction of Ngn2 only led to a clear expression for Cux1. The Ctip2 expression was rather weak, while Tbr1 was not detectable (Figure 7 B). These data support the previous results of the immunocytochemistry analyses. To quantify expression levels of the different cortical layer specific markers, we performed quantitative real-time PCR analyses of neuronal cultures differentiated for 8 weeks with or without induction of the transgenes. Besides Tbr1, Ctip2 and Cux1, we also included Tle4 in our analyses as a marker specific for corticofugal neurons of the cortical layer V. Gene expression values of hPSC-FN and hPSC-N derived neurons were analyzed in relation to the expression values of hPSC-FN derived neurons with no transgene induction. Here we found a more than 1-fold increase in the expression of the layer V marker Ctip2 in hPSC-FN derived neurons. The expression of the other layer V marker Tle4 showed also an increase of 0,25-fold. The upper layer marker Cux1 exhibited a minor increase of 0,1-fold. Only the layer VI marker Tbr1 showed a 0,4-fold decrease (Figure 7 C).

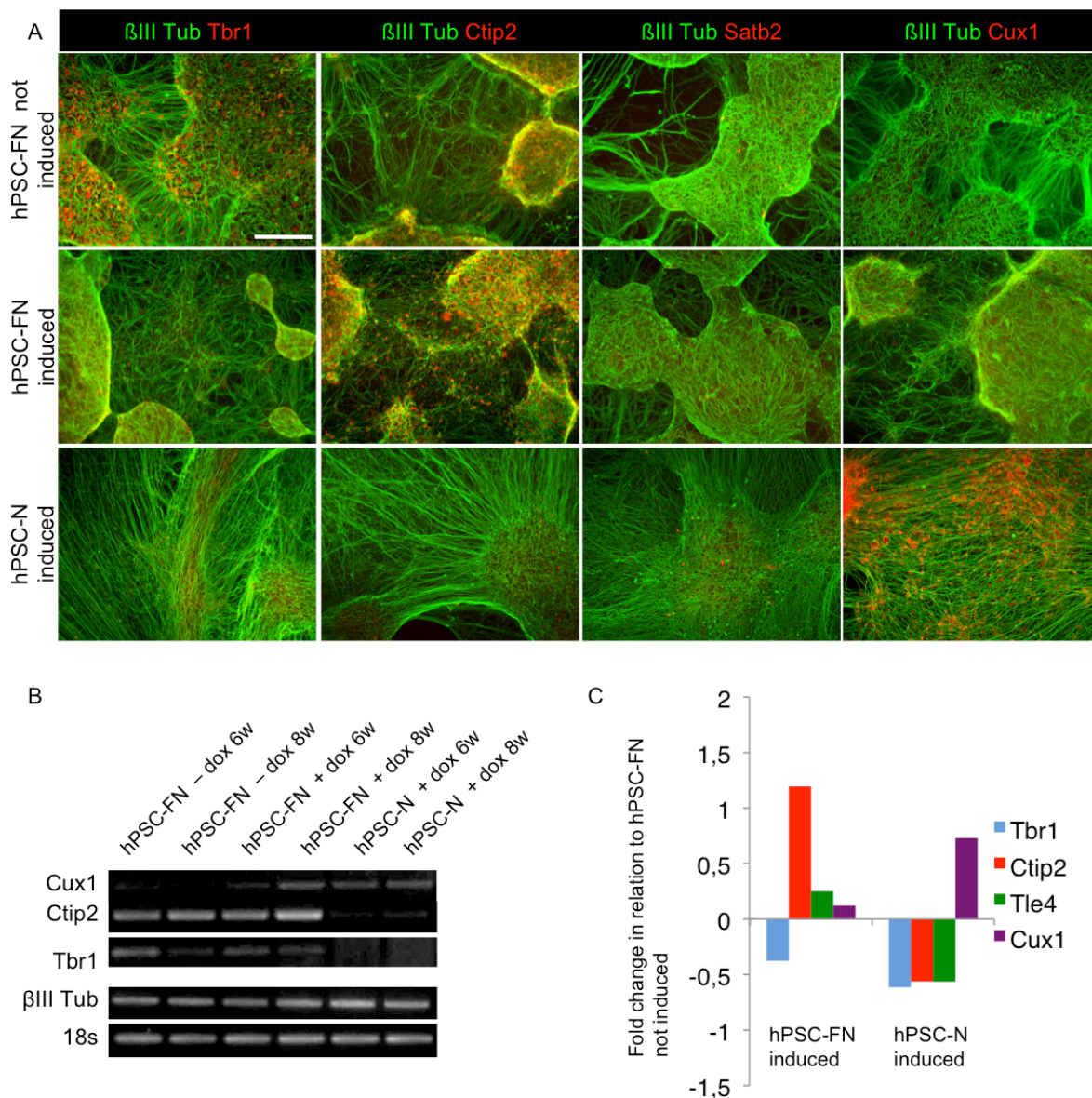


Figure 7 Transgenic Fezf2 expression instructs deep cortical layer identity. *A: Immunocytochemical characterization of 8 weeks old neurons. Neurons with no induction of Fezf2 (F) and Ngn2 (N) show many neurons stained positive for Tbr1 and Ctip2. Markers for upper cortical layers (Satb2 and Cux1) are almost absent (upper panel). Induction of hPSC-FN shows many neurons stained positive for Ctip2. Tbr1 and upper cortical markers are almost absent (middle panel). The absence of Fezf2 shows a huge number of Cux1 positive neurons. Also Satb2 staining shows more positive neurons. Tbr1 and Ctip2 positive neurons are much less (lower panel). Scale bar 100 μ m. B: PCR characterization of 6 weeks and 8 weeks old neurons. Cux1 signal is strongest in hPSC-N line and weaker in the induced hPSC-FN line. The uninduced hPSC+FN line shows no Cux1 signal. Ctip2 signal is strongest in the induced hPSC-FN line and is also strong in the uninduced hPSC-FN line. The hPSC-N line shows no detection of Ctip2 signal. Tbr1 signal is strongest in the uninduced hPSC-FN line. Weak signal is observable in the induced hPSC-FN line. N-line shows no signal. C: quantitative real-time PCR analyses of neurons. Induced hPSC-FN line shows more expression of Ctip2, Tle4 and Cux1 and less expression of Tbr1 compared to the uninduced hPSC-FN line. The hPSC-N line shows less expression of Tbr1, Ctip2 and Tle4 but more expression of Cux1. Performed together with Julia Ladewig.*

In contrast, hPSC-N derived neurons displayed only an increase for the upper layer marker *Cux 1* (0,7-fold). The layer VI marker *Tbr1* (0,6-fold) as well as the layer V markers *Ctip2* (0,6-fold) and *Tle4* (0,6-fold) showed a clear decrease (Figure 7 C).

Thus, the results of the quantitative real-time PCRs go in line with the previous analyses indicating that ectopic expression of *Fezf2* during the cortical differentiation of PSC led to the induction of a deep cortical layer identity.

Taken together these data illustrate that the ectopic expression of the transcription factors *Fezf2* and *Ngn2* lead to an increase in the expression of the cortical layer V marker *Ctip2* as well as to the corticofugal marker *Tle4* suggesting efficient direct induction of PSC into cortical layer 5 neurons. Interestingly, this data suggests that ectopic expression of the pro-neural transcription factor *Ngn2* exclusively converted PSC into neurons with an upper layer identity.

4.1.3 Transcription factor based direct conversion of human fibroblasts into corticofugal neurons

It could be shown that the ectopic expression of the pro-neural transcription factors *Ascl1* (A) and *Ngn2* (N) can convert human fibroblasts into functional induced neurons (iN; Ladewig *et al.*, 2012; Liu *et al.*, 2013; Vierbuchen *et al.*, 2010). When combining pro-neural TF with brain region specific transcription factors, iN with distinct regional identities could be generated (Pfisterer *et al.*, 2011; Son *et al.*, 2011). We wanted to explore whether combining *Ascl1* and *Ngn2* with the deep cortical layer specific transcription factor *Fezf2* is sufficient to directly convert human fibroblasts into corticofugal neurons.

4.1.3.1 Generation and validation of human fibroblasts carrying tet-on controllable *Ascl1*, *Ngn2* and *Fezf2* constructs

We transduced human skin fibroblasts derived from a healthy control individual (CTRL; for more details see Chapter 3.6) with a construct carrying the transcription factors *Ascl1* (A) and *Ngn2* (N) (CTRL-AN) exclusively or with the construct carrying the transcription factors *Ascl1*, *Ngn2* in combination with a construct carrying *Fezf2* (F) (CTRL-FAN; Figure 8 A). The transgenes, encoded on these constructs, were

doxycycline inducible. The production of the lentiviral particles and the transduction of fibroblasts are described in chapters 3.3 – 3.5. To verify whether the introduced transgenes are indeed expressed following doxycycline induction, PCR analyses using RNA isolated from transduced cells after four days of doxycycline treatment were performed. cDNAs were amplified using transgene specific primer pairs (listed in materials, chapter 2.5.6). Here we could confirm the expression of A and N in CTRL-FAN and CTRL-AN fibroblasts (Figure 8 A). As expected, expression of Fetz2 was only detectable in CTRL-FAN fibroblasts (Figure 8 A). These data confirmed that treatment with doxycycline leads to robust transgene induction in transduced fibroblast lines.

4.1.3.2 Direct conversion of human FAN-fibroblasts into corticofugal neurons

Highly efficient direct conversion of AN-fibroblasts into functional iNs could be shown by an implementation of synergistic SMAD pathway inhibition in combination with an inhibition of GSK3 β (Ladewig *et al.*, 2012). We applied this protocol to convert FAN- and AN-fibroblasts into iN cells and analyzed the derived cultures 28 days following doxycycline induction for the expression of neuronal marker by immunocytochemistry. CTRL-FAN-derived cells were found to give rise to β III-tubulin positive induced neurons (Figure 8 B). A fraction of the generated induced neurons co-expressed the neuronal marker Map2 (Figure 8 C). Expression of the cortical layer specific markers Tbr1 (layer VI) and Ctip2 (layer V) could also be detected (Figure 8 D, E).

To further verify the cellular identify of the CTRL-FAN-derived neurons, we performed qRT-PCR using specific primer pairs for genes, which were described to be specific for corticofugal neurons of the deep cortical layers including ER81, Clim1, Dkk3, Crym and Wnt7b (Ye *et al.*, 2015). Gene expression values of CTRL-FAN-derived iNs were analyzed in relation to the expression value of CTRL-AN-derived iNs. Here we found that the gene expression for ER81 ($1,64 \pm 0,2444$), Clim1 ($1,484 \pm 0,1668$) and Crym ($2,738 \pm 0,4659$) was significantly increased in CTRL-FAN-derived neurons. The expression of Dkk3 was enhanced in comparison to neurons derived from the CTRL-AN line, too ($2,191 \pm 0,1409$) (Figure 8 F). Only the Wnt7b expression was not as distinct as the other markers. This data indicate that ectopic expression of

the transcription factor Fezf2 (F) in combination with the expression of Ascl1 and Ngn2 leads to the generation of corticofugal-like iNs.

Corticofugal neurons cannot only be characterized by marker expression but also by their specific morphology. It was described that these neurons, which extend projections to the brain stem and the spinal chord, exhibit pyramidal cell bodies, (Molyneaux *et al.*, 2007).

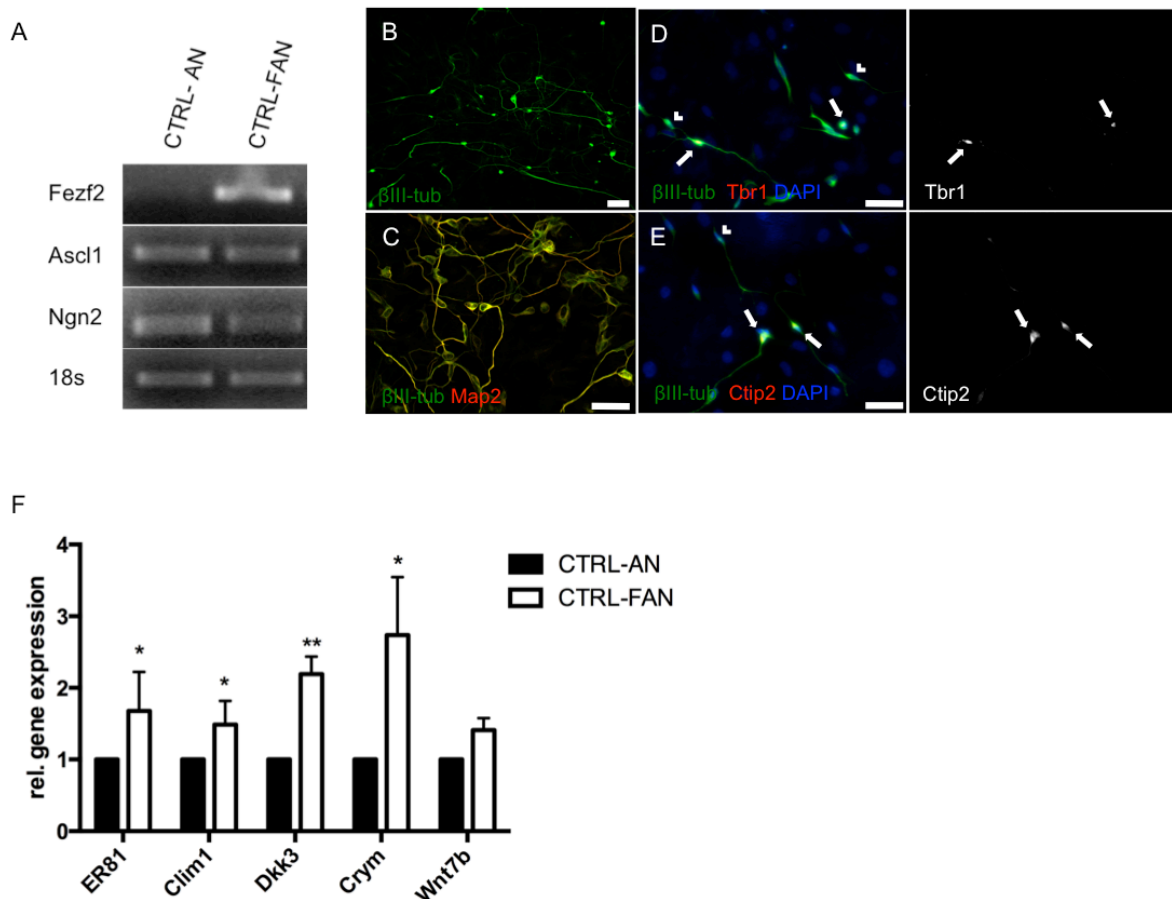


Figure 8 FAN-derived iNs show a corticofugal-like marker expression and morphology. A: Validation of transgenic gene expression after 4 days doxycycline treatment. CTRL-AN displays an expression signal for the transgenes Ascl1 and Ngn2, but lacking the expression of Fezf2. CTRL-FAN shows a transgenic expression for Fezf2, Ascl1 and Ngn2. B-E: Immunocytochemical analyses of 28 days old neurons for neuronal markers β III-tubulin (B), Map2 (C), Tbr1 (D) and Ctip2 (E). F: quantitative real time PCR analyses of 28 days old iNs. Deep layer markers are differentially expressed throughout neurons with (FAN) and without (AN) Fezf2 expression. Neurons derived from an FAN line show in most cases an elevated expression of the markers. Data presented as mean + SD. For statistical analysis an unpaired t-test was used ($n=3$; * $p \leq 0,05$; ** $p \leq 0,01$). Scale bars: 50 μ m.

In a first set of analyses we investigated the morphology of the cell bodies in our iN cultures 23 days following doxycycline induction. To visualize the iNs, we stained the cells for β III-tubulin. In our analysis we distinguished between cell bodies with a

pyramidal and a round morphology (Figure 9 A). Here we found a significant increase in the portion of pyramidal neurons in the CTRL-FAN-derived population ($37,52\% \pm 3,070$) compared to CTRL-AN-derived cells ($19,61\% \pm 3,405$; Figure 9 B).

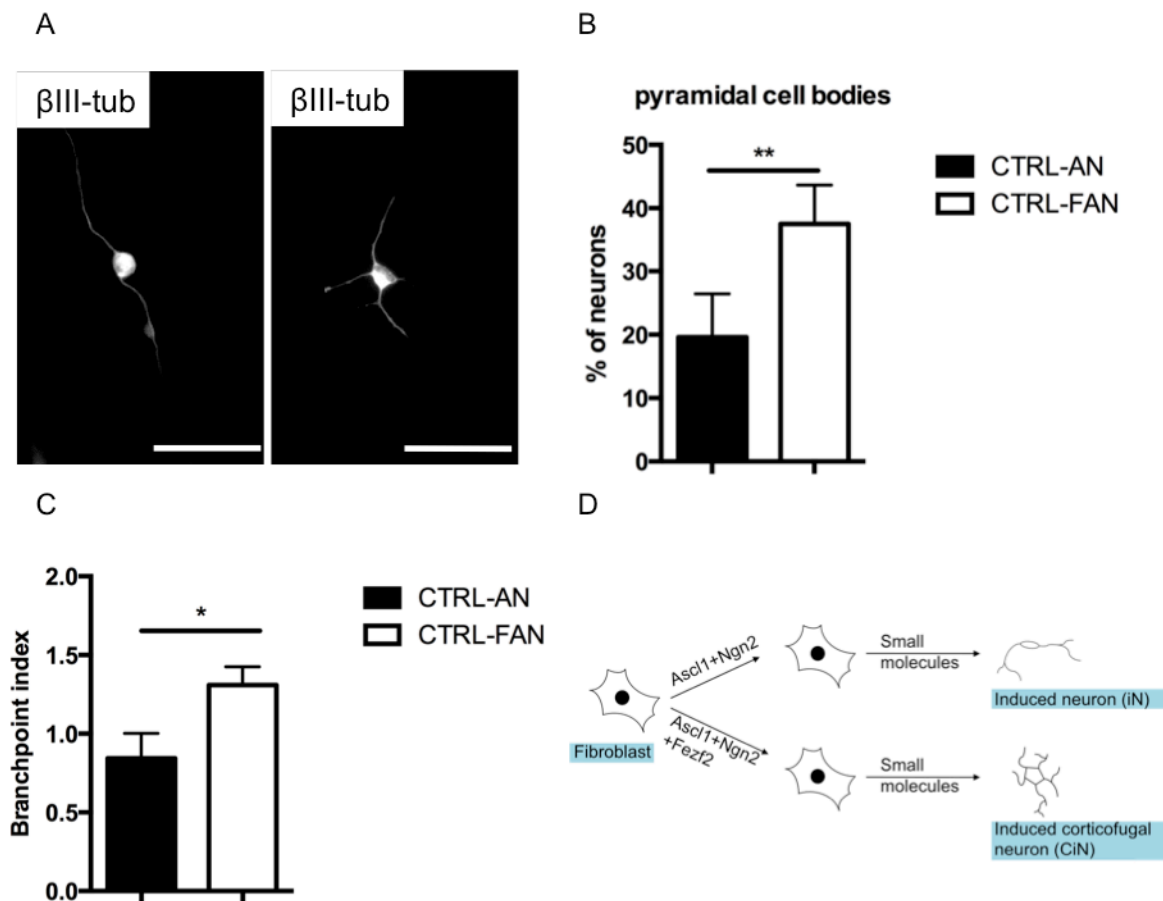


Figure 9 FAN-derived iNs show an increase in pyramidal cell bodies A: Representative images of a neuron with a round cell body (left) and a pyramidal shaped cell body (right). B: Quantification of cell bodies with a pyramidal cell body. 19,61% of CTRL-AN-derived iNs and 37,52 of CTRL-FAN-derived iNs had a pyramidal cell body. C: Quantification of differently shaped cell bodies of 23 days old neurons. Neurons derived from an FAN show more pyramidal cell bodies than AN neurons ($n=4$). D: Quantification of the branchpoint index for each neuronal population. CTRL-FAN-derived iNs shows an average of $1,309 \pm 0,06778$; CTRL-AN-derived iNs: $0,8438 \pm 0,09156$. Data presented as mean + SD. For statistical analysis an unpaired t-test was used ($n=3$; $*p \leq 0,05$). E: Schematic overview of the transcription factor based direct conversion. Introduction of *Fezf2* led to neurons with corticofugal-like phenotypes (CiNs). Data presented as mean + SD. For statistical analysis an unpaired t-test was used ($n=4$; $**p \leq 0,01$) Scale bars: $50\mu\text{m}$.

In a next set of experiments, we analyzed the morphology of the CTRL-FAN and CTRL-AN-derived iNs cells 28 days following doxycyline induction in more detail. To that end, we developed a branching assay. In this assay, each branchpoint of an iN was counted and the mean value was calculated. The branching assay revealed a significantly increase in branchpoints in CTRL-FAN-derived iNs compared to CTRL-

AN- derived iNs (Figure 9 C). These data indicate that introduction of the transcription factor *Fezf2* leads to a generation of iNs with a higher morphological complexity.

The morphology analyses together with the expression analyses suggest that ectopic expression of *Fezf2* in combination with *Ascl1* and *Ngn2* lead to the generation of iN cell with corticofugal-like phenotypes, which we will term in the following CiNs (Figure 9 D).

4.2 CiNs to model malformations of cortical development (CDM)

4.2.1 Generation of CiNs derived from Miller-Dieker-Syndrome patient fibroblasts

Fibroblasts from two patients (MDS1 and MDS2) suffering from Miller Dieker syndrome (MDS), a very severe form of lissencephaly (see chapter 2.4.4), were subjected to our developed CiN protocol. In brief, we used the construct carrying the transcription factors *Ascl1*, *Ngn2* as well as *Fezf2* for the transduction of MDS1- (MDS1-FAN) as well as MDS2-derived fibroblasts (MDS2-FAN).

The expression of the transgenes in each line was validated by PCR following 4 days of doxycycline treatment (Figure 10 A). Here we could confirm the efficient induction of the introduced transcription factors *Fezf2*, *Ascl1* and *Ngn2* upon doxycycline induction. Following the first validation step, MDS1-FAN and MDS2-FAN fibroblasts were subjected to the direct conversion protocol (see chapter 3.7). Cells were analyzed 28 days following transgene induction for the expression of pan-neuronal markers as well as markers specific for corticofugal neurons of the deep cortical layers including *ER81*, *Clim1*, *Dkk3*, *Crym* and *Wnt7b* (Ye *et al.*, 2015).

Immunocytochemistry revealed that cells derived from both MDS lines were found to give rise to β III-tubulin positive iNs (Figure 10 B). The expression of regional specific markers was analyzed via quantitative real-time PCR. Gene expression values of MDS1-iNs and MDS2-iNs were analyzed in relation to the expression value of the CTRL-AN-derived iNs. MDS2-iNs showed a significant increase in the expression of *ER81* ($6,799 \pm 1,472$), *Clim1* ($6,679 \pm 0,9157$), *Dkk3* ($52,71 \pm 6,590$), *Crym* ($4,311 \pm 2,214$) and *Wnt7b* ($4,378 \pm 0,2921$) in relation to the expression value of CTRL-AN-derived iNs line. MDS1-iNs displayed a significant upregulation in the expression of

ER81 ($1,460 \pm 0,2382$), *Clim1* ($2,177 \pm 0,5435$) and *Dkk3* ($4,914 \pm 0,3388$) (Figure 10 C). The expression levels of *Crym* ($2,824 \pm 1,657$) and *Wnt7b* ($3,664 \pm 1,025$) were increased in relation to the CTRL-AN-derived iNs, but the difference was not significant (Figure 10 B).

These data indicate that MDS1-FAN fibroblasts as well as MDS2-FAN fibroblasts could efficiently be converted into neurons with corticofugal like marker expression. Hence they are called in the following MDS-CiNs.

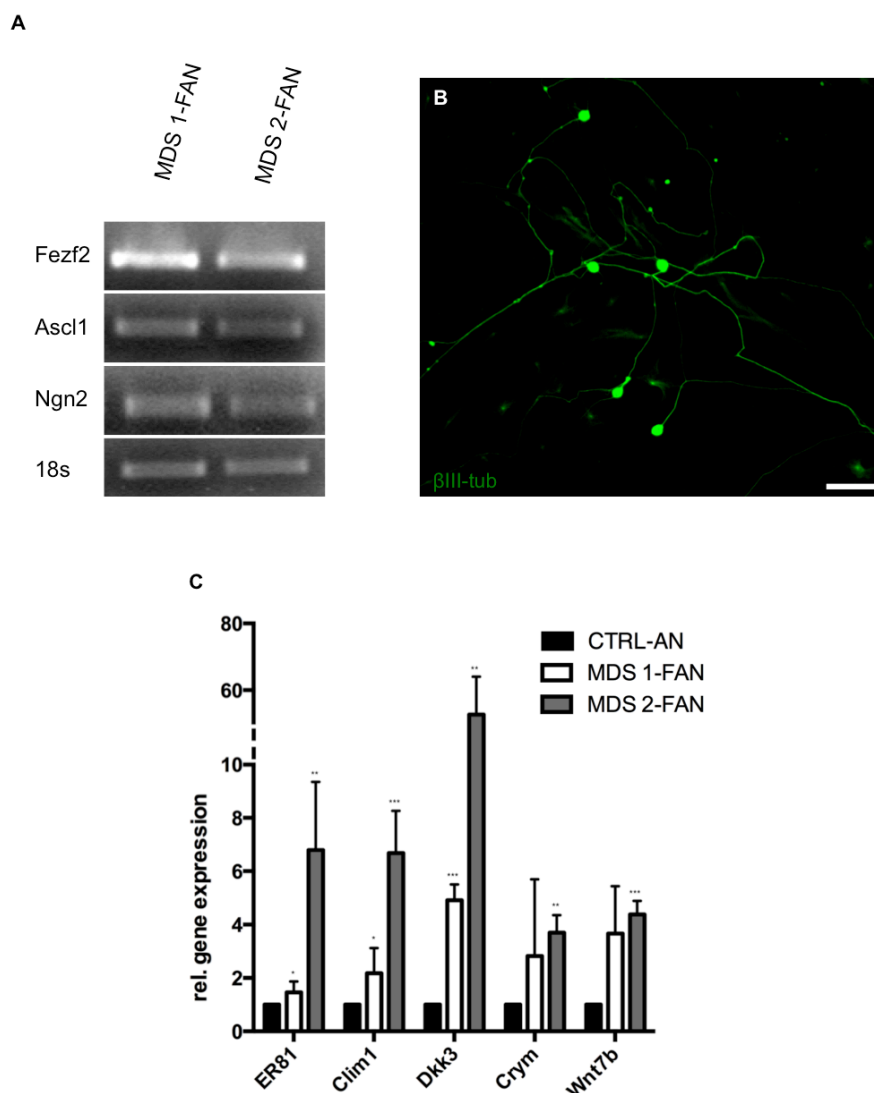


Figure 10 Characterization of Miller-Dieker-Syndrome patients-derived iNs. A: Validation of transgenic gene expression in MDS1-FAN and MDS2-FAN lines after 4 days of doxycycline induction. Both MDS-FAN lines show a transgenic expression for *Fezf2*, *Ascl1* and *Ngn2* B: Immunocytochemistry analysis of 28 days old iNs for neuronal markers β III-tubulin. C: Quantitative real time PCR analyses for the expression of regional specific markers in of 28 days old MDS1-iNs and MDS2-iNs in relation to CTRL-AN-derived iNs., MDS1-FAN-iNs and MDS2-iNs show an up-regulation to the analyzed markers in relation to CTRL-AN-derived iNs. Data presented as mean + SD. For statistical analysis an unpaired t-test was used ($n=3$; $*p \leq 0,05$; $**p \leq 0,01$; $***p \leq 0,001$).

4.2.2 Phenotypic characterization of MDS patient-derived CiNs

4.2.2.1 Characterization of lissencephaly patient-derived CiNs migration behavior

MDS represents a severe form of lissencephaly, which is characterized by a haploinsufficiency on chromosome 17p13.3 harbouring a lot of different genes including *PAFAH1B1* and *YWHAE*, which are encoding for Lis1 and 14.3.3 ϵ respectively (Cardoso *et al.*, 2003; Chong *et al.*, 1997; Dobyns *et al.*, 1983; Hattori *et al.*, 1994; Reiner *et al.*, 1993; Schwartz *et al.*, 1988). Both genes were described to interact with NDEL1 an intracellular multicomplex, which is important for the regulation of microtubule dynamics and the cytoplasmic dynein (Wynshaw-Boris 2007). Deletion of those genes leads to a misregulation of microtubule stability and dynein dysfunction, which was described to lead to impaired neuronal migration (Moon and Wynshaw-Boris 2013).

To investigate whether MDS-derived CiNs recapitulate the disease phenotype *in vitro*, we analyzed the migration behavior of CTRL-CiNs and MDS1-CiNs by performing a motility assay. To that end we used live cell-imaging microscopy to investigate neuronal movements in 35 days old CiNs over a time period of 2 days. After imaging, the motility was quantified by tracking single neurons over time (Figure 11 A + B).

Thereafter, the speed of each neuron was calculated. At the end, the speed of CTRL-derived CiNs was compared to the speed of MDS-derived CiNs. The tracking of the CiNs is visualized in Figure 8 A + B as colored lines. The CTRL-derived CiNs showed colored lines, which extend over the visual field, whereas the MDS-derived CiNs were moving more back and forth in a smaller area of the field (Figure 11 A+B). The dot blot displays every tracked CiN as a single dot. The higher the dots are located in this diagram, the more motile and faster were the neurons (Figure 11 C). The comparison of CTRL-derived CiNs and MDS-derived CiNs indicates that the MDS-derived CiNs appeared to be less motile (Figure 11 C). This result was reinforced by a quantification of the mean speed of the CiNs. This quantification revealed a significant difference between CTRL-derived CiNs and MDS-derived CiNs (Figure 11 D).

These data indicate that MDS-derived CiNs indeed feature the hallmark of an impaired migration and by that recapitulating the disease phenotype *in vitro*.

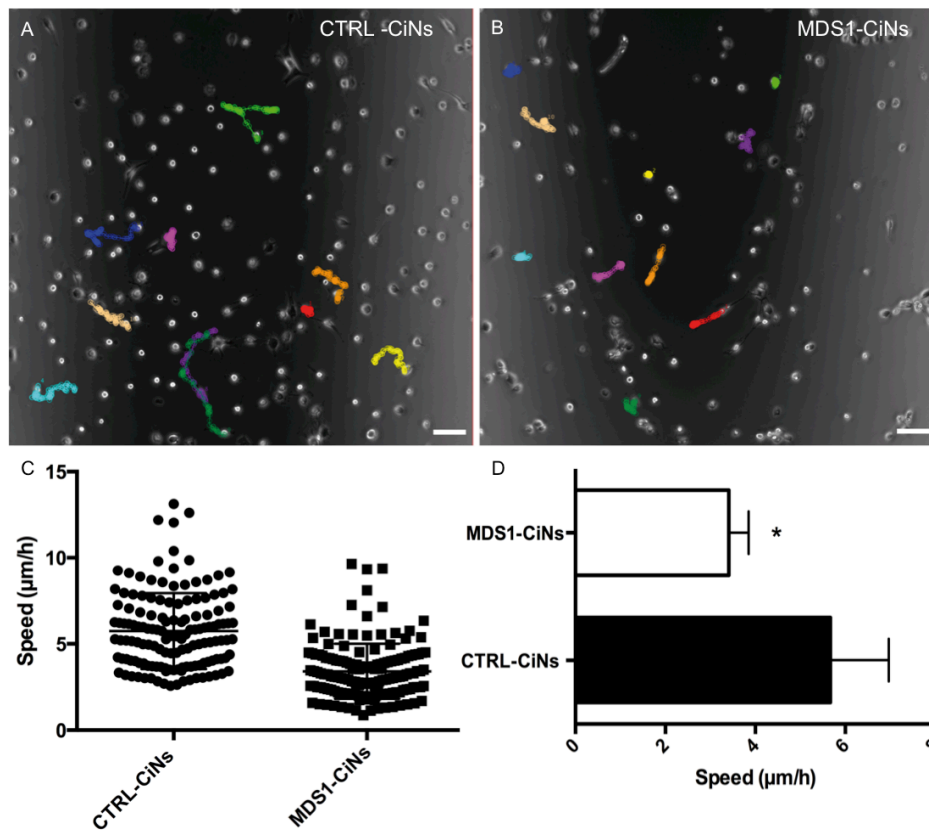


Figure 11 MDS-derived CiNs are less motile than CTRL-derived CiNs. A+B: Representative images of traced CTRL-FAN-CiNs (A) and MDS 1-FAN-CiNs (B). Every colored line is a traced CiN. C+D: Quantification of neuronal speed. Dot blot represents every single traced CiN (C; CTRL: n=143; MDS: n=155). Comparison of the mean speed reveals a greater speed in CTRL-FAN (D). Data presented as mean + SD. For statistical analysis an unpaired t-test was used (n=3; *p ≤ 0,05). Scale bar: 250µm.

4.2.2.2 Morphological phenotyping of MDS-derived CiNs

Corticofugal neurons of the deep cortical layers exhibit a neuronal subtype specific complex branching structure with a lot of branchpoints and they extend their projections subcerebral to the brain stem and spinal cord (Molyneaux *et al.*, 2007). Biopsy data from MDS-patients reveal immature neuronal morphologies with a reduced branching pattern and thereby a decrease in complexity (Sheen *et al.*, 2006). To identify whether MDS-derived CiNs recapitulate the *in vivo* observed phenotypic alterations *in vitro*, we applied the already developed branching assay to 23 days and 28 days old CTRL- and MDS-derived CiNs. More specifically, we

counted each branchpoint of at least 150 CiNs per condition and calculated the mean value termed branchpoint index. This branchpoint index thus represents the degree of complexity of either CTRL- or MDS-derived CiNs, respectively.

When subjecting 23 days old CTRL and MDS-derived CiNs to the branching assay, we found CiNs with a variety of different numbers of branchpoints ranging from no or one branchpoint to up to twelve branchpoints per CiN (Figure 12 A). While CTRL-CiNs displayed many processes with a lot of branchpoints, MDS1- as well as MDS2-CiNs show rather simple morphologies with either no process or one process without a branchpoint (Figure 12 B-D). When calculating the branchpoint index 23 d after doxycycline induction CTRL-CiNs showed a significant higher branchpoint index ($1,338 \pm 0,1083$) then the MDS-derived CiNs (MDS1-CiNs: $0,6041 \pm 0,03557$; MDS2-CiNs $0,3263 \pm 0,03786$; Figure 12 E).

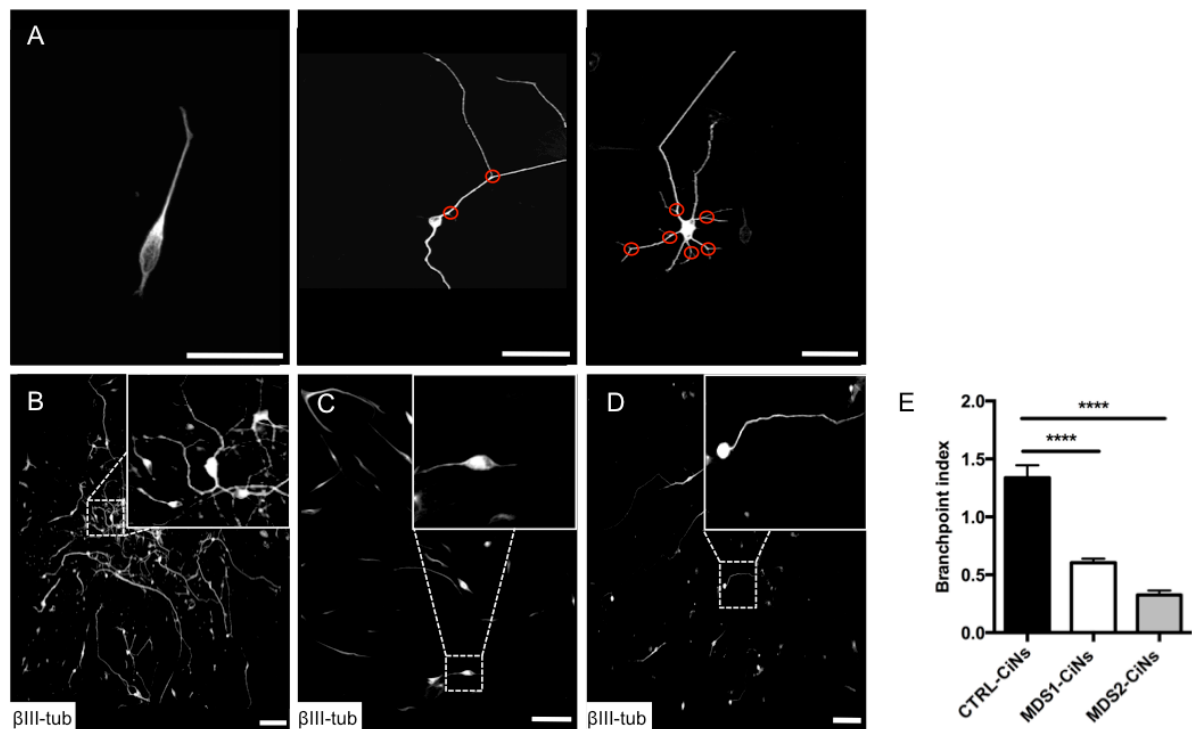


Figure 12 MDS-derived CiNs show morphological alterations after 23 days. A: Representative images of CiNs with no, two or six branchpoints (indicated by red circle). B-D: Immunofluorescence analyses of CTRL-CiNs (B), MDS1-CiNs (C) and MDS2-CiNs (D) stained for the pan-neuronal marker β III-tubulin. E: Quantification of the branchpoint index for each neuronal population. Data presented as mean + SD. For statistical analysis an unpaired t-test was used ($n=4$; **** $p \leq 0,0001$) Scale bars: A: $50\mu\text{m}$; B-E: $100\mu\text{m}$.

When performing the branching assay with CiNs 28 days after doxycycline induction, we found a similar result as described for 23 days old CiNs. In more detail, the CTRL-CiNs exhibited an increased amount of branches and seemed to be more

complex in comparison to MDS1-CiNs and MDS2-CiNs, which showed a lot of CiNs with no branchpoint or only one or two branchpoints (Figure 13 A-C). When investigating the branchpoint index, we got a result, which had the same distribution as our branching assay with 23 days old CiNs. The CTRL-CiNs represent a more complex population showing a score of $1,274 \pm 0,1185$ (Figure 13 D). The branchpoint score of MDS 1-CiNs was again significantly lower ($0,6323 \pm 0,03339$) compared to CTRL-derived CiNs. Also the score of MDS2-CiNs was significantly lower than the score of CTRL-CiNs, even though it was slightly increased ($0,4506 \pm 0,04759$) (Figure 13 D).

These data indicate that the MDS-derived CiNs develop less complex morphologies in comparison to CTRL-derived CiNs. By that our data recapitulate the morphological alterations described in MDS *in vivo* in an *in vitro* cell culture system.

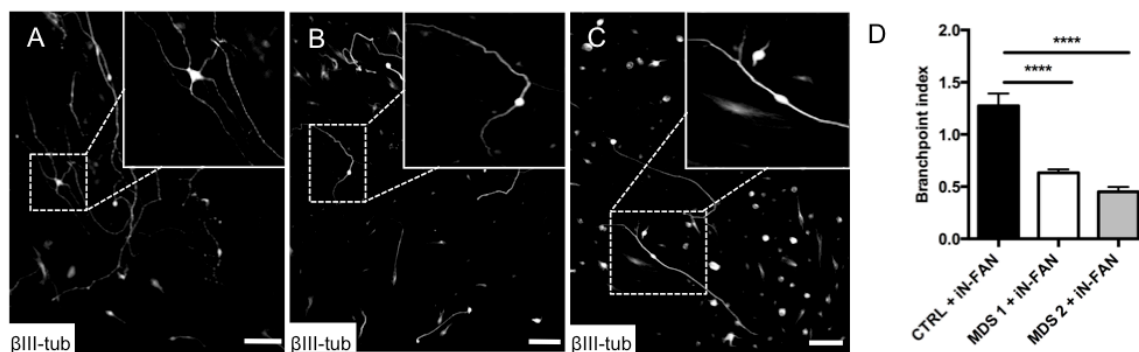


Figure 13 MDS-derived CiNs show morphological alterations after 28 days. A-C: Immunofluorescence analyses of CTRL-CiNs (A), MDS1-CiNs (B) and MDS2-CiNs (C) stained for the pan-neuronal marker β III-tubulin. D: Quantification of the branchpoint index for each neuronal population. Data presented as mean + SD. For statistical analysis an unpaired t-test was used ($n=4$; **** $p \leq 0,0001$) Scale bars: 100 μ m.

4.2.3 Mechanistic principles underlying the phenotypic changes in MDS-derived CiNs

MDS is linked with a haploinsufficiency on chromosome 17p13.3, harbouring a lot of different genes including *PAFAH1B1* and *YWHAE*, which are encoding for LIS1 and 14.3.3 ϵ respectively (Cardoso *et al.*, 2003; Chong *et al.*, 1997; Dobyns *et al.*, 1983; Hattori *et al.*, 1994; Reiner *et al.*, 1993; Schwartz *et al.*, 1988). Heterozygous deletions or mutations of *LIS1* were described to be the most usual cause of lissencephaly (Kato and Dobyns, 2003). The strong phenotype in MDS was shown to be due to the deletion of 14.3.3 in addition to LIS1, as 14.3.3 ϵ stabilizes the LIS1-

we found two microRNAs, namely microRNA-22 and microRNA-132, which were described to be involved in neuronal polarization, neuronal migration as well as neurite- and axonal outgrowth (Figure 14 B). (Hancock *et al.*, 2014; Vo *et al.*, 2005; Volvert *et al.*, 2014) (detailed description in chapter 1.1.2).

4.2.3.1 Generation of CiNs with a gain- and loss-of-function of microRNA-22 and microRNA-132

To experimentally test whether microRNA-22 and/ or microRNA-132 might have an impact on the disease specific phenotypic alterations observed in our *in vitro* model, we analyzed whether the phenotypic alterations are associated with an altered expression pattern of either microRNA-22 or microRNA-132.

In a first set of experiments, we confirmed reduced expression levels of microRNA-22 and microRNA-132 in CTRL-CiN and MDS1-CiNs by performing quantitative real-time PCRs. Here we could show that both microRNAs exhibit significantly reduced expression levels in MDS1-CiNs compared to CTRL-CiNs (Figure 15 A).

In a next set of experiments, we performed gain- and loss-of-function studies to investigate a possible contribution of both microRNAs to our identified phenotypic alterations in MDS-derived CiNs. For the gain-of-function experiments we used for each microRNA a vector where the gene expression could be induced by using doxycycline due to an integrated tet-on system. Furthermore, the constructs exhibited a puromycin resistance cassette¹. Following the generation of lentiviral particles (see chapter 3.4), we transduced MDS1-FAN fibroblasts with either microRNA-22 (MDS1-FAN-miR-22) or microRNA-132 (MDS1-FAN-miR-132). Thus it was possible to overexpress the microRNAs in MDS-derived CiNs, which possess usually a reduced expression.

The MDS1-FAN-miR-22 and MDS1-FAN-miR-132 fibroblasts were then subjected to our direct conversion protocol. 28 days following transgene induction, the expression level of microRNA22 and microRNA 132 was validated via quantitative real-time PCRs. To that end, MDS1-miR-22-CiNs were analyzed for microRNA-22 expression levels and MDS1-miR-132-CiNs for expression levels of microRNA-132. The expression levels of MDS1-miR-22-CiNs and MDS1-miR-132-CiNs were normalized

¹ Cloning was performed by Tom Lickiss

to the expression level of MDS1-CiNs. The expression analyses revealed that MDS1-miR22-CiNs exhibited a $2,077 \pm 0,5380$ -fold increase in microRNA-22 expression levels and MDS1-miR132-CiNs a $13,54 \pm 5,294$ -fold increase in expression levels of microRNA-132 (Figure 15 B+C). These data reveal that the transduction was successful and both microRNAs could be overexpressed in MDS cells.

For the loss-of-function experiments microRNA sponges can be used. These sponges are oligonucleotides, designed to target the expression of a specific microRNA. The sponges are located in the cytoplasm and bind complementary to the mature microRNA. By that, the binding of the microRNA to its target mRNA is prevented leading to the inactivation of the microRNA function and target mRNA translation. To use sponges for our loss-of-function experiments, we used a doxycycline inducible and puromycin selectable vector with coding sequences for either a microRNA-22 sponge, or a microRNA-132 sponge². Following the generation of lentiviral particles, we transduced CTRL-FAN fibroblasts with either the vector coding for the microRNA-22 sponge (CTRL-FAN-sp-22), or the vector coding for the microRNA-132 sponge (CTRL-FAN-sp-132). After transduction, the fibroblasts were converted along our direct conversion protocol for 28 days and both sponges were validated via quantitative real-time PCRs. We analyzed the microRNA-22 or microRNA-132 expression in CTRL-sp-22-CiNs and CTRL-sp-132-CiNs, respectively. Expression values of CTRL-sp-22-CiNs and CTRL-sp-132-CiNs were normalized to the expression value of CTRL-CiNs. Here we found that CTRL-sp-22-CiNs showed a significant decrease in microRNA-22 expression ($0,4833 \pm 0,07172$) and CTRL-sp-132-CiNs a significant decrease in microRNA-132 expression ($0,364 \pm 0,02963$) (Figure 15 D+E).

These data confirm that the transduction of the fibroblasts was successful and that the sponges functioned, by decreasing the respective microRNA expression in CTRL-CiNs.

² Cloning was performed by Tom Lickiss

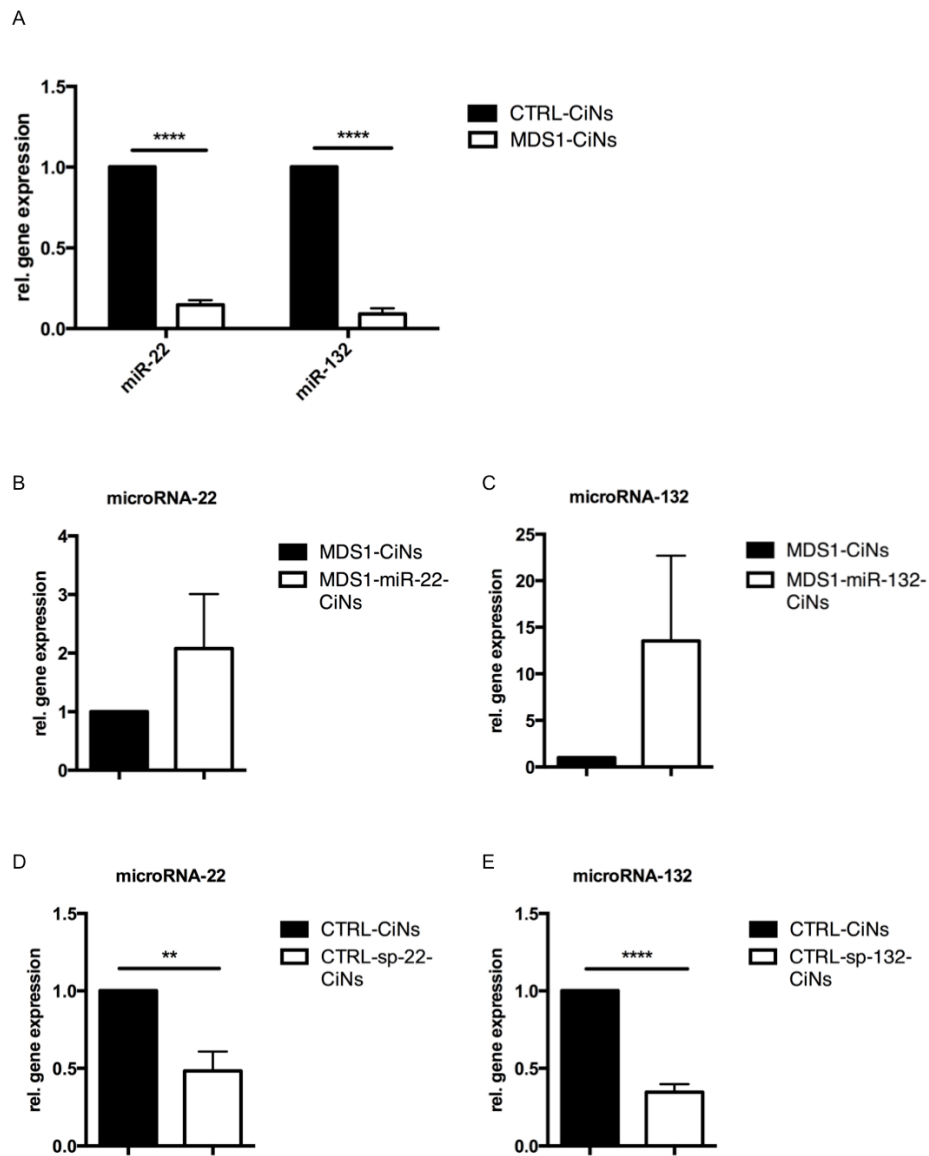


Figure 15 Validation of microRNA expression in CiNs derived from MDS- and transduced fibroblasts. A: Expression of microRNA-22 and microRNA-132 in CTRL-CiNs and MDS1-CiNs. Expression values of MDS1-CiNs were normalized to expression values of CTRL-CiNs. B: Expression of microRNA-22 in MDS1-CiNs and MDS1-miR-22-CiNs. C: Expression of microRNA-132 in MDS1-CiNs and MDS1-miR-132-CiNs. D: Expression of microRNA-22 in CTRL-CiNs and CTRL-sp-22-CiNs. E: Expression of microRNA-132 in CTRL-CiNs and CTRL-sp-132-CiNs. Expression values of CiNs with a microRNA overexpression were normalized to expression values of MDS-CiNs. Expression values of CiNs with a sponge were normalized to expression values of CTRL-CiNs. 28d old CiNs were used for all experiments. Data presented as mean + SD. For statistical analysis an unpaired t-test was used ($n=3$; $**p \leq 0,01$; $****p \leq 0,0001$).

4.2.3.2 microRNA-22 and microRNA-132 impact CiN migration

To decipher whether microRNA-22 and/or microRNA-132 contribute to the well-studied migration defect in MDS, we investigated migration in MDS1-CiNs versus

MDS1-miR-22-CiNs or MDS1-miR-132-CiNs. To that end, we performed motility assays as described in chapter 4.2.2.1. Following 35 days of doxycycline induction, CiNs of the three different lines were imaged and tracked. When analyzing the motility of the CiNs in a dot blot, we found that the majority of the MDS1-CiNs did not move faster than 5 $\mu\text{m}/\text{h}$. In comparison, the CiNs, which were derived from MDS1-FAN-miR-22 and MDS1-FAN-miR-132 fibroblasts, showed an increased speed (Figure 16 A). This difference in speed was reinforced by the calculation of the average speed of the three different CiN populations. MDS1-FAN-CiNs showed an average speed of $3.4 \pm 0,4415 \mu\text{m}/\text{h}$, whereas the MDS1-FAN-miR-22-CiNs and MDS1-FAN-miR-132-CiNs exhibited averages of $7.4 \pm 0,7191 \mu\text{m}/\text{h}$ and $6.7 \pm 0,09014 \mu\text{m}/\text{h}$, respectively (Figure 16 B).

These data indicate that there is a significant increase in neuronal speed, upon ectopic expression of microRNA-22 or microRNA-132 in MDS-CiNs. Interestingly, CiNs possessing an overexpression of either microRNA-22 or microRNA-132 exhibited even a higher neuronal speed than control-derived CiNs (see chapter 4.2.2.1)

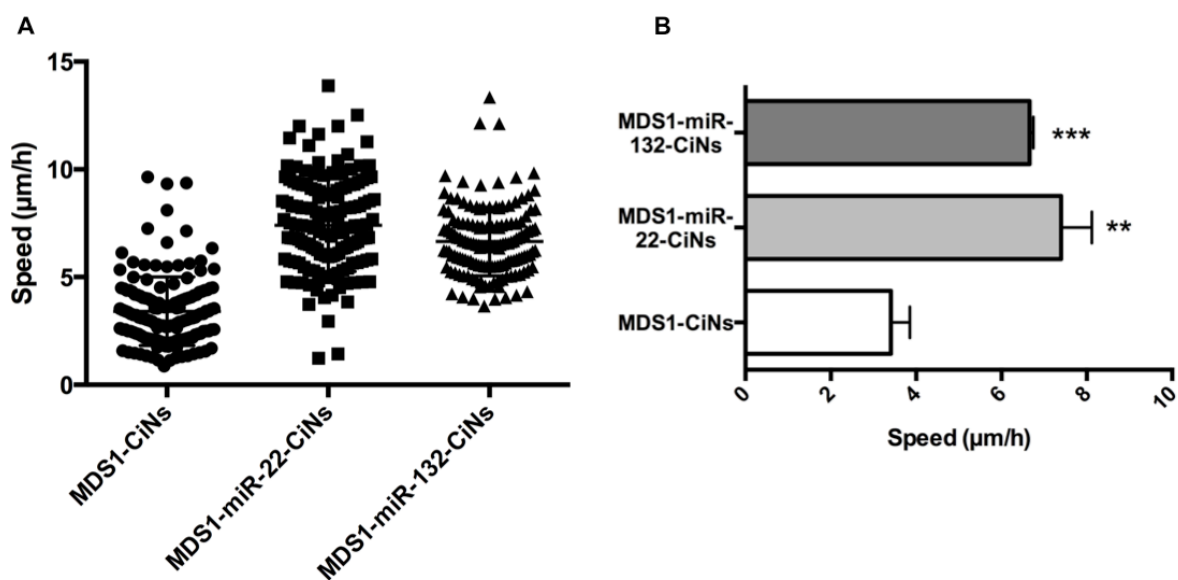


Figure 16 Migration aberrations in MDS-derived CiNs are correlated to microRNA expression. A+B: Quantification of neuronal speed. Dot blot represents every single traced neuron (A; MDS1-CiNs: $n=155$; MDS1-miR-22-CiNs: $n=150$; MDS1-miR-132-CiNs: $n=150$). Comparison of the mean speed revealed a greater speed CiNs with an overexpression of either microRNA-22, or microRNA-132. (B). Data presented as mean + SD. For statistical analysis an unpaired t-test was used ($n=3$; ** $p \leq 0,01$; *** $p \leq 0,001$).

4.2.3.3 MicroRNA-22 and microRNA-132 impact CiN morphology

To investigate whether the identified morphological alterations in MDS-derived CiNs are associated with the altered expression of microRNA-22 or microRNA-132, we analyzed the neuronal morphology of MDS1-miR-22-CiNs, MDS1-miR-132-CiNs, CTRL-sp-22-CiNs and CTRL-sp-132-CiNs as described in chapter 4.2.2.1. In brief, we performed a branching assay in the different CiN populations following 23 or 28 days of doxycycline induction.

In a first set of branching assays we analyzed if an ectopic expression of microRNA-22 and/or microRNA-132 in a MDS background might impact the CiN morphology. Therefore we compared our results with the morphology of MDS1-CiNs without an ectopic expression of one of the microRNAs.

When comparing the neuronal populations at day 23, we found that ectopic expression of microRNA-22 or microRNA-132 significantly increased the amount of branches (Figure 17 A-C). Compared to $0,6041 \pm 0,03557$ in MDS1-FAN-CiNs, MDS1-FAN-miR-22-CiNs showed a branchpoint index of $0,7594 \pm 0,02398$ (Figure 17 D). The branchpoint index of MDS1-FAN-miR-132-CiNs was $0,9645 \pm 0,1426$ (Figure 17 D).

Our analyses with 28 days old CiNs, which were derived from the three different fibroblast lines, showed a significantly increased amount of branches in regard to an ectopic expression of microRNA-22 or microRNA-132, too (Figure 17 E-G). At this time point, MDS-CiNs had a branchpoint index of $0,6323 \pm 0,03339$, compared to $0,7141 \pm 0,02042$ and $0,9942 \pm 0,09095$ for MDS1-miR-22-CiNs and MDS1-miR-132-CiNs, respectively (Figure 17 H). These data reveal that the ectopic expression of microRNA-22 or microRNA-132 significantly increased the amount of branches after 28 days. Taking the analyses of both time points together, our data indicate that the ectopic expression of microRNA-22 and microRNA-132 increases branching in MDS-derived CiNs.

To further delineate the impact of microRNA-22 and microRNA-132 on neuronal branching, we performed loss-of-function experiments. Therefore we investigated the neuronal branching in CTRL-CiNs, CTRL-sp-22-CiNs and CTRL-sp-132-CiNs. Here we found a significantly decreased branching in CTRL-sp-22-CiNs and CTRL-sp-132-CiNs compared to CTRL-CiNs after 23 days (Figure 18 A-C). CTRL-CiNs displayed a branchpoint index of $1,338 \pm 0,1083$, while the CTRL-sp-22-CiNs and

CTRL-sp-132-CiNs showed a branchpoint index of $0,4550 \pm 0,03784$ and $0,3005 \pm 0,05272$, respectively (Figure 18 D).

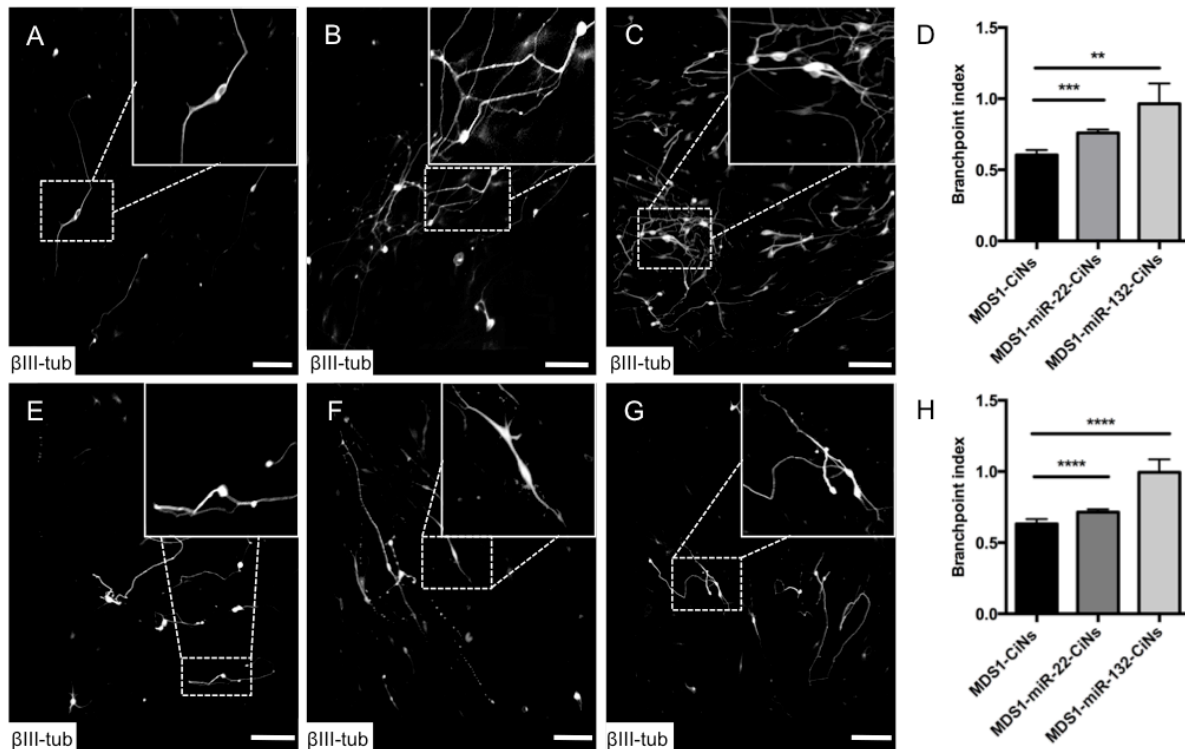


Figure 17 Ectopic expression of microRNA-22 and microRNA-132 leads to increased neuronal branching. A-C: Immunofluorescence analysis of MDS-derived CiNs (A) and CiNs with an ectopic expression of microRNA-22 (B) and microRNA-132 (C) stained for the pan neuronal marker β III-tubulin 23 days following transgene induction. D: Quantification of the branchpoint index for each neuronal population 23 days following transgene induction. E-G: Immunofluorescence analysis of MDS-derived CiNs (E) and CiNs with an ectopic expression of microRNA-22 (F) and microRNA-132 (G) stained for the pan neuronal marker β III-tubulin 28 days following transgene induction. H: Quantification of the branchpoint index for each neuronal population 28 days following transgene induction. Data presented as mean + SD. For statistical analysis an unpaired t-test was used ($n=4$; ** $p \leq 0,01$; *** $p \leq 0,001$; **** $p \leq 0,0001$). Scale bars: $100\mu\text{m}$.

Similarly, our loss-of-function experiments with 28 days old CiNs showed a significant decrease in neuronal branching in CTRL-sp-22-CiNs and CTRL-sp-132-CiNs compared to CTRL-CiNs (Figure 18 E-G). Here the branchpoint index of CTRL-CiNs was $1,274 \pm 0,1185$, whereas CTRL-sp-22-CiNs and CTRL-sp-132-CiNs exhibited a branchpoint index of $0,4897 \pm 0,1162$ and $0,4543 \pm 0,02340$, respectively (Figure 18 H).

Taken together these data show an association of the morphological alterations and the expression of the microRNAs. An ectopic expression of one of the microRNAs could improve the MDS branching pattern, whereupon the CiNs are still not as

complex as the control derived CiNs. In contrast a loss-of-function of one of the microRNAs shows a dramatic effect resulting in CiNs exhibiting even less branching compared to MDS-derived CiNs. Thereby this data confirms and strengthens our findings that microRNA-22 and microRNA-132 impact the neuronal morphology in MDS.

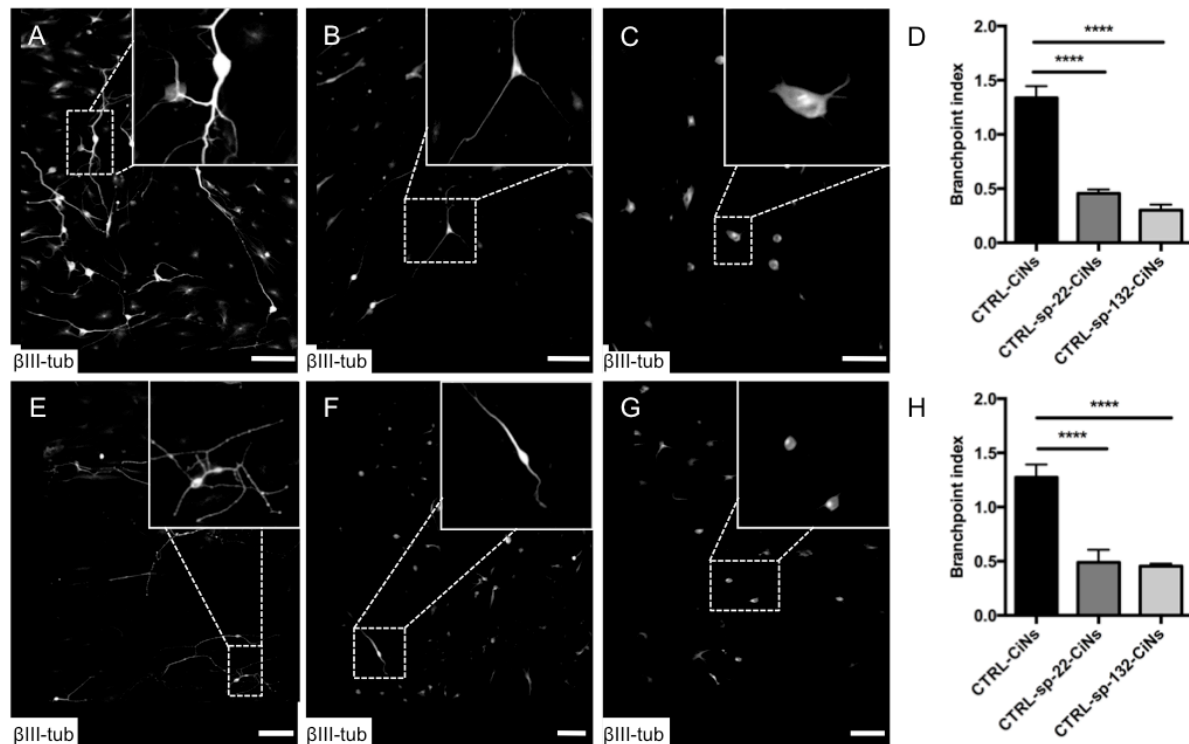


Figure 18 Loss-of-function of microRNA-22 and microRNA-132 leads to decreased neuronal branching. A-C: Immunofluorescence analysis of control-derived CiNs (A) and CiNs sponged for microRNA-22 (B) and microRNA-132 (C) stained for the pan neuronal marker β III-tubulin 23 days following transgene induction. D: Quantification of the branchpoint index for each neuronal population 23 days following transgene induction. E-G: Immunofluorescence analysis of control-derived CiNs (E) and CiNs sponged for microRNA-22 (F) and microRNA-132 (G) stained for the pan neuronal marker β III-tubulin 28 days following transgene induction. H: Quantification of the branchpoint index for each neuronal population 28 days following transgene induction. Data presented as mean + SD. For statistical analysis an unpaired *t*-test was used ($n=4$; ** $p \leq 0,01$; *** $p \leq 0,001$; **** $p \leq 0,0001$). Scale bars: 100 μ m.

4.2.4 microRNA-22 impacts CiN morphology via the PTEN / PDK1 signaling pathway

It was described that microRNA-22 plays a role in cortical development and neural cell differentiation (Bar *et al.*, 2010; Volvert *et al.*, 2014). This description is

strengthened by our results of the gain and loss-of-function experiments (see chapter 4.2.3.2) suggesting that microRNA-22, as well as microRNA-132, is involved in the development of the morphology of CiNs. To further analyze the role of microRNA-22 in cortical development, we set out to investigate how this microRNA is associated with neuronal development by searching for a possible regulation downstream of microRNA-22.

First we performed an unbiased screen for all possible target interactions of microRNA-22 using the miRTarBase (<http://mirtarbase.mbc.nctu.edu.tw>). After collecting 76 possible targets, we performed a gene ontology analysis by clustering the targets depending on their functional characteristics. Besides others, we found target genes described to regulate neuronal differentiation and the development of neuronal projections. In this context, we identified the phosphatase and tensin homologue PTEN as one of the microRNA-22 target genes. It was shown that the inhibition of PTEN promotes neurite outgrowth in an actin dependent manner (Adler *et al.*, 2006; Ning *et al.*, 2010). In addition, it was shown to play an important role by downregulating the Akt signaling pathway (Ohtake and Hayat 2015; Tsujita and Itoh 2015). It dephosphorylates and thereby represses PIP3 function, which results in a downregulation of all downstream members and in the end to a disruption of the Akt signaling pathway. The disruption of the Akt pathway leads to a decreased dephosphorylation of the microtubules, which is important for axonal outgrowth and thereby for the neuronal morphology (Kath *et al.*, 2018). Interestingly, PTEN was already described to be regulated by microRNA-22 in the context of cell cycle progression and cell survival (Bar *et al.*, 2010). Bar and colleagues also showed that PTEN expression is inhibited by microRNA-22 (Bar *et al.*, 2010).

To investigate whether microRNA-22 indeed targets PTEN in CiNs, we analyzed PTEN expression levels by performing quantitative real-time PCRs with CTRL-, CTRL-sp-22-, MDS1- and MDS1-miR-22-CiNs. When comparing the expression levels in CTRL-CiNs with the expression in CTRL-sp-22-CiNs, we found a 5-fold increase in CiNs expressing the sponge for microRNA-22 (Figure 19 B). When comparing expression levels of MDS1- and MDS1-miR-22-CiNs, we found a significant decrease of PTEN expression in CiNs with an ectopic expression of microRNA-22 (Figure 19 B). Thus our results indicate the described interaction between microRNA-22 and PTEN. In more detail our data show that a depletion of microRNA-22 led to an increased PTEN expression since it is not longer inhibited.

Vice versa ectopic expression led to a decreased expression in regard to a stronger inhibition of PTEN.

We further investigated downstream partners connected to the microRNA-22/PTEN signaling including the phosphoinositide-dependent kinase 1 (PDK1), which is important for the activation of Akt and is usually inhibited by PTEN. Here we found that ectopic expression of microRNA-22 resulted in a 5,5-fold increase of PDK1 expression (Figure 19 C). Vice versa a loss-of-function of microRNA-22 led to a significant decrease in PDK1 expression (Figure 19 C). These results go in line with our PTEN analyses. An ectopic expression of microRNA-22 results in a stronger inhibition of PTEN. Thereby the inhibition of PDK1 via PTEN is attenuated and the expression of PDK1 is increased. In contrast, loss-of-function of microRNA-22 diminishes the PTEN inhibition. PTEN is highly expressed, which inhibits and thereby reduces PDK1 expression.

Our results suggest that microRNA-22 impact CiN morphology via the PTEN/PDK1 signaling cascade. A loss of microRNA-22 expression leads to a disruption of the signaling pathway. Thereby the ratio of deetyrosinated microtubules is reduced, which disrupts axonal outgrowth and the morphology of the neurons is altered (Figure 19 A).

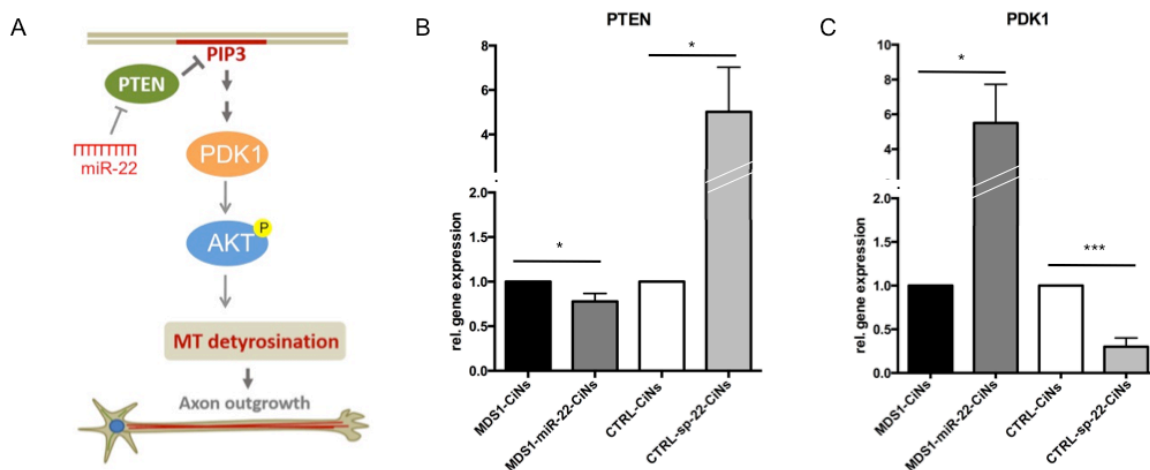


Figure 19 Involvement of microRNA-22 in PTEN/Akt-signaling. A: Schematic overview of our proposed involvement of microRNA-22 in PTEN/Akt-signaling (modified from Kath et al., 2018). B: Gene expression analyses of PTEN in case of a loss-of-function and an ectopic expression of microRNA-22. Gene expression of CTRL-sp-22-CiNs was normalized to the expression in CTRL-CiNs. Gene expression of MDS1-miR-22-CiNs was normalized to the expression in MDS1-CiNs C: Gene expression analyses of PDK1 in case of a loss-of-function and an ectopic expression of microRNA-22. Normalizations were similar to PTEN analyses. For gene expression analyses 28d old CiNs were used. Data presented as mean + SD. For statistical analyses an unpaired t-test was used. (n=3; *p ≤ 0,05; ***p ≤ 0,001).

4.2.5 microRNA-132 impacts CiN morphology via p250GAP / Rac1-signaling

MicroRNA-132 was described to be involved in cortical development, specifically in neurite growth and building the neurite morphology (Clovis *et al.*, 2012; Hancock *et al.*, 2014; Vo *et al.*, 2005). To further analyze the impact of microRNA-132 on neuronal development, we performed an unbiased screen for all possible target interactions of microRNA-132 using the miRTarBase. We found 175 possible targets, which we clustered by performing a gene ontology analysis. According to the analysis, p250GAP was suggested to be a direct target of microRNA-132. p250GAP is a member of the Rho family of small GTPases, which are known to be regulators of the actin cytoskeletal organization (Hall 1998; Nakazawa *et al.*, 2003; Nobes and Hall 1995; Ridley and Hall 1992; Van Aelst and D'Souza-Schorey 1997). In regard to microRNA-132, it was reported to be negatively regulated by microRNA-132 (Vo *et al.*, 2005).

To investigate whether microRNA-132 indeed targets p250GAP in CiNs, we analyzed p250GAP expression levels by performing quantitative real-time PCRs with CTRL-, CTRL-sp-132-, MDS1- and MDS1-miR-132-CiNs. By comparing the expression levels in CTRL-CiNs with the levels in CTRL-sp-132-CiNs, we found a 2,1-fold increase in CiNs expressing the sponge for microRNA-132 (Figure 20 B). Along this line, the comparison of expression levels in MDS1-CiNs and MDS1-miR-132-CiNs revealed a significant decrease of p250GAP expression in CiNs with an ectopic expression of microRNA-132 (Figure 20 B).

Thus, our data confirm the described interaction between microRNA-132 and p250GAP. The ectopic expression of microRNA-132 resulted in an increased inhibition of p250GAP, whereas a loss of microRNA-132 led to enhanced expression of p250GAP.

Next, we further investigated downstream partners connected to the microRNA-132/p250GAP signaling including the small GTPase Rac1. Rac1 is known to regulate actin dynamics through an activation of WAVE (Miki *et al.*, 1998; Stradal *et al.*, 2004). Subsequently WAVE interacts with the Arp2/3 complex, which is responsible for the initiation of actin filament branches on existing filaments (Pilo Boyl *et al.*, 2007; reviewed by Pollard 2007; Takenawa and Miki, 2001). Usually it is inhibited by p250GAP.

Here we found that ectopic expression of microRNA-132 resulted in a 6-fold increase of Rac1 expression (Figure 20 C). On the other hand a loss-of-function of microRNA-132 led to a significant decrease in Rac1 expression (Figure 20 C). These results go in line with our p250GAP analyses. An ectopic expression of microRNA-132 leads to a stronger inhibition of p250GAP. Thereby the inhibition of Rac1 through p250GAP is attenuated and the expression of Rac1 is increased. Contrary, loss-of-function of microRNA-132 diminishes the p250GAP inhibition. p250GAP is highly expressed, which inhibits and thereby reduces Rac1 expression.

Our results suggest that microRNA-132 impact CiN morphology via the p250GAP/Rac1 signaling cascade. A loss of microRNA-132 would lead to a disruption of Rac1 signaling. Thereby the downstream members WAVE and Arp2/3 would not be activated and the building of new actin branches would be disrupted resulting in a neuronal morphology with less branches (Figure 20 A).

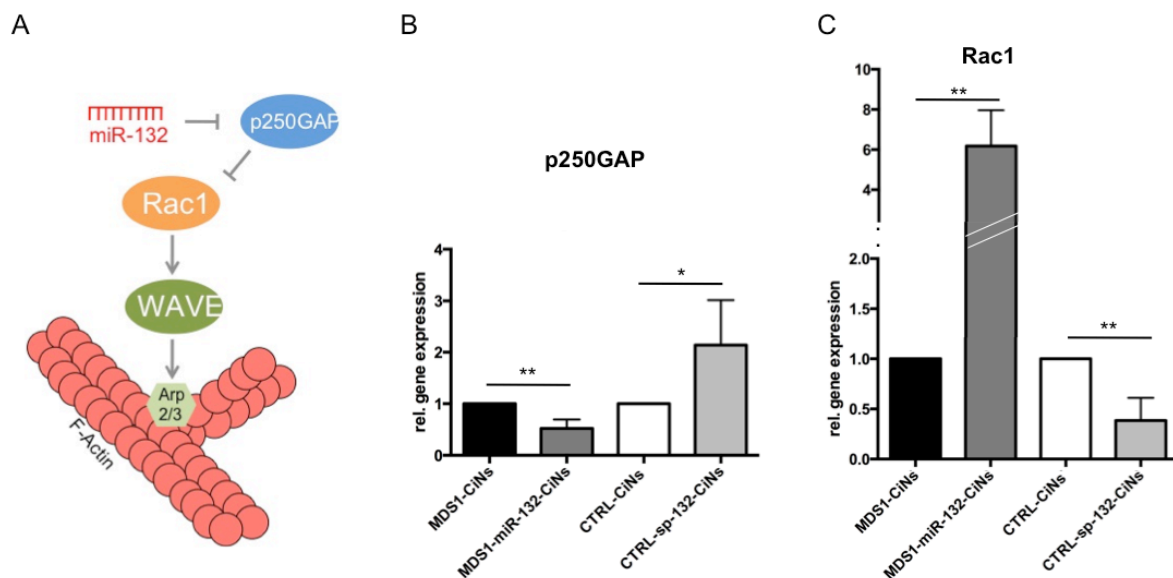


Figure 20 Involvement of microRNA-132 in Rac1-signaling. A: Schematic overview of our proposed regulation of F-actin through microRNA-132. B: Gene expression analyses of p250GAP in case of a loss-of-function and an ectopic expression of microRNA-132. Gene expression CTRL-sp-132-CiNs was normalized to the expression CTRL-CiNs. Gene expression of MDS-miR-132-CiNs was normalized to the expression in MDS1-CiNs. C: Gene expression analyses of Rac1 in case of a loss-of-function and an ectopic expression of microRNA-132. Normalizations were similar to p250GAP analyses. For gene expression analyses 28d old CiNs were used. Data presented as mean + SD. For statistical analyses an unpaired t-test was used ($n=3$; $*p \leq 0,05$; $**p \leq 0,01$; $***p \leq 0,001$).

5. Discussion

A fundamental prerequisite for CNS disease modeling *in vitro* is the generation of human patient specific cell populations. In order to obtain this, tools and techniques for the production of pure subtype specific cell types need to be developed. Thereby disease associated cell types could be generated and analyzed for modeling of the respective disease.

In the presented study, cortical layer specific neurons, namely corticofugal neurons, were induced by combining the directed differentiation of PSCs with the transcription factor-based conversion. Furthermore, a transcription factor-based direct programming approach has been developed for the generation of corticofugal neurons from human fibroblasts of a healthy control and two patients suffering from the most severe form of lissencephaly, the Miller-Dieker Syndrome.

5.1 Fezf2 induces deep cortical layer identity

5.1.1 Differentiation of hiPSCs into human cortical layer specific neurons

Several transcription factors, alone or combined, have been so far described as candidates for the directed differentiation of PSCs toward specific cell types. For instance, the combination of *Ascl1* and *Dlx2* results in the generation of GABAergic neurons, whereas the combination of *Ascl1*, *Nurr1* and *Lmx1a* leads to dopaminergic neurons (Sun *et al.*, 2016; Yang *et al.*, 2017). Excitatory neurons, such as cortical neurons, were described to be successfully generated by *Ascl1*, *Ngn2* or *NeuroD1* (Chanda *et al.*, 2014; Thoma *et al.*, 2012; Zhang *et al.*, 2013). Since we wanted to specifically generate corticofugal neurons, we included the TF *Fezf2* to our combination of *Ascl1* and *Ngn2*. We decided to use *Fezf2*, because substantial work had been conducted especially in the mouse model showing that *Fezf2* can be an important regulator for the instruction of corticofugal identity. Loss of *Fezf2* in null mutant mice led to a failure in the fate specification of subcerebral neurons, a subclass of corticofugal neurons (Molyneaux *et al.*, 2005), whereas ectopic expression of *Fezf2* in neural progenitors of the mouse brain are able to give rise to any major type of projection neuron within the layer V of the mature mouse motor

cortex (Rouaux and Arlotta, 2010; Tantirigama *et al.*, 2016). Furthermore, *in vivo* experiments in mice showed that ectopic Fezf2 expression in postmitotic neurons, like callosal neurons, has the power to convert them into corticofugal neurons (Rouaux and Arlotta, 2013). In this study we show that Fezf2 expression can direct the differentiation of human PSCs to the induction of corticofugal neurons *in vitro*. During the development of the human neocortex, the different neuronal subtypes are sequentially differentiated according to an inside-out manner starting with the early born neurons of the layer VI following the layers V-II (Rakic *et al.*, 2009). This sequential differentiation was abolished in our hiPSC differentiation with Fezf2. The dominant expression of Ctip2 and Tle4 in the neurons indicates a corticofugal identity since Ctip2 is known to be specific for corticofugal neurons of layer V and Tle4 was reported to be specifically expressed in layer V neurons (Molyneaux *et al.*, 2007). Moreover, neuronal markers for different layers than layer V showed no appreciable expression. Neither Tbr1, which is sequentially expressed corticothalamic neurons within layer VI (Molyneaux *et al.*, 2007), nor the upper layer marker Cux1 were well expressed in the neuronal population. These results go in line with previous studies in mice, which suggested that Fezf2 is critical for the development of deep-layer cortical neurons, particularly for the development of corticospinal motor neurons, which belong to the group of subcerebral projection neurons in layer V (Chen *et al.*, 2005; Molyneaux *et al.*, 2005; Molyneaux *et al.*, 2007; Rouaux and Arlotta, 2010). The essential role of Fezf2 was emphasized by showing that the transgenic expression of Ngn2 alone resulted in the generation of a neuronal subpopulation, too. But here, callosal neurons of the upper cortical layer instead of corticofugal neurons were predominantly generated, as it was previously reported (Zhang *et al.*, 2013). In addition to the performed experiments, the induced neurons could be further characterized in regard to their identity by performing RNA sequencing (RNA-seq) to analyze their transcriptome. In contrast to qPCRs, it is more robust and it gives information about the expression of an enormous number of genes each time. There, the neurons should show an enhanced expression for distinct corticofugal marker in response to transgenic Fezf2 expression. Another important characterization would be an analysis of the neuronal morphology. Corticofugal neurons are described to have a more elaborated dendritic tree than other neuronal types. Therefore the complexity of the different neuronal populations

could be quantified. Then, *Fezf2*-derived neurons should show a more complex dendritic tree.

Nevertheless, these findings emphasize the successful induction of cortical layer specific neurons suggesting that *Fezf2* acts as a master regulator for the induction of corticofugal identity in hiPSC-derived neurons.

5.1.2 Direct conversion of human fibroblasts into human cortical layer specific neurons

To accelerate the efficient generation of corticofugal neurons, we set out to directly convert human fibroblasts by using the transcription factor based direct conversion.

For a rapid conversion of human fibroblasts to corticofugal neurons, we used the transcription factors *Fezf2* and *Ngn2* again. Furthermore, we added with *Ascl1* another transcription factor to the previous combination, since *Ascl1* expression was previously shown to be important for the direct conversion of fibroblasts (Ladewig *et al.*, 2012; Pang *et al.*, 2011; Vierbuchen *et al.*, 2010). In combination with the three transcription factors, we included small molecules to increase the conversion efficiency (adopted from Ladewig *et al.*, 2012).

By applying the transcription factors in combination with small molecules, we demonstrate the successful direct conversion of human fibroblasts to corticofugal neurons in response to transgenic *Fezf2* expression. Again, it is not proven whether the directly induced neurons are fully functional. Also here, further experiments have to be performed by analyzing the electrophysiological properties of the directly induced neurons. Furthermore, single cell RNA sequencing analyses would give additional information about the conversion by showing that fibroblast-specific genes are downregulated and neuronal genes are upregulated.

Similarly to our iPSC studies, the directly induced *Fezf2*-derived neurons showed a *Ctip2* expression indicating a corticofugal fate (Rouaux and Arlotta, 2013). In contrast to our results with hiPSC-derived neurons, this generated neuronal population showed also *Tbr1* positive corticothalamic neurons of layer VI, although transgenic *Fezf2* was induced. An explanation for this could be that the transgenic *Fezf2* was not expressed in sporadic cells after culturing them for several passages, since we exhibited a predominant generation of corticothalamic neurons by differentiating hiPSCs without transgenic *Fezf2* expression. Moreover, induced neurons showed a

significant upregulation of genes, which were reported to be specific for corticofugal neurons, upon transgenic *Fezf2* expression (Ye *et al.*, 2015). Additionally to these findings, morphological analyses of the cell soma revealed a phenotype, which is characteristic for corticofugal neurons. The induction of transgenic *Fezf2* led to an increase in neurons with a pyramidal shaped cell soma. These neurons are referred as pyramidal neurons. Large pyramidal cell somas are characteristic for corticofugal neurons from layer V of the neocortex (Molyneaux *et al.*, 2007). Besides this, more experiments could be done to further characterize the directly induced neurons. One possibility could be to perform whole cell patch clamp recordings. There, *Fezf2*-derived neurons should show an increased membrane time constant and a decreased membrane resistance due to the larger cell body and more complex dendritic tree of corticofugal neurons (Zuccotti *et al.*, 2014). Again, a promising experiment would be a whole transcriptome RNA sequencing to emphasize the corticofugal-like signature in gene expression.

Taking everything into account, we demonstrate with these findings that it is also possible to generate corticofugal neurons directly from human fibroblasts by using the combination of the TFs *Ascl1*, *Ngn2* and *Fezf2*.

5.1.3 Direct conversion of somatic cells versus differentiation of PSCs

As demonstrated, the transcription factor based direct conversion, as well as the differentiation of PSCs were feasible to induce corticofugal neurons.

A clear advantage of directly converting somatic cell is the short generation time. Mature and functional neurons could be induced from fibroblasts within two weeks, whereas the differentiation of PSCs is a labour-intensive process (Vierbuchen *et al.*, 2010). The donor cells have to be reprogrammed, before they are in a second step differentiated into the desired cell type. In contrast, the direct conversion technique consists of just a single-step and thereby accelerates the generation of mature cell types.

In return, using PSCs has the benefit of an unlimited expandability while maintaining a pluripotent state. It is also possible to expand somatic cells, like fibroblasts, *in vitro*, but the cells often change their epigenetic signature and lose their differentiation capability. On the other side, the extensive propagation of PSCs increases the risk of various kinds of mutations, like point mutations, copy number variations or karyotypic

abnormalities (Bai *et al.*, 2015; Garitaonandia *et al.*, 2015; Maitra *et al.*, 2005; Mitalipova *et al.*, 2005; Sebastiano *et al.*, 2014; Ronen and Benvenisty, 2012; Weissbein *et al.*, 2014). Directly transdifferentiated cells were found to have a greater karyotypic stability than PSC-derived cells (Weissbein *et al.*, 2014).

When it comes to disease modeling, the speed of the direct conversion technique is a big plus. Thereby target cells of a great cohort of patients can be efficiently generated providing a great sample size for analyses. Because of that, this technique could be also beneficial for pharmacological screens. In addition, it improves especially the modeling of neurodegenerative diseases, because directly induced cells retain the age signature of the starter cells (Mertens *et al.*, 2015).

As one part of this work we demonstrate the capability of using directly converted neurons to model a cortical malformation as a prove-of-principle.

In regard to disease modeling, differentiating PSCs holds the advantage that it is possible to genetically engineer their genome in an efficient manner due to the already discussed great expandability (Li *et al.*, 2014). Thereby disease-associated mutations can be introduced into healthy control cells or rescued in patient cells.

On this account transplantation studies demonstrated great promises for the regenerative medicine and possible cell replacement therapies. Espuny-Camacho and colleagues demonstrated that pyramidal neurons derived from human PSCs can integrate into a mouse brain in vivo (Espuny-Camacho *et al.*, 2013). More recently it was shown that human iPS-derived dopaminergic progenitor cells survived and functioned as midbrain dopaminergic neurons in a primate model of Parkinsons Disease (Kikuchi *et al.*, 2017). With respect to their high proliferative capacity, transplantation of PSC-derived cell populations can be dangerous. Undifferentiated cells inside the population could be transplanted, which could result in the formation of tumors. With regard to this, prolonged differentiation and purification was attempted to reduce this risk (Doi *et al.*, 2014).

In contrast, direct conversion of somatic cells to another somatic cell avoids the risk of tumor formation, because only postmitotic cells are used. Additionally no oncogenes are being used, since the lack of reprogramming.

5.2 Transcription factor based direct conversion as a powerful tool to study cortical development malformations

These discussed techniques offer great opportunities to generate tissue specific cells, which were so far not easily accessible in human, and utilize them for analyses. One of those difficult accessible cell types are cortical neurons. These cells are part of the neocortex in the human brain, which is arranged with an incomparable complexity. Within this work we could show that a specific neuronal subtype of the neocortex, namely corticofugal neurons, can be generated from human fibroblasts.

Within the last years different studies demonstrated how directly induced neurons could be applied to model different neurological diseases. For instance they were used to study neurodegenerative diseases like amyotrophic lateral sclerosis (ALS), frontotemporal dementia (FTD) or Parkinson's disease (Caiazzo *et al.*, 2011; Kim *et al.*, 2011; Son *et al.*, 2011; Wen *et al.*, 2014). Furthermore chemical induced neurons were utilized to explore new insights into Alzheimer's disease (Hu *et al.*, 2015).

In this work we wanted to investigate whether the induced corticofugal neurons can be used to model the most severe form of the neurodevelopmental disorder lissencephaly, namely Miller-Dieker Syndrome (MDS), by applying the transcription factor based direct conversion protocol to fibroblasts derived from MDS patients.

Lissencephaly is associated with a group of cortical development malformations. Often described as a migrational disorder, the cortical plate of a MDS brain is disorganized and consists of only four instead of six layers (Sheen *et al.*, 2006). The regionalization of the neurons is consequently disrupted and early born neurons, which normally populate the deep layers of the cortical plate, are suddenly located within the upper layers (Sheen *et al.*, 2006).

In this work we could successfully show that corticofugal neurons of the deep cortical layers can be induced by directly converting fibroblasts, which were derived from MDS patients.

Despite the fact that there could be done more validations like immunocytochemical and morphological analyses, as they were performed for the characterization of control INs, the corticofugal identity of patient-derived iNs is strongly pointed out by gene expression analyses. The patient-derived iNs shared the same upregulation of the five specific corticofugal genes as we saw with iNs derived from a healthy control,

concluding that our direct conversion protocol can be successfully applied to MDS patient cells, too (Ye *et al.*, 2015).

Similarly to the characterization of control-derived iNs, we did not analyze iNs in regard to their functionality. Therefore further experiments have to be performed by analyzing the electrophysiological properties of the patient-derived iNs.

Nevertheless these data indicate the specific induction of corticofugal neurons, generated for the first time by the direct conversion of MDS-derived fibroblasts.

5.3 Impaired neuronal morphology and behavior in MDS

As we were able to generate corticofugal neurons from MDS patient-derived fibroblasts, we next used the patient specific CiNs for analyses.

Excessive studies in mouse models and postmortem human brains led to the predominant model that MDS and less severe lissencephaly variants are caused by a defect in neuronal migration (Gambello *et al.*, 2003; Hirotsune *et al.*, 1998; Kato and Dobyns 2003; Toyo-oka *et al.*, 2003; Youn *et al.*, 2009). Especially *LIS1* emerged as a key factor concerning neuronal migration. Reduced levels of *LIS1* were reported to lead to defects in neuronal migration in mice (Hirotsune *et al.*, 1998; Smith *et al.*, 2000).

To validate the functionality of our *in vitro* system, the migration of MDS patient-derived CiNs was analyzed.

Conducting time-lapse studies we could recapitulate this migration defect in MDS patient-derived CiNs. In comparison to control-derived CiNs, CiNs from patients showed a significant decrease in motility. Although our assay does not give information about a directed migration of the CiNs, the motility of a neuron provides important information about the migration capacity of a neuronal population. To analyze the directed migration of the CiNs, additional chemotaxis assays have to be conducted by applying a chemoattractant inside a Boyd- or Dunn Chamber.

These data showed that our *in vitro* system is applicable to study the lissencephaly pathogenesis. Thus it provides the opportunity to study the disease pathogenesis in a human relevant cellular and genetic context, whereas studies in mice may not appropriately analyze certain aspects during cortical development, since the mouse brain is naturally lissencephalic.

While the neuronal migration defect (Hirotsune *et al.*, 1998; Smith *et al.*, 2000) and the resulting disrupted cortical layering (Sheen *et al.*, 2006; Saito *et al.*, 2011) was extensively studied, the morphology of the postmitotic neurons of lissencephalic brains remained less explored. In this regard, Sheen and colleagues reported that the neurons appear immature by analyzing brain tissue sections of MDS patients (Sheen *et al.*, 2006). Interestingly, we observed significant differences in the complexity of neuronal branching between control- and patient-derived CiNs. Control-derived CiNs showed a distinctive branching along their neurites, whereas the branching of patient-derived neurons was severely reduced. In many cases, the branches were even totally absent. This significant decrease of neuronal complexity in patient-derived neurons was not abolished over time, since it is demonstrated at two different time points.

To strengthen this data, the branching of CiNs could be analyzed in more detail, e.g. by specifying primary and secondary branches. Also interesting would be to see, whether there is a difference in the axon length between control- and patient-derived CiNs.

However this observation is strong evidence for a failed cytoskeletal development in patient-derived CiNs. Consequently, the development of dendrite and the axon is impaired. For the formation of axons and dendrites the neurite extension is the first essential step (Sainath and Gallo 2015). The neurite is formed by a regulation of the cytoskeleton within the neuronal cell body to produce actin rich filopodia. Reorganization of the actin cytoskeleton drives this morphological change (Sainath and Gallo 2015). After the formation of the neurites, dendrites and axons evolve, which are important for the transport of afferent and efferent signals. The arrangement of the dendrites has great impact for the processing of neural information (London and Häusser 2005; Spruston 2008). The dendritic branching pattern varies with the neuronal type. Thereby it influences the way in which a neuron receives the information (Stuart *et al.*, 2000). This means that the complexity of a neuron is correlated to the particular assignment of it (Elston 2000; Poirazi and Mel 2001). Thus the disrupted development of the axon and dendrites in MDS patient-derived CiNs leads to a reduction in signal transduction and processing within the neuronal network.

Collectively, we suggest that the decrease in neuronal complexity is, in addition to the disorganization of the cortical plate, crucial for the described mental retardation in MDS.

5.4 microRNAs: important regulators besides LIS1 and YWHAE

All cases of MDS are known to be connected with a haploinsufficiency on chromosome 17p13.3., involving 2116 genes, which are consequently deleted on one of the chromosome pair (Schwartz *et al.* 1988; Dobyns *et al.* 1991; Ledbetter *et al.* 1992). This leads to a reduced gene expression of this huge number of genes in MDS patients.

In the past, the lissencephaly pathology was extensively investigated by using knockouts in rodents. Thereby *LIS1* and *YWHAE* have been emerged as key factors being crucial for lissencephaly (Hirotsune *et al.*, 1998; Toyo-oka *et al.*, 2003; Gambello *et al.*, 2003; Youn *et al.*, 2009). But even though MDS has been extensively modeled by analyzing *LIS1* and *YWHAE* mutants in rodents, a model, which allows the recapitulation of the complete genetic defects of MDS, was missing. In this work it was possible to work with MDS patient cells by directly converting them specifically to corticofugal neurons for the first time. Using directly induced neurons holds the advantage that the neurons can be genetically manipulated in a simple way and important cellular processes of the *in vivo* brain development can be recapitulated *in vitro* (Eiraku *et al.*, 2008; Gaspard *et al.*, 2008). Thereby it is possible to conduct rescue experiments or analyzing specific signaling pathways, which control disease related processes.

On our search for genes, which might contribute to neurite outgrowth, neuronal branching and neuronal migration, we identified two microRNAs, namely microRNA-22 and microRNA-132. Like *LIS1* and *YWHAEE*, both microRNAs were encoded on the deleted region in MDS. So far, they were not described in association with lissencephaly, but they were known to be involved in neuronal polarization, neuronal migration as well as neurite- and axonal outgrowth (Hancock *et al.*, 2014; Vo *et al.*, 2005; Volvert *et al.*, 2014).

When performing gain-of-function experiments, we found that a restoration of either microRNA-22 or microRNA-132 in MDS-derived CiNs leads to a significant increase in neuronal motility. This shows that the expression levels of the microRNAs have an

impact on neuronal migration and that the extensively studied defect in neuronal migration in MDS is not only due to *LIS1* and *YWHAE*. In case of microRNA-22 Volvert and colleagues described a role for the regulation of the expression of Doublecortin (Dcx), a microtubule-associated protein, which is important for the establishment of neuronal polarization and radial migration (Volvert *et al.*, 2014). Surprisingly, CiNs with an overexpression of either microRNA-22 or microRNA-132 possessed an even higher motility than control-derived CiNs. This excessive rescue effect could be due the elevated microRNA expression levels, which could overcome the effect of the *LIS1* and *YWHAE* deletion. CiNs with an overexpression of microRNA-132, for example, showed the strongest increase, which correlates with the analyses of the microRNA expression levels, where the overexpression of microRNA-132 displayed the highest level. It could also be that the overexpression is too strong, which is why the microRNA expression levels would be higher than in the control. To analyze whether this would have an influence on the phenotype, it would be interesting to overexpress the microRNAs in the control line and investigate if the motility of the derived CiNs is increased compared to the unaffected control-derived CiNs. In that case, it would be strong evidence for the involvement of these microRNAs in neuronal migration. To further strengthen the correlation between the microRNA expression and neuronal migration it would be beneficial to conduct also loss-of-function experiments to see whether the neuronal migration is affected upon a decrease of microRNA expression. Furthermore, it would be interesting to see if there is a synergistic effect in response to an altered expression of the microRNAs in combination with *LIS1* and/or *YWHAE* observable.

The importance of microRNA-22 and microRNA-132 for modeling MDS was further encouraged by analyzing the neuronal morphology with respect to both microRNAs. When conducting gain-of-function experiments as well as loss-of-function experiments we found that the morphological changes correlate with the expression pattern of either microRNA-22 or microRNA-132. This suggests that both microRNAs are important regulators for the development of axons and dendrites. A restoration of the expression of one of the microRNAs in MDS-derived neurons resulted in a rescue of neuronal complexity. CiNs with an overexpression of either microRNA-22 or microRNA-132 possessed a much more complex dendritic pattern as the untreated diseased neurons. Again, CiNs with an overexpression of microRNA-132 showed a greater effect, which is probably due to a stronger overexpression. In contrast to our

motility assays, gain-of-function of microRNA-22 or microRNA-132 did not reach the complexity levels of control-derived neurons. The downregulation of each microRNA shows even more striking results. Control-derived neurons with a downregulation of microRNA-22 or microRNA-132 suddenly suffered from a massive loss of neuronal complexity. In correlation with the observed expression levels of microRNA-22 and microRNA-132 in CiNs with a downregulation of one of the microRNAs, CiNs with a downregulation of microRNA-132 exhibited the most impaired morphology. Those neurons exhibited even less dendritic branching than MDS patient-derived CiNs. This dramatic effect was surprising, as the microRNA expression levels in CiNs carrying a sponge were higher than the expression levels in MDS-derived CiNs. The exact reason for this result remains elusive. Also here, the branching could be evaluated more specifically by differentiating between primary and secondary branches to underline these remarkable findings.

The influence of these microRNAs on neuronal development is not new. It was shown that introduction of microRNA-132 into primary cortical neurons stimulated the neurite outgrowth (Vo *et al.*, 2005). Furthermore developing projection neurons of the embryonic mouse neocortex exhibited delays in neurite outgrowth and an impairment in radial migration with a reduced expression of microRNA-132 (Clovis *et al.*, 2012). Similar results were observed in hippocampal neurons of young adult mice (Magill *et al.*, 2010). But in this work we describe for the first time that these microRNAs are crucial for the development of corticofugal neurons of the deep cortical layers and thereby are important regulators in the MDS model.

Altogether this work highlights two novel factors besides *LIS1* and *YWHAEE* for the lissencephaly model.

5.5 Impaired axonal outgrowth in MDS patients

As already mentioned, the use of MDS patient cells offered the possibility to generate genetically manipulated corticofugal neurons and analyze important cellular processes of the *in vivo* brain development in an altered genetic background *in vitro*. Thereby possible effectors downstream of the microRNAs could be investigated causing the disease phenotype. Therefore signaling pathways controlling disease related processes like the cytoskeletal regulation were analyzed.

This work shows that microRNA-22 regulates PTEN in a negative manner. More specifically, we found that an increase of microRNA expression led to a decrease of PTEN expression on mRNA levels. Conversely, a decrease of microRNA expression resulted in elevated expression of PTEN. Transferred to the MDS model, PTEN expression is stronger due to a partial lack of microRNA-22 expression.

PTEN arose to be an important regulator of neuronal development. Amongst others it is involved in developmental disorders, including neuropathies and different kind of cancers (Knafo and Esteban 2017; Kreis *et al.*, 2014; Mester and Eng 2013; Zhou and Parada 2012). More importantly it was previously described as a negative regulator of cell motility and that PTEN inhibition promotes neurite outgrowth (Gu *et al.*, 1999; Iijima 2002; Kath *et al.*, 2018; Liliental *et al.*, 2000). The involvement of PTEN in the building of neuronal architectures can be explained through its influence in the PI3K/Akt signalling pathway. In the past, this pathway was described to play a role in axon growth (Atwal *et al.*, 2000; Jiang *et al.*, 2005; Kuruvilla *et al.*, 2000; Markus *et al.*, 2002; Shi *et al.*, 2003). PTEN negatively regulates this pathway via a dephosphorylation of phosphatidylinositol-3,4,5-triphosphate (PIP3) to a diphosphate (PIP2) (Bar and Dikstein 2010).

We identified that microRNA-22 influences the PI3K/Akt signaling pathway via PTEN by analyzing the gene expression of PDK1. PDK1 is a member of the PI3K/Akt signaling pathway by being an important activator of Akt. The analysis indicates that a higher expression of microRNA-22 leads to significantly more PDK1 gene expression and vice versa. This observation verifies the discussed role of PTEN, namely that high microRNA expression leads to reduced PTEN expression levels, which in turn results in a reduced dephosphorylation of PIP3. Since PIP3 activates PDK1, the PDK1 expression is enhanced upon PTEN inhibition, as we showed in our analyses. Consequently, the Akt kinase activity is enhanced. Akt is described to promote together with GSK3 β the dephosphorylation of microtubules, which is important for the developing axon since elevated level of dephosphorylation promotes the outgrowth of developing axons (Kath *et al.* 2018). With regard to that, elevated dephosphorylation of microtubules were obtained by a lack of PTEN expression (Kath *et al.*, 2018).

Taking all this into account, this work proposes the following mechanistic model: Under normal circumstances microRNA-22 inhibits PTEN expression. Thereby there is no distraction of the PI3K/Akt signalling pathway. There is a high intracellular level

of PIP3, which leads to an activation of PDK1 and subsequently Akt. This activation of the PI3K/Akt signalling pathway keeps then the dephosphorylation of microtubules up and promotes the outgrowth of developing axons.

Conversely to this, in a lissencephalic brain it is vice versa. The heterozygous depletion of microRNA-22 results in increased PTEN expression. We postulate that the PI3K/Akt signaling pathway is thereby disrupted due to reduced levels of PDK1 and Akt. Along our hypothesis reduced levels of dephosphorylated microtubules are the consequence, leading to reduced axonal outgrowth and a decrease in neuronal complexity (see Figure 19).

Altogether it demonstrates that the microRNA-22 is involved in the regulation of axonal outgrowth via the PI3K/Akt signaling pathway.

5.6 Perturbed actin fiber formation in MDS

Similar to the analysis of the regulative mechanism downstream of microRNA-22, we investigated regulators downstream of microRNA-132, explaining the morphological alterations in MDS patient-derived CiNs additionally to previous findings. A direct target screen revealed p250GAP as a candidate. This was substantiated by a report of Vo and colleagues, who described the small GTPase p250GAP as a direct target of microRNA-132 (Vo *et al.*, 2005).

This work shows that p250GAP is negatively regulated by microRNA-132. In specific, we found that an increase of microRNA-132 expression decreases the expression of p250GAP on mRNA level. In contrast, a decrease of microRNA-132 expression resulted in an increased expression of p250GAP. Transferred to the MDS model, p250GAP expression is increased upon a partial lack of microRNA-132 expression.

The connection between microRNA-132 and p250GAP in regard to neuronal development was previously demonstrated by showing that both factors are involved in the mediation of dendritic growth and the formation of dendritic spines (Impey *et al.*, 2010; Wayman *et al.*, 2008). We assumed that this could be the result of a failed actin remodeling due to a disruption of the Rac signaling pathway. p250GAP is involved in the Rac signaling pathway by regulating Rac1 in a negative manner (Magill *et al.*, 2010). The Rac signaling pathway itself is an important regulator of actin remodeling in matters of building the cytoskeleton. The cytoskeleton of the brain includes three different filamentous structures: actin filaments, microtubules and

neurofilaments. Central for cytoskeletal dynamics are the actin filaments and microtubules (Coles and Bradke 2015). The remodeling of the cytoskeleton is necessary for the migration and growth of neurons. Our analyses indeed prove the inhibitory function of p250GAP. It is shown that CiNs exhibited always an increased expression of Rac1 in response to an increased expression of microRNA-132 due to reduced levels of p250GAP. Conversely, a decrease of microRNA-132 reduces also the Rac1 expression upon increased p250GAP levels. The decrease in Rac1 expression has a dramatic effect on the CiNs, since Rac1 is very important for neuronal development. It possesses a unique role in actin remodelling (Nobes and Hall, 1995; Hall, 1998). It promotes the expression of the WAVE-complex, whereas the WAVE-complex induces cytoskeletal remodelling through a direct interaction with the Arp2/3-complex (Takenawa and Miki 2001; Pilo Boyl *et al.*, 2007). That Arp2/3-complex is known to be an actin filament nucleator that binds the side of an existing actin filament and nucleates a new filament (Spillane and Gallo 2014). This is enabled through regulatory proteins like the Wiskott-Aldrich syndrome protein (WASp), which include the three motifs V (verprolin homology), C (connecting) and A (acidic). Those VCA domains act as mediators and consolidate the Arp2/3-complex and the first subunit of the daughter filaments. This daughter filament is then fixed with its pointed end at the mother filament, usually at the side (reviewed by Pollard 2007). At the end, a new actin branch at the side of a filament develops. Reduction of Rac1 expression would lead to a disruption of this actin remodeling.

The results of this work and the previously described role of microRNA-132 let us propose the following model of actin regulation via microRNA-132. Healthy neurons possess a normal level of microRNA-132 expression leading to a reduced expression level of p250GAP. Thereby the activity of the Rac signaling pathway is not disrupted through p250GAP and the actin remodeling takes place.

In contrast, the expression of microRNA-132 is reduced in the lissencephalic brain. Thus the inhibition of p250GAP is less strong and it negatively regulates the Rac signaling pathway. Because of this, the actin remodeling is disrupted and through this disruption the dendritic arborization of the neurons is reduced and leading to a decrease in neuronal complexity (see Figure 20 A).

Collectively these results indicate the important role of microRNA-132 in actin remodeling by acting via the Rac signaling pathway.

5.8 Conclusions

This thesis describes the efficient generation of human cortical layer specific neurons from either human iPSCs or directly from human fibroblasts. More specifically, we used a directed differentiation combined with transcription factor based induction to convert human iPSC or human fibroblasts into corticofugal neurons of the cortical layer V. Furthermore it demonstrates the role of *Fezf2* as a key factor for instructing a corticofugal identity in human cortical neurons.

In addition to the generation of human cortical layer specific neurons, it highlights the acquired opportunity through these techniques by employing the generated corticofugal neurons to model a cortical malformation, specifically the Miller-Dieker Syndrome. In terms of modeling the most severe form of lissencephaly, it recapitulates migration defects caused by this disease. In addition, it delineates a failed branching of the neurons by showing that diseased neurons are less complex developed as their healthy counterparts. In addition, it describes for the first time the involvement of two microRNAs, namely microRNA-22 and microRNA-132, with regard to MDS. By introducing these two novel regulators, we demonstrate not only their influence in morphological phenotypes, but also their involvement in the genetic regulation behind the phenotype. Thereby this thesis gives new revealing insights about the Miller-Dieker Syndrome.

6. Abbreviations

Abbreviation	Full name
AD	Alzheimer's Disease
ALK	Anaplastic lymphoma kinase
ALS	Amyotrophic lateral sclerosis
ASCL1	achaete-scute family bHLH transcription factor 1
BDNF	Brain-derived neurotrophic factor
bFGF	Basic fibroblasts growth factor
BMP	Bone morphogenetic protein
BRN2 (POU3F2)	POU class 3 homeobox 2
BSA	Bovine serum albumin
CaCl ₂	Calciumchloride
CACNA1H	Calcium voltage-gated channel subunit alpha1 H
cAMP	Cyclic adenosinmonophosphate
Cdc42	Cell division cycle 42
CDM	Cortical development malformation
cDNA	Complementary DNA
CiN	Corticofugal-like neuron
CLIM1 (LDB2)	LIM domain binding 2
cm	Centimeter
CNS	Central nervous system
CoREST	REST corepressor 1
CP	Cortical plate
CRYM	Crystallin mu
Ct	Cycle threshold
CTIP2 (BCL11B)	B cell CLL/lymphoma 11B
CTRL	Control
CUX1	Cut like homeobox 1
DABCO	1,4-Diazabicyclo[2.2.2]octan
DACH1	Dachshund family transcription factor 1
DAPI	4,6 Diamidino-2-phenylindole
db cAMP	Dibutyryl-cAMP
DCX	Doublecortin
DEPC	Diethyl pyrocarbonate

DKK3	Dickkopf WNT signaling pathway inhibitor 3
DLX5	Distal-less homeobox 5
DMEM	Dulbecco's Modified Eagle Medium
DMSO	Dimethyl sulfoxide
DNA	Deoxyribonucleic acid
dNTP	Desoxynucleoside triphosphate
DOX	Doxycycline
e.coli	Escherichia coli
EDTA	Ethylenediaminetetraacetic acid
EGF	Epidermal growth factor
EN1	Engrailed homeobox 1
ER81 (ETV1)	ETS variant 1
ESC	Embryonic stem cell
FCS	Fetal calf serum
FEZF2	Fez family zinc finger 2
FGF2	Fibroblast growth factor 2
FOXA2	Forkhead box A2
FOXG1	Forkhead box G1
FTD	Frontotemporal dementia
GABA	Gamma-Aminobutyric acid
GATA2	GATA binding protein 2
GDNF	Glial cell-derived neurotrophic factor
GO	Gene ontology
GOI	Gene of interest
gt	Goat
h	Hour(s)
H ₂ O	Water
HCl	Hydrogen chloride
HEPES	4-(2-hydroxyethyl)-1-piperazineethanesulfonic acid
IL	Interleukin
IP	Intermediate progenitors
iPS cell	Induced pluripotent stem cell
iN	Induced neuron
ISL1	Isl LIM homeobox 1
Kcl	Kaliumchloride
KLF4	Krüppel like factor 4

KOSR	Knockout serum replacement
l	Liter
LAAP	L-ascorbic-acid-2-phosphat
LED	Light-emitting diode
LHX3	LIM homeobox 3
LHX6	LIM homeobox 6
LIS1 (PAFAH1B1)	Platelet activating factor acetylhydrolase 1b regulatory subunit 1
LMX1A	LIM homeobox transcription factor 1 alpha
LMX1B	LIM homeobox transcription factor 1 beta
Ln	Laminin
MAP2	Microtubule associated protein 2
MDS	Miller-Dieker Syndrome
MgCl ₂	Magnesiumchloride
MYOD1	Myogenic differentiation 1
µg	Microgram
mg	Milligram
µm	Micrometer
mM	Millimolar
µM	Micromolar
min	Minute(s)
miR, miRNA	microRNA
ml	Milliliter
mRNA	messenger RNA
ms	Mouse
MSX1	Msh homeobox 1
MYT1L	Myelin transcription factor 1 like
Na ₂ HPO ₄	Disodium phosphate
NaCl	Sodiumchloride
NC	Neuron conversion medium
NDEL1	NudE neurodevelopment protein 1 like 1
ng	Nanogram
NGMC	Neuronal generation medium
NGN2 (NEUROG2)	Neurogenin 2
NPC	Neural progenitor cell
NM	Neural maturation medium

nPTB (PTBP2)	Polypyrimidine tract binding protein 2
NURR1 (NR4A2)	Nuclear receptor subfamily 4, group A, member 2
OCT 3/4 (POU5F1)	POU class 5 homeobox 1
OSVZ	Outer subventricular zone
OTX2	Orthodenticle homeobox 2
PAX6	Paired box 6
p250GAP (ARHGAP32)	Rho GTPase activating protein 32
PBS	Phosphate buffered saline
PCR	Polymerase chain reaction
PKD1	Pyruvate dehydrogenase kinase 1
PDX1	Pancreatic and duodenal homeobox 1
PEG 6000	Polyethylene glycol 6000
Pen / Strep	Penicillin-Streptomycin
PFA	Paraformaldehyde
PITX3	Paired like homeodomain 3
PO	Poly-ornithine
pre-miRNA	precursor microRNA
pri-miRNA	primary microRNA
PTBP1	Polypyrimidine tract-binding protein 1
PTEN	Phosphatase and tensin homolog
puroR	Puromycin resistance
RA	Retinoic acid
RAC1	Rac family small GTPase 1
RANBP17	Ran-binding protein 17
rb	Rabbit
REST	RE1 silencing transcription factor
RELN	Reelin
RGC	Radial glia cell
RISC complex	RNA-induced silencing complex
RNA	Ribonucleic acid
RNA-seq	RNA sequencing
RT	Room temperature
RT-PCR	Reverse transcriptase PCR
RT-qPCR	Real time quantitative PCR
s	Seconds
SD	Standard deviation

SHH	Sonic hedgehog
SIRT1	Sirtuin 1
SKI	Ski proto-oncogene
SOX2	Sex determining region Y- box 2
SVZ	Subventricular zone
TAP	Transient amplifying daughter cell
TBR1	T-box brain 1
TC	Tissue culture
TE	Trypsin/EDTA
Tetfree FCS	Tetracycline free fetal calf serum
tetOn	Tetracycline regulatable gene induction system
TF	Transcription factor
TGF β 1	Transforming growth factor
TLE4	Transducin like enhancer of split 4
Tris	Tris(hydroxymethyl)aminomethane
UTR	Untranslated region
VZ	Ventricular zone
WASp	Wiskott-Aldrich syndrome protein
WNT	Wingless/Integrated
WNT7b	Wnt family member 7B

7. Abstract

Until recently, lineage commitment and differentiation have been considered to be unidirectional and irreversible. This traditional view has dramatically changed with the advent of cellular reprogramming and direct cell fate conversion. Today, almost any given somatic cell can, in principle, be efficiently transferred into any other desired cellular phenotype. These techniques offer great opportunities to generate tissue specific cells, which were so far not easily accessible in human. The human brain, which is equipped with almost incomparable complexity, certainly is the most prominent example for such a tissue. The human cortex for instance is composed of a 6-layer structure, and each layer contains specific neuronal subtypes subserving distinct functions. The behavior of the cortical neurons can be disrupted in developmental disorders including lissencephaly, a cortical malformation associated with defects in neuronal migration and maturation.

In this thesis we use transcription factor-based direct conversion techniques, for the generation of cortical subtype-specific neurons from human induced pluripotent stem cell (iPSC) and human fibroblasts and utilize the derived neurons to investigate phenotypic changes associated with lissencephaly. In more detail, we identified a TF, which is sufficient to induce a deep layer corticofugal fate in cortical differentiated iPSC and in human fibroblasts. When generating induced corticofugal neurons (CiNs) from lissencephaly patients and healthy controls, we observed a decrease in neuronal complexity. In particular, we found significantly reduced neuronal branching in patient-derived CiNs. We suggest that two microRNAs, which are heterozygous deleted in the patient samples, play a role in the observed phenotypic changes. Gain- and loss-of-function studies in patient- and control-derived CiNs confirmed a role of both microRNAs in the disease phenotype. Finally, we identified microRNA downstream pathways involved in neuronal branching to be dis-regulated specifically in patient-derived CiNs.

Our data indicate that direct programming serves as promising technique for the generation of cortical layer specific human neurons and the analyses of neuronal behavior *in vitro*.

8. Zusammenfassung

Bis vor Kurzem wurde angenommen, dass die Differenzierung von Zellen und deren Bindung an ihre Abstammung irreversibel und nur in eine Richtung gerichtet ist. Mit der Entwicklung der zellulären Reprogrammierung und der direkten Konversion hat sich diese Sichtweise komplett geändert. Heutzutage ist es möglich fast jede somatische Zelle in einen anderen gewünschten Zelltyp in effizienter Weise umzuwandeln. Diese entwickelten Techniken offerieren große Möglichkeiten, wie z.B. spezifische Zellen des menschlichen Körpers zu generieren, die bislang nicht so frei zugänglich waren. Ein Beispiel dafür ist das menschliche Gehirn, welches das komplexeste aller menschlichen Organe ist. Allein der zerebrale Kortex besteht aus einer laminierten Struktur mit sechs verschiedenen Schichten, welche aus spezifischen neuronalen Subtypen bestehen, die jeweils verschiedene Funktionen innehaben. Bei Entwicklungsstörungen des zentralen Nervensystems (ZNS) verhalten sich jene Neurone anders als gewöhnlich. Ein Beispiel dafür ist die Lissenzephalie, die sich durch eine Fehlbildung des zerebralen Kortex äußert und mit Defekten in der Migration und Reifung der Neurone assoziiert ist.

In dieser Arbeit haben wir mittels Transkriptionsfaktoren-basierten Konversionsverfahren subtyp-spezifische kortikale Neurone aus humanen induziert pluripotenten Stammzellen und humanen Fibroblasten hergestellt. Diese Neurone wurden anschließend für die Analyse phänotypischer Abweichungen im Bezug auf Lissenzephalie benutzt. Im Einzelnen haben wir einen Transkriptionsfaktor identifiziert, dessen Expression ausreicht, um aus iPSC und humanen Fibroblasten kortikofugale Neurone zu erzeugen. Im Zuge der Erzeugung kortikofugaler Neurone von Lissenzephalie Patienten und gesunden Kontrollen, haben wir eine Verminderung der Komplexität der Neurone beobachten können. Im Speziellen haben wir eine signifikante Abnahme in der Verzweigung der Neurone bei Lissenzephalie Patienten feststellen können. Im Weiteren legen wir nahe, dass die Expression zweier microRNAs, die bei den Patientenzellen heterozygot deletiert sind, mit den beobachteten morphologischen Unterschieden assoziiert sein könnte. Gain- und loss-of-function Experimente mit kortikofugalen Neuronen, die von Patienten und Kontrollen abgeleitet worden sind, bestätigen den Einfluss beider microRNAs. Am Ende haben wir zudem zwei Signalwege identifiziert, in denen jeweils eine der microRNAs involviert ist. Diese Signalwege sind beide in der Entwicklung der

neuronalen Verzweigung involviert und zeigen eine fehlerhafte Regulation in Neuronen, die von Patienten abgeleitet wurden.

Zusammengefasst zeigt diese Arbeit, dass die direkte Konversion eine vielversprechende Methode für die Erzeugung von spezifischen Subtypen kortikaler Neurone und der anschließenden Analyse deren Verhaltens *in vitro* ist.

9. References

- Abelson, J.F., Kwan, K.Y., O’Roak, B.J., Baek, D.Y., Stillman, A.A., et al. (2005). Sequence variants in SLITRK1 are associated with Tourette’s syndrome. *Science* 310, 317–20
- Adler, C.E., Fetter, R.D., Bargmann, C.I. (2006). UNC-6/Netrin induces neuronal asymmetry and defines the site of axon formation. *Nat Neurosci.* 9, 511–518
- Alcamo, E.A., Chirivella, L., Dautzenberg, M., Dobрева, G., Farinas, I., Grosschedl, R., McConnell, S.K. (2008). *Satb2* regulates callosal projection neuron identity in the developing cerebral cortex. *Neuron* 57, 364–377
- Ambros, V. (2004). The functions of animal microRNAs. *Nature* 431, 350–355
- Andersson, E., Tryggvason, U., Deng, Q., Friling, S., Alekseenko, Z., Robert, B., Perlmann, T., Ericson, J. (2006). Identification of intrinsic determinants of midbrain dopamine neurons. *Cell* 124(2), 393–405
- Angevine, J. B. Jr & Sidman, R. L. (1961). Autoradiographic study of cell migration during histogenesis of cerebral cortex in mouse. *Nature* 192, 766–768
- Arlotta, P., Molyneaux, B.J., Chen, J., Inoue, J., Kominami, R., Macklis, J.D. (2005). Neuronal subtype-specific genes that control corticospinal motor neuron development in vivo. *Neuron* 45, 207–221
- Atwal, J.K., Massie, B., Miller, F.D., Kaplan, D.R. (2000). The TrkB-Shc site signals neuronal survival and local axon growth via MEK and P13-kinase. *Neuron* 27, 265–277
- Bai, Q., Ramirez, J.M., Becker, F., Pantesco, V., Lavabre- Bertrand, T., Hovatta, O., Lemaitre, J.M., Pellestor, F., De Vos, J. (2015). Temporal analysis of genome alterations induced by single-cell passaging in human embryonic stem cells. *Stem Cells Dev.* 24, 653–662
- Bar, N., Dikstein, R. (2010). miR-22 forms a regulatory loop in PTEN/AKT pathway and modulates signaling kinetics. *PLoS One* 5(5)
- Barkovich, A.J., Guerrini, R., Kuzniecky, R.I., Jackson, G.D., Dobyns, W.B. (2012). A developmental and genetic classification for malformations of cortical development: update 2012. *Brain* 135 (Pt 5), 1348–69
- Bartel, D. P. (2004). MicroRNAs: genomics, biogenesis, mechanism, and function. *Cell* 116, 281–297
- Bayer, S. A. & Altman, J. (1991). in *Neocortical Development* 255 (Raven, New York).
- Berenguer, J., Herrera, A., Vuolo, L., Torroba, B., Llorens, F., Sumoy, L., and Pons, S. (2013). MicroRNA 22 regulates cell cycle length in cerebellar granular neuron precursors. *Mol. Cell. Biol* 33, 2706–2717

- Bershteyn, M., Nowakowski, T.J., Pollen, A.A., et al. (2017). Human iPSC-Derived Cerebral Organoids Model Cellular Features of Lissencephaly and Reveal Prolonged Mitosis of Outer Radial Glia. *Cell Stem Cell* 20(4), 435–449
- Bi, W., Sapir, T., Shchelochkov, O.A., Zhang, F., Withers, M.A., Hunter, J.V., Levy, T., Shinder, V., Peiffer, D.A., Gunderson, K.L., et al. (2009). Increased LIS1 expression affects human and mouse brain development. *Nat. Genet.* 41, 168–177
- Bock, C., Kiskinis, E., Verstappen, G., Gu, H., Boulting, G., Smith, Z.D., Ziller, M., Croft, G.F., Amoroso, M.W., Oakley, D.H., et al. (2011). Reference Maps of human ES and iPS cell variation enable high-throughput characterization of pluripotent cell lines. *Cell* 144, 439–452
- Borchert, G.M., Lanier, W., Davidson, B.L. (2006). RNA polymerase III transcribes human microRNAs. *Nat Struct Mol Biol* 13, 1097–1101
- Brennecke, J., Stark, A., Russell, R.B., Cohen, S.M. (2005). Principles of microRNA-target recognition. *PLoS Biol* 3, e85
- Broccoli, V., Caiazzo, M. & Dell'anno, M.T. J. (2011). Setting a highway for converting skin into neurons *Mol. Cell. Biol.* 3, 322–323
- Bystron, I., Rakic, P., Molnár, Z., and Blakemore, C. (2006). The first neurons of the human cerebral cortex. *Nat. Neurosci.* 9, 880–886
- Cai, X., Hagedorn, C.H., Cullen, B.R. (2004). Human microRNAs are processed from capped, polyadenylated transcripts that can also function as mRNAs. *Rna* 10, 1957–1966
- Caiazzo, M., Dell'Anno, M.T., Dvoretzkova, E., Lazarevic, D., Taverna, S., Leo, D., Sotnikova, T.D., Menegon, A., Roncaglia, P., Colciago, G., Russo, G., Carninci, P., Pezzoli, G., Gainetdinov, R.R., Gustincich, S., Dityatev, A., Broccoli, V. (2011). Direct generation of functional dopaminergic neurons from mouse and human fibroblasts. *Nature* 476, 224–227
- Candiani, S., Moronti, L., De Pietri Tonelli, D., Garbarino, G., Pestarino, M. (2011). A study of neural-related microRNAs in the developing amphioxus. *Evodevo* 2, 15
- Cardoso, C., Leventer, R.J., Ward, H.L., Toyo-Oka, K., Chung, J., Gross, A., Martin, C.L., Allanson, J., Pilz, D.T., Olney, A.H., et al. (2003). Refinement of a 400-kb critical region allows genotypic differentiation between isolated lissencephaly, Miller-Dieker syndrome, and other phenotypes secondary to deletions of 17p13.3. *Am. J. Hum. Genet.* 72, 918–930
- Carthew, R.W., Sontheimer, E.J. (2009). Origins and mechanisms of miRNAs and siRNAs. *Cell* 36, 642-655
- Casarosa, S., Fode, C., and Guillemot, F. (1999). Mash1 regulates neurogenesis in the ventral telencephalon. *Development* 126, 525–534

- Chambers, S.M. et al. (2009). Highly efficient neural conversion of human ES and iPS cells by dual inhibition of SMAD signaling. *Stuart Nat. Biotechnol.* 27, 275–280
- Chanda, S., Ang, C.E., Davila, J., et al. (2014). Generation of induced neuronal cells by the single reprogramming factor ASCL1. *Stem Cell Reports* 3(2), 282–296
- Chen, B., Wang, S.S., Hattox, A.M., Rayburn, H., Nelson, S.B., McConnell, S.K. (2008). The Fezf2-Ctip2 genetic pathway regulates the fate choice of subcortical projection neurons in the developing cerebral cortex. *Proceedings of the National Academy of Sciences U S A* 105, 11382–11387
- Cheng, L.C., Pastrana, E., Tavazoie, M., and Doetsch, F. (2009). miR-124 regulates adult neurogenesis in the subventricular zone stem cell niche. *Nat. Neurosci.* 12, 399–408
- Choi, J., Costa, M.L., Mermelstein, C.S., Chagas, C., Holtzer, S., Holtzer, H. (1990). MyoD converts primary dermal fibroblasts, chondroblasts, smooth muscle, and retinal pigmented epithelial cells into striated mononucleated myoblasts and multinucleated myotubes. *Proc Natl Acad Sci U S A* 87, 7988–7992
- Chong, S.S., Pack, S.D., Roschke, A.V., Tanigami, A., Carrozzo, R., Smith, A.C.M., Dobyns, W.B., and Ledbetter, D.H. (1997). A revision of the lissencephaly and Miller-Dieker syndrome critical regions in chromosome 17p13.3. *Hum. Mol. Genet.* 6, 147–155
- Ciani, L. & Salinas, P.C. (2005). WNTs in the vertebrate nervous system: from patterning to neuronal connectivity. *Nat. Rev. Neurosci* 6, 351–362
- Clovis, Y.M., Enard, W., Marinaro, F., Huttner, W.B., and De Pietri Tonelli, D. (2012). Convergent repression of Foxp2 3'UTR by miR-9 and miR-132 in embryonic mouse neocortex: implications for radial migration of neurons. *Development* 139, 3332–3342
- Colasante, G., Lignani, G., Rubio, A., Medrihan, L., Yekhlef, L., Sessa, A., Massimino, L., Giannelli, S.G., Sacchetti, S., Caiazzo, M., et al. (2015). Rapid Conversion of Fibroblasts into Functional Forebrain GABAergic Interneurons by Direct Genetic Reprogramming. *Cell Stem Cell* 17, 719–734
- Coles, C.H., Bradke, F. (2015). Coordinating Neuronal Actin–Microtubule Dynamics. *Curr Biol.* 25, R677– R691
- Curran, T., D'Arcangelo, G. (1998). Role of reelin in the control of brain development. *Brain Res Brain Res Rev* 26, 285-94
- D'Arcangelo, G., Miao, G.G., Chen, S.C., Soares, H.D., Morgan, J.I., Curran, T. (1995). A protein related to extracellular matrix proteins deleted in the mouse mutant reeler. *Nature* 374, 719–23
- Davis, R.L., Weintraub, H., Lassar, A.B. (1987). Expression of a single transfected cDNA converts fibroblasts to myoblasts. *Cell* 51, 987–1000

- Davis, T.H., Cuellar, T.L., Koch, S.M., Barker, A.J., Harfe, B.D., et al. (2008). Conditional loss of Dicer disrupts cellular and tissue morphogenesis in the cortex and hippocampus. *J. Neurosci.* 28, 4322–30
- De Pietri Tonelli, D., Pulvers, J.N., Haffner, C., Murchison, E.P., Hannon, G.J., Huttner, W.B. (2008). miRNAs are essential for survival and differentiation of newborn neurons but not for expansion of neural progenitors during early neurogenesis in the mouse embryonic neocortex. *Development* 135, 3911–21
- Derer, P., Nakanishi, S. (1983). Extracellular matrix distribution during neocortical wall ontogenesis in “normal” and “reeler” mice. *J Hirnforsch* 24, 209–24
- Dobyns, W.B., Stratton, R.F., Parke, J.T., Greenberg, F., Nussbaum, R.L., Ledbetter, D.H. (1983). Miller-Dieker syndrome: lissencephaly and monosomy 17p. *J Pediatr* 102, 552–558
- Dobyns, W.B., Curry, C.J., Hoyme, H.E., Turlington, L., Ledbetter, D.H. (1991). Clinical and molecular diagnosis of Miller-Dieker syndrome. *Am J Hum Genet.* 48(3), 584–94
- Doi, D., Samata, B., Katsukawa, M., Kikuchi, T., Morizane, A., Ono, Y., Sekiguchi, K., Nakagawa, M., Parmar, M., Takahashi, J. (2014). Isolation of human induced pluripotent stem cell-derived dopaminergic progenitors by cell sorting for successful transplantation. *Stem Cell Reports* 2(3), 337–50
- Edbauer, D., Neilson, J. R., Foster, K. A., Wang, C.-F., Seeburg, D. P., Batterton, M. N., Tada, T., Dolan, B. M., Sharp, P. A. and Sheng, M. (2010). Regulation of synaptic structure and function by FMRP-associated microRNAs miR-125b and miR-132. *Neuron* 65, 373–384
- Eiraku, M., Watanabe, K., Matsuo-Takasaki, M., Kawada, M., Yonemura, S., Matsumura, M., Wataya, T., Nishiyama, A., Muguruma, K., Sasai, Y. (2008). Self-organized formation of polarized cortical tissues from ESCs and its active manipulation by extrinsic signals. *Cell Stem Cell* 3, 519–532
- Elston, G.N. (2000). Pyramidal cells of the frontal lobe: All the more spinous to think with. *J. Neurosci.* 20, RC95
- Espuny-Camacho, I., Michelsen, K.A., Gall, D., Linaro, D., Hasche, A., Bonnefont, J., Bali, C., Orduz, D., Bilheu, A., Herpoel, A., et al. (2013). Pyramidal neurons derived from human pluripotent stem cells integrate efficiently into mouse brain circuits in vivo. *Neuron* 77, 440–456.
- Fasano, C.A., Chambers, S.M., Lee, G., Tomishima, M.J., and Studer, L. (2010). Efficient derivation of functional floor plate tissue from human embryonic stem cells. *Cell Stem Cell* 6, 336–347
- Feng, R., Desbordes, S.C., Xie, H., Tillo, E.S., Pixley, F., Stanley, E.R., Graf, T. (2008). PU.1 and C/EBP α / β convert fibroblasts into macrophage-like cells. *Proc Natl Acad Sci U S A* 105, 6057–6062

- Ferrer, I., Fernandez-Alvarez, E. (1977). Lissencephaly: agyria. A study using the Golgi technic. *J Neurol Sci* 34, 109–120
- Francis, F., Meyer, G., Fallet-Bianco, C., Moreno, S., Kappeler, C., Socorro, A.C., Tuy, F.P., Beldjord, C., and Chelly, J. (2006). Human disorders of cortical development: from past to present. *Eur. J. Neurosci.* 23, 877–893
- Friedman, R.C., Farh, K.K., Burge, C.B., Bartel, D.P. (2009). Most mammalian mRNAs are conserved targets of microRNAs. *Genome Res* 19(1), 92–105
- Fuccillo, M., Joyner, AL. & Fishell, G. (2006). Morphogen to mitogen: the multiple roles of hedgehog signalling in vertebrate neural development. *Nat. Rev. Neurosci* 7, 772–783
- Gambello, M.J., Darling, D.L., Yingling, J., Tanaka, T., Gleeson, J.G., and Wynshaw-Boris, A. (2003). Multiple dose-dependent effects of Lis1 on cerebral cortical development. *J. Neurosci.* 23, 1719–1729
- Gaspard, N., Bouchet, T., Hourez, R., Dimidschstein, J., Naeije, G., van den Aemele, J., Espuny-Camacho, I., Herpoel, A., Passante, L., Schiffmann, S.N., Gaillard, A., Vanderhaeghen, P. (2008). An intrinsic mechanism of corticogenesis from embryonic stem cells. *Nature* 455, 351–357
- Garitaonandia, I., Amir, H., Boscolo, F.S., Wambua, G.K., Schultheisz, H.L., Sabatini, K., Morey, R., Waltz, S., Wang, Y.C., Tran, H., Leonardo, T.R., Nazor, K., Slavin, I., Lynch, C., Li, Y., Coleman, R., Gallego Romero, I., Altun, G., Reynolds, D., Dalton, S., Parast, M., Loring, J.F., Laurent, L.C. (2015). Increased risk of genetic and epigenetic instability in human embryonic stem cells associated with specific culture conditions. *PLoS One* 10(2), e0118307
- Gelman, D. M., and Marín, O. (2010). Generation of interneuron diversity in the mouse cerebral cortex. *Eur. J. Neurosci.* 31, 2136–2141
- Gleeson, J.G., Lin, P.T., Flanagan, L.A., Walsh, C.A. (1999). Doublecortin is a microtubule-associated protein and is expressed widely by migrating neurons. *Neuron* 23, 257–271
- Goffinet, A.M., Lyon, G. (1979). Early histogenesis in the mouse cerebral cortex: a Golgi study. *Neurosci Lett* 14, 61–6
- Goffinet, A.M. (1979). An early development defect in the cerebral cortex of the reeler mouse. A morphological study leading to a hypothesis concerning the action of the mutant gene. *Anat Embryol (Berl)* 157, 205–16
- Gu, J., Tamura, M., Pankov, R., Danen, E.H.J., Takino, T., Matsumoto, K., et al. (1999). Shc and Fak Differentially Regulate Cell Motility and Directionality Modulated by Pten. *J Cell Biol.* 146, 389–404
- Hall, A. (1998). Rho GTPases and the actin cytoskeleton. *Science* 279, 509–514

- Han, W., Kwan, K.Y., Shim, S., Lam, M.M., Shin, Y., Xu, X., Zhu, Y., Li, M., Sestan, N. (2011). TBR1 directly represses Fezf2 to control the laminar origin and development of the corticospinal tract. *Proc Natl Acad Sci U S A* *108*, 3041–3046
- Hancock, M.L., Preitner, N., Quan, J., Flanagan, J.G., (2014). MicroRNA-132 is enriched in developing axons, locally regulates Rasa1 mRNA, and promotes axon extension. *J. Neurosci.* *34*, 66–78
- Hansen, D.V., Lui, J.H., Flandin, P., Yoshikawa, K., Rubenstein, J.L., Alvarez-Buylla, A., and Kriegstein, A.R. (2013). Non-epithelial stem cells and cortical interneuron production in the human ganglionic eminences. *Nat. Neurosci.* *16*, 1576–1587
- Hattori, M., Adachi, H., Tsujimoto, M., Arai, H., and Inoue, K. (1994). Miller-Dieker lissencephaly gene encodes a subunit of brain platelet-activating factor acetylhydrolase [corrected]. *Nature* *370*, 216–218
- Hevner, R. F. *et al.* (2003). Beyond laminar fate: toward a molecular classification of cortical projection/pyramidal neurons. *Dev. Neurosci.* *25*, 139–151
- Hirotsune, S., Fleck, M.W., Gambello, M.J., Bix, G.J., Chen, A., Clark, G.D., Ledbetter, D.H., McBain, C.J., and Wynshaw-Boris, A. (1998). Graded reduction of Pafah1b1 (Lis1) activity results in neuronal migration defects and early embryonic lethality. *Nat. Genet.* *19*, 333–339
- Hoerder-Suabedissen, A., Molnar, Z. (2013). Molecular diversity of early-born subplate neurons. *Cereb Cortex* *23*, 1473–83
- Howard, B.M., Zhicheng Mo, Filipovic, R., Moore, A.R., Antic, S.D., and Zecevic, N. (2008). Radial glia cells in the developing human brain. *Neuroscientist* *14*, 459–473
- Hu, B.Y., Weick, J.P., Yu, J., Ma, L.X., Zhang, X.Q., Thomson, J.A., and Zhang, S.C. (2010). Neural differentiation of human induced pluripotent stem cells follows developmental principles but with variable potency. *Proc. Natl. Acad. Sci. USA* *107*, 4335–4340
- Hu, W., Qiu, B., Guan, W., Wang, Q., Wang, M., Li, W., Gao, L., Shen, L., Huang, Y., Xie, G., Zhao, H., Jin, Y., Tang, B., Yu, Y., Zhao, J., Pei, G. (2015). Direct Conversion of Normal and Alzheimer’s Disease Human Fibroblasts into Neuronal Cells by Small Molecules. *Cell Stem Cell* *17*, 204–212
- Huh, C.J., Zhang, B., Victor, M.B., Dahiya, S., Batista, L.F., Horvath, S., and Yoo, A.S. (2016). Maintenance of age in human neurons generated by microRNA-based neuronal conversion of fibroblasts. *eLife* *5*, e18648
- Iefremova, I., Manikakis, G., Krefft, O., Jabali, A., Weynans, K., Wilkens, R., Marsoner, F., Brändl, B., Müller, F.J., Koch, P., Ladewig, J. (2017). An organoid-based model of cortical development identifies non-cell-autonomous defects in Wnt signaling contributing to Miller-Dieker syndrome. *Cell Rep.* *19*, 50–59

- Iijima, M., Devreotes, P. (2002). Tumor Suppressor PTEN Mediates Sensing of Chemoattractant Gradients. *Cell* 109, 599–610
- Im, H.I., Kenny, P.J. (2012). MicroRNAs in neuronal function and dysfunction. *Trends Neurosci.* 35(5), 325-34
- Impey, S., Davare, M., Lasiek, A., Fortin, D., Ando, H., Varlamova, O., Obrietan, K., Soderling, T.R., Goodman, R.H., Wayman, G.A. (2010). An activity-induced microRNA controls dendritic spine formation by regulating Rac1-PAK signaling. *Mol Cell Neurosci* 43, 146–156
- Inoue, K., Wakao, H., Ogonuki, N., Miki, H., Seino, K., Nambu-Wakao, R., Noda, S., Miyoshi, H., Koseki, H., Taniguchi, M., Ogura, A. (2005). Generation of cloned mice by direct nuclear transfer from natural killer T cells. *Curr Biol.* 15, 1114–1118
- Jiang, H., Guo, W., Liang, X., Rao, Y. (2005). Both the establishment and the maintenance of neuronal polarity require active mechanisms: critical roles of GSK-3beta and its upstream regulators. *Cell* 120, 123–135
- Jossin, Y., Bar, I., Ignatova, N., Tissir, F., De Rouvroit, C.L., Goffinet, A.M. (2003). The reelin signaling pathway: some recent developments. *Cereb Cortex* 13, 627-33
- Jossin, Y., Cooper, J.A. (2011). Reelin, Rap1 and N-cadherin orient the migration of mul- tipolar neurons in the developing neocortex. *Nat Neurosci.* 14, 697–703
- Jovicic, A., Zaldivar Jolissaint, J.F., Moser, R., Silva Santos Mde, F., Luthi-Carter, R. (2013). MicroRNA-22 (miR-22) overexpression is neuroprotective via general anti-apoptotic effects and may also target specific Huntington's disease-related mechanisms. *PLoS One* 8(1)
- Kassai, H., Terashima, T., Fukaya, M., Nakao, K., Sakahara, M., Watanabe, M., Aiba, A. (2008). Rac1 in cortical projection neurons is selectively required for midline crossing of commissural axonal formation. *Eur J Neurosci.* 28(2), 257-67
- Kath, C., Goni-Oliver, P., Müller, R., Schultz, C., Haucke, V., Eickholt, B., Schmoranzer, J. (2018). PTEN suppresses axon outgrowth by down-regulating the level of deetyrosinated microtubules. *PLoS One* 13(4)
- Kato, M., and Dobyns, W.B. (2003). Lissencephaly and the molecular basis of neuronal migration. *Hum. Mol. Genet.* 12, R89–R96
- Kawase-Koga, Y., Otaegi, G., Sun, T. (2009). Different timings of Dicer deletion affect neurogenesis and gliogenesis in the developing mouse central nervous system. *Dev. Dyn.* 238, 2800–12
- Kikuchi, T., Morizane, A., Doi, D., Magotani, H., Onoe, H., Hayashi, T., Mizuma, H., Takara, S., Takahashi, R., Inoue, H., et al. (2017). Human iPS cell-derived dopaminergic neurons function in a primate Parkinson's disease model. *Nature* 548(7669), 592-596

- Kim, J., Inoue, K., Ishii, J., Vanti, W.B., Voronov, S.V., Murchison, E. et al. (2007). A microRNA feedback circuit in midbrain dopamine neurons. *Science* 317, 1220–1224
- Kim, V.N., Han, J., Siomi, M.C. (2009). Biogenesis of small RNAs in animals. *Nat Rev Mol Cell Biol.* 10, 126-139
- Kim, J., Su, S.C., Wang, H., Cheng, A.W., Cassady, J.P., Lodato, M.A., Lengner, C.J., Chung, C.Y., Dawlaty, M.M., Tsai, L.H., Jaenisch, R. (2011). Functional integration of dopaminergic neurons directly converted from mouse fibroblasts. *Cell Stem Cell* 9(5), 413–9
- Knafo, S., Esteban, J.A. (2017). PTEN: Local and Global Modulation of Neuronal Function in Health and Disease. *Trends Neurosci.* 40, 83–91
- Kondo, M., Scherer, D.C., Miyamoto, T., King A.G., Akashi, K., Sugamura, K., Weissman I.L. (2000). Cell-fate conversion of lymphoid-committed progenitors by instructive actions of cytokines. *Nature* 407, 383–386
- Kreis, P., Leondaritis, G., Lieberam, I., Eickholt, B.J. (2014). Subcellular targeting and dynamic regulation of PTEN: implications for neuronal cells and neurological disorders. *Front Mol Neurosci.* 7, 23
- Kriks, S., Shim, J.W., Piao, J., Ganat, Y.M., Wakeman, D.R., Xie, Z., Carrillo-Reid, L., Auyeung, G., Antonacci, C., Buch, A., et al. (2011). Dopamine neurons derived from human ES cells efficiently engraft in animal models of Parkinson’s disease. *Nature* 480, 547–551
- Krol, J., Loedige, I. and Filipowicz, W. (2010). The widespread regulation of microRNA biogenesis, function and decay. *Nat. Rev. Genet.* 11, 597-610
- Kuruvilla, R., Ye, H., Ginty, D.D. (2000). Spatially and functionally distinct roles of the PI3-K effector pathway during NGF signaling in sympathetic neurons. *Neuron* 27, 499–512
- Kutner, R. H., Puthli, S., Marino, M. P., & Reiser, J. (2009). Simplified production and concentration of HIV-1-based lentiviral vectors using HYPERFlask vessels and anion exchange membrane chromatography. *BMC biotechnology*, 9, 10
- Ladewig, J., Mertens, J., Kesavan, J., Doerr, J., Poppe, D., Glaue, F., Herms, S., Wernet, P., Kögler, G., Müller, F.J., et al. (2012). Small molecules enable highly efficient neuronal conversion of human fibroblasts. *Nat. Methods* 9, 575–578
- Landgraf, P., Rusu, M., Sheridan, R., Sewer, A., Iovino, N., et al. (2007). A mammalian microRNA expression atlas based on small RNA library sequencing. *Cell* 129, 1401–1414
- Ledbetter, S.A., Kuwano, A., Dobyns, W.B., and Ledbetter, D.H. (1992). Microdeletions of chromosome 17p13 as a cause of isolated lissencephaly. *Am. J. Hum. Genet.* 50, 182–189

- Lee, Y., Kim, M., Han, J., Yeom, K.H., Lee, S., et al. (2004). MicroRNA genes are transcribed by RNA polymerase II. *Embo J* 23, 4051–4060
- Leone, D.P., Heavner, W.E., Ferenczi, E.A., Dobрева, G., Huguenard, J.R., Grosschedl, R., and McConnell, S.K. (2015). *Satb2* Regulates the Differentiation of Both Callosal and Subcerebral Projection Neurons in the Developing Cerebral Cortex. *Cereb. Cortex* 25, 3406–3419
- Lewis, B.P., Burge, C.B., and Bartel, D.P. (2005). Conserved seed pairing, often flanked by adenosines, indicates that thousands of human genes are microRNA targets. *Cell* 120, 15–20
- Li, X.J., Zhang, X., Johnson, M.A., Wang, Z.B., Lavaute, T., Zhang, S.C. (2009). Coordination of sonic hedgehog and Wnt signaling determines ventral and dorsal telencephalic neuron types from human embryonic stem cells. *Development* 136, 4055–4063
- Li, M., Suzuki, K., Kim, N.Y., Liu, G.H., Izpisua Belmonte, J.C. (2014). A cut above the rest: targeted genome editing technologies in human pluripotent stem cells. *J. Biol. Chem.* 289, 4594–4599
- Li, X., Zuo, X., Jing, J., Ma, Y., Wang, J., Liu, D., Zhu, J., Du, X., Xiong, L., Du, Y., et al. (2015). Small-Molecule-Driven Direct Reprogramming of Mouse Fibroblasts into Functional Neurons. *Cell Stem Cell* 17, 195–203
- Liliental, J., Moon, S.Y., Lesche, R., Mamillapalli, R., Li, D., Zheng, Y., et al. (2000). Genetic deletion of the *Pten* tumor suppressor gene promotes cell motility by activation of *Rac1* and *Cdc42* GTPases. *Curr Biol.* 10, 401–404
- Liu, A. & Niswander, L.A. (2005). Bone morphogenetic protein signalling and vertebrate nervous system development. *Nat. Rev. Neurosci* 6, 945–954
- Liu, M.L., Zang, T., Zou, Y., Chang, J.C., Gibson, J.R., Huber, K.M., and Zhang, C.L. (2013). Small molecules enable neurogenin 2 to efficiently convert human fibroblasts into cholinergic neurons. *Nat. Commun.* 4, 2183
- Liu, M.L., Zang, T., Zhang, C.L. (2015) Direct Lineage Reprogramming Reveals Disease-Specific Phenotypes of Motor Neurons from Human ALS Patients. *Cell Reports* 14, 115–128
- London, M., Häusser, M. (2005). Dendritic computation. *Annu. Rev. Neurosci.* 28, 503–32
- Lui, J.H., Hansen, D.V., and Kriegstein, A.R. (2011). Development and evolution of the human neocortex. *Cell* 146, 18–36
- Luo, C., Lee, Q.Y., Wapinski, O., et al. (2019). Global DNA methylation remodeling during direct reprogramming of fibroblasts to neurons. *Elife* 8, e40197

- Ma, T., Wang, C., Wang, L., Zhou, X., Tian, M., Zhang, Q., Zhang, Y., Li, J., Liu, Z., Cai, Y., et al. (2013). Subcortical origins of human and monkey neocortical interneurons. *Nat. Neurosci.* *16*, 1588–1597
- Maden, M. (2007). Retinoic acid in the development, regeneration and maintenance of the nervous system. *Nat. Rev. Neurosci* *8*, 755–765
- Magill, S. T., Cambronne, X. A., Luikart, B. W., Lioy, D. T., Leighton, B. H., Westbrook, G. L., Mandel, G. and Goodman, R. H. (2010). microRNA-132 regulates dendritic growth and arborization of newborn neurons in the adult hippocampus. *Proc. Natl. Acad. Sci. USA* *107*, 20382-20387
- Makeyev, E.V., Zhang, J., Carrasco, M.A. & Maniatis, T. (2007). The MicroRNA miR-124 promotes neuronal differentiation by triggering brain-specific alternative pre-mRNA splicing. *Mol. Cell* *27*, 435–448
- Mall, M., Kareta, M.S., Chanda, S., Ahlenius, H., Perotti, N., Zhou, B., Grieder, S.D., Ge, X., Drake, S., Euong Ang, C., et al. (2017). Myt1l safeguards neuronal identity by actively repressing many non-neuronal fates. *Nature* *544*, 245–249
- Marin-Padilla, M. (1978). Dual origin of the mammalian neocortex and evolution of the cortical plate. *Anat Embryol (Berl)* *152*, 109–26
- Marin-Padilla, M. (1992). Ontogenesis of the pyramidal cell of the mammalian neocortex and developmental cytoarchitectonics: a unifying theory. *J Comp Neurol* *321*, 223–40
- Markus, A., Zhong, J., Snider, W.D. (2002). Raf and akt mediate distinct aspects of sensory axon growth. *Neuron* *35*, 65–76
- Mason, I. (2007). Initiation to end point: the multiple roles of fibroblast growth factors in neural development. *Nat. Rev. Neurosci* *8*, 583–596
- Masserdotti, G., Gascon, S., Götz, M. (2016). Direct neuronal reprogramming: learning from and for development. *Development* *143*, 2494-2510
- Maitra A et al. (2005). Genomic alterations in cultured human embryonic stem cells. *Nat. Genet.* *37*, 1099–1103
- McKenna, W.L., Betancourt, J., Larkin, K.A., Abrams, B., Guo, C., Rubenstein, J.L., Chen, B. (2011). Tbr1 and Fezf2 regulate alternate corticofugal neuronal identities during neocortical development. *J Neurosci.* *31*, 549–564
- McKenna, W.L., Ortiz-Londono, C.F., Mathew, T.K., Hoang, K., Katzman, S., and Chen, B. (2015). Mutual regulation between Satb2 and Fezf2 promotes subcerebral projection neuron identity in the developing cerebral cortex. *Proc. Natl. Acad. Sci. USA* *112*, 11702–11707
- McNeill, E., Van Vactor, D. (2012). MicroRNAs shape the neuronal landscape. *Neuron* *75*, 363–379

- Mertens, J., Paquola, A.C.M., Ku, M., Hatch, E., Böhnke, L., Ladjevardi, S., McGrath, S., Campbell, B., Lee, H., Herdy, J.R., Gonçalves, J.T., Toda, T., Kim, Y., Winkler, J., Yao, J., Hetzer, M.W., Gage, F.H. (2015). Directly Reprogrammed Human Neurons Retain Aging-Associated Transcriptomic Signatures and Reveal Age-Related Nucleocytoplasmic Defects. *Cell Stem Cell* 17(6), 705-718
- Mester, J., Eng, C. (2013). When Overgrowth Bumps Into Cancer: The PTEN-Opathies. *Am J Med Genet C Semin Med Genet.* 163, 114–121
- Miki, H., Suetsugu, S., Takenawa, T. (1998). WAVE, a novel WASP-family protein involved in actin reorganization induced by Rac. *EMBO J* 17, 6932–6941
- Mitalipova, M.M., Rao, R.R., Hoyer, D.M., Johnson, J.A., Meisner, L.F., Jones, K.L., Dalton, S., Stice, S.L. (2005). Preserving the genetic integrity of human embryonic stem cells. *Nat. Biotechnol.* 23, 19–20
- Miyoshi, K., Miyoshi, T., Siomi, H. (2010). Many ways to generate microRNA-like small RNAs: non-canonical pathways for microRNA production. *Mol Genet Genomics* 284(2), 95–103
- Molyneaux, B.J., Arlotta, P., Hirata, T., Hibi, M., Macklis, J.D. (2005). Fezl is required for the birth and specification of corticospinal motor neurons. *Neuron* 47, 817–831
- Molyneaux, B.J., Arlotta, P., Menezes, J.R.L., Macklis, J.D. (2007). Neuronal subtype specification in the cerebral cortex. *Nature Reviews Neuroscience* 8, 427–437
- Moon, H.M., & Wynshaw-Boris, A. (2013). Cytoskeleton in action: Lissencephaly, a neuronal migration disorder. *Wiley Interdiscip. Rev. Dev. Biol.* 2, 229–245
- Mountcastle, V.B. (1998). *The Cerebral Cortex*. Harvard University Press, Cambridge, Massachusetts
- Mukhtar, T., Taylor, V. (2018). Untangling Cortical Complexity During Development. *J Exp Neurosci.* 12
- Nagamani, S.C., Zhang, F., Shchelochkov, O.A., Bi, W., Ou, Z., Scaglia, F., Probst, F.J., Shinawi, M., Eng, C., Hunter, J.V., et al. (2009). Microdeletions including YWHAE in the Miller-Dieker syndrome region on chromosome 17p13.3 result in facial dysmorphisms, growth restriction, and cognitive impairment. *J. Med. Genet.* 46, 825–833
- Nakazawa, T., Watabe, A.M., Tezuka, T., Yoshida, Y., Yokoyama, K., Umemori, H., Inoue, A., Okabe, S., Manabe, T., Yamamoto, T. (2003). p250GAP, a novel brain-enriched GTPase-activating protein for Rho family GTPases, is involved in the N-methyl-d-aspartate receptor signaling. *Mol Biol Cell.* 14(7), 2921-34
- Nefzger, C.M., Haynes, J.M., Pouton, C.W. (2011). Directed expression of Gata2, Mash1, and Foxa2 synergize to induce the serotonergic neuron phenotype during in vitro differentiation of embryonic stem cells. *Stem Cells* 29, 928–939

- Nicholas, C.R., Chen, J., Tang, Y., Southwell, D.G., Chalmers, N., Vogt, D., Arnold, C.M., Chen, Y.J., Stanley, E.G., Elefanty, A.G., et al. (2013). Functional maturation of hPSC-derived forebrain interneurons requires an extended time-line and mimics human neural development. *Cell Stem Cell* 12, 573–586
- Nichols, A.J., Olson, E.C. (2010). Reelin promotes neuronal orientation and dendritogenesis during preplate splitting. *Cereb Cortex* 20, 2213–23
- Ning, K., Drepper, C., Valori, C.F., Ahsan, M., Wyles, M., Higginbottom, A., et al. (2010). PTEN depletion rescues axonal growth defect and improves survival in SMN-deficient motor neurons. *Hum Mol Genet.* 19, 3159–3168
- Nobes, C.D., Hall, A. (1995). Rho, rac and cdc42 GTPases: regulators of actin structures, cell adhesion and motility. *Biochem Soc Trans* 23, 456–459
- Noctor, S. C., Martinez-Cerdeno, V., Ivic, L. & Kriegstein, A. R. (2004) Cortical neurons arise in symmetric and asymmetric division zones and migrate through specific phases. *Nature Neurosci.* 7, 136–144
- Nowakowski, T.J., Mysiak, K.S., O’Leary, T., Fotaki, V., Pratt, T., Price, D.J. (2013). Loss of functional Dicer in mouse radial glia cell-autonomously prolongs cortical neurogenesis. *Dev. Biol.* 382, 530–37
- Olson, E.C. (2014). Analysis of preplate splitting and early cortical development illuminates the biology of neurological disease. *Front Pediatr.* 2, 121
- Osheroff, H., Hatten, M.E. (2009). Gene expression profiling of preplate neurons destined for the subplate: genes involved in transcription, axon extension, neurotransmitter regulation, steroid hormone signaling, and neuronal survival. *Cereb Cortex* 19, 126–34
- Ozsolak, F., Poling, L.L., Wang, Z., Liu, H., Liu, X.S., et al. (2008). Chromatin structure analyses identify miRNA promoters. *Genes Dev* 22, 3172–3183
- Packer, A.N., Xing, Y., Harper, S.Q., Jones, L., and Davidson, B.L. (2008). The bifunctional microRNA miR-9/miR-9* regulates REST and CoREST and is downregulated in Huntington’s disease. *J. Neurosci.* 28, 14341–14346
- Pang, T., Atefy, R., Sheen, V. (2008). Malformations of cortical development. *Neurologist.* 14(3), 181–191
- Pang, Z.P., Yang, N., Vierbuchen, T., Ostermeier, A., Fuentes, D.R., Yang, T.Q., Citri, A., Sebastiano, V., Marro, S., Südhof, T.C., Wernig, M. (2011). Induction of human neuronal cells by defined transcription factors. *Nature* 476, 220–223
- Pasca, S.P., Portmann, T., Voineagu, I., Yazawa, M., Shcheglovitov, A., Pasca, A.M., Cord, B., Palmer, T.D., Chikahisa, S., Nishino, S., Bernstein, J.A., Hallmayer, J., Geschwind, D.H., Dolmetsch, R.E. (2011). Using iPSC-derived neurons to uncover cellular phenotypes associated with Timothy syndrome. *Nat. Med* 17, 1657–1662

- Pfisterer, U., Kirkeby, A., Torper, O., Wood, J., Nelander, J., Dufour, A., Bjorklund, A., Lindvall, O., Jakobsson, J., Parmar, M. (2011). Direct conversion of human fibroblasts to dopaminergic neurons. *Proc Natl Acad Sci U S A* 108(25), 10343-8
- Pfisterer, U., Ek, F., Lang, S., Soneji, S., Olsson, R., Parmar, M. (2016). Small molecules increase direct neural conversion of human fibroblasts. *Scientific reports* 6, 38290
- Pilo-Boyl, P., Di Nardo, A., Mülle, C., Sassoe-Pognetto, M., Panzanelli, P., Mele, A., Kneussel, M., Costantini, V., Perlas, E., Massimi, M., Vara, H., Giustetto, M., Witke, W. (2007). Profilin2 contributes to synaptic vesicle exocytosis, neuronal excitability, and novelty-seeking behavior. *EMBO J* 26, 2991–3002
- Pollard, T.D. (2007). Regulation of Actin Filament Assembly by Arp2/3 Complex and Formins. *Annual Review of Biophysics and Biomolecular Structure* 36:1, 451-477
- Poirazi, P., Mel, B.W. (2001). Impact of active dendrites and structural plasticity on the memory capacity of neural tissue. *Neuron* 29, 779–796
- Rakic, P. (1974). Neurons in rhesus monkey visual cortex: systematic relation between time of origin and eventual disposition. *Science* 183, 425–427
- Rakic, P. (1988). Specification of cerebral cortical areas. *Science* 241, 170–176
- Rakic, P. (2007). The radial edifice of cortical architecture: from neuronal silhouettes to genetic engineering. *Brain Res Rev.* 55, 204–219
- Rakic, P. (2009) Evolution of the neocortex: a perspective from developmental biology. *Nat Rev Neurosci* 10(10), 724–735.
- Reiner, O., Carrozzo, R., Shen, Y., Wehnert, M., Faustinella, F., Dobyns, W.B., Caskey, C.T., and Ledbetter, D.H. (1993). Isolation of a Miller-Dieker lissencephaly gene containing G protein beta-subunit-like repeats. *Nature* 364, 717–721
- Reiner, O., Sapir, T. (2013). LIS1 functions in normal development and disease, *Curr. Opin. Neurobiol.* 23, 951–956
- Remenyi, J., van den Bosch, M.W., Palygin, O., Mistry, R.B., McKenzie, C., Macdonald, A., Hutvagner, G., Arthur, J.S., Frenguelli, B.G., Pankratov, Y. (2013). miR-132/212 knockout mice reveal roles for these miRNAs in regulating cortical synaptic transmission and plasticity. *PLoS One* 8, e62509
- Ridley, A.J., and Hall, A. (1992). The small GTP-binding protein Rho regulates the assembly of focal adhesions and actin stress fibers in response to growth factors. *Cell* 70, 389–399
- Romero, D.M., Bahi-Buisson, N., Francis, F. (2018). Genetics and mechanisms leading to human cortical malformations. *Semin Cell Dev Biol.* 76, 33-75
- Ronen, D., Benvenisty, N. (2012). Genomic stability in reprogramming. *Curr. Opin. Genet. Dev.* 22, 444–449

- Rouaux, C., Arlotta, P. (2010). Fezf2 directs the differentiation of corticofugal neurons from striatal progenitors in vivo. *Nat Neurosci.* 13(11), 1345–1347
- Rouaux, C., Arlotta, P. (2013). Direct lineage reprogramming of post-mitotic callosal neurons into corticofugal neurons in vivo. *Nat Cell Biol.* 15(2), 214–222
- Sainath, R., Gallo, G. (2015). Cytoskeletal and signaling mechanisms of neurite formation. *Cell Tissue Res.* 359(1), 267-78
- Saito, T., Hanai, S., Takashima, S., Nakagawa, E., Okazaki, S., Inoue, T., Miyata, R., Hoshino, K., Akashi, T., Sasaki, M., et al. (2011). Neocortical layer formation of human developing brains and lissencephalies: consideration of layer-specific marker expression. *Cereb. Cortex* 21, 588–596
- Salta, E., Lau, P., Sala Friegerio, C., Coolen, M., Bally-Cuif, L., De Strooper, B. (2014). A Self-Organizing miR-132/Ctbp2 Circuit Regulates Bimodal Notch Signals and Glial Progenitor Fate Choice during Spinal Cord Maturation. *Developmental Cell* 30(4), 423 - 436
- Schwartz, C.E., Johnson, J.P., Holycross, B., Mandeville, T.M., Sears, T.S., Graul, E.A., Carey, J.C., Schroer, R.J., Phelan, M.C., Szollar, J., Flannery, D.B., Stevenson, R.E. (1988). Detection of submicroscopic deletions in band 17p13 in patients with the Miller- Dieker syndrome. *Am J Hum Genet* 43, 597–604
- Schwartz, J.C., Younger, S.T., Nguyen, N.B., Hardy, D.B., Monia, B.P., Corey, D.R., Janowski, B.A. (2008). Antisense transcripts are targets for activating small RNAs. *Nat Struct Mol Biol* 15(8), 842–848
- Sebastiano, V., Zhen, H.H., Haddad, B., Bashkirova, E., Melo, S.P., Wang, P., Leung, T.L., Siprashvili, Z., Tichy, A., Li, J., Ameen, M., Hawkins, J., Lee, S., Li, L., Schwertschcow, A., Bauer, G., Lisowski, L., Kay, M.A., Kim, S.K., Lane, A.T., Wernig, M., Oro, A.E. (2014). Human COL7A1-corrected induced pluripotent stem cells for the treatment of recessive dystrophic epidermolysis bullosa. *Sci Transl Med* 6(264), 264ra163
- Sheen, V.L., Ferland, R.J., Neal, J. et al. (2006). Neocortical neuronal arrangement in Miller Dieker syndrome. *Acta Neuropathol* 111(5), 489-96
- Sheppard, A.M., Pearlman, A.L. (1997). Abnormal reorganization of preplate neurons and their associated extracellular matrix: an early manifestation of altered neocortical development in the reeler mutant mouse. *J Comp Neurol* 378, 173–9
- Shi, Y., Kirwan, P., Smith, J., Robinson, H.P., and Livesey, F.J. (2012). Human cerebral cortex development from pluripotent stem cells to functional excitatory synapses. *Nat. Neurosci.* 15, 477–486
- Shi, S.H., Jan, L.Y., Jan, Y.N. (2003). Hippocampal neuronal polarity specified by spatially localized mPar3/mPar6 and PI 3-kinase activity. *Cell* 112, 63–75

- Shibata, M., Nakao, H., Kiyonari, H., Abe, T., Aizawa, S. (2011). MicroRNA-9 regulates neurogenesis in mouse telencephalon by targeting multiple transcription factors. *J Neurosci* 31, 3407–3422
- Shibata, M., Gulden, F.O., Sestan, N. (2015). From trans to cis: transcriptional regulatory networks in neocortical development. *Trends Genet.* 31(2), 77-87
- Shim S, Kwan KY, Li M, Lefebvre V, Sestan N. (2012). Cis-regulatory control of corticospinal system development and evolution. *Nature.* 486:74–79
- Smith, D.S., Niethammer, M., Ayala, R., Zhou, Y., Gambello, M.J., Wynshaw-Boris, A., and Tsai, L.H. (2000). Regulation of cytoplasmic dynein behaviour and microtubule organization by mammalian Lis1. *Nat. Cell Biol.* 2, 767–775
- Son, E.Y., Ichida, J.K., Wainger, B.J., Toma, J.S., Rafuse, V.F., Woolf, C.J., and Eggan, K. (2011). Conversion of mouse and human fibroblasts into functional spinal motor neurons. *Cell Stem Cell* 9, 205–218
- Spillane, M., Gallo, G. (2014). Involvement of Rho-family GTPases in axon branching. *Small GTPases.* 5, e27974.
- Spruston, N. (2008). Pyramidal neurons: dendritic structure and synaptic integration. *Nat. Rev. Neurosci.* 9(3), 206–21
- Stark, K.L., Xu, B., Bagchi, A., Lai, W.S., Liu, H., Hsu, R., Wan, X., Pavlidis, P., Mills, A.A., Karayiorgou, M., Gogos, J.A. (2008). Altered brain microRNA biogenesis contributes to phenotypic deficits in a 22q11-deletion mouse model. *Nat Genet* 40, 751–760
- Stradal, T.E., Rottner, K., Disanza, A., Confalonieri, S., Innocenti, M., Scita, G. (2004). Regulation of actin dynamics by WASP and WAVE family proteins. *Trends Cell Biol* 14, 303–311
- Stuart, G., Spruston, N., and Häusser, M. (2000). *Dendrites*. Oxford University Press, Cary, NC
- Tabata, H., Nakajima, K. (2003). Multipolar migration: the third mode of radial neuronal migration in the developing cerebral cortex. *J Neurosci* 23, 9996–10001
- Takahashi, K., and Yamanaka, S. (2006). Induction of pluripotent stem cells from mouse embryonic and adult fibroblast cultures by defined factors. *Cell* 126, 663-676
- Takenawa, T., Miki, H. (2001). WASP and WAVE family proteins: key molecules for rapid rearrangement of cortical actin filaments and cell movement. *J Cell Sci* 114, 1801–1809
- Tantirigama, M.L.S., Oswald, M.J., Clare, A.J., Wicky, H.E., Day, R.C., Hughes, S.M., Empson, R.M. (2016) Fezf2 expression in layer 5 Mol Neurobiol (2018) 55:642–651 projection neurons of mature mouse motor cortex. *J Comp Neurol* 524(4), 829–845

- Tao, Y., & Zhang, S. C. (2016). Neural Subtype Specification from Human Pluripotent Stem Cells. *Cell stem cell*, *19*(5), 573–586
- Taverna, E., Götz, M., & Huttner, W.B. (2014). The cell biology of neurogenesis: toward an understanding of the development and evolution of the neocortex. *Annu. Rev. Cell Dev. Biol.* *30*, 465–502
- Thoma, E.C., Wischmeyer, E., Offen, N., Maurus, K., Siren, A.L., Scharl, M., Wagner, T. U., (2012). Ectopic expression of neurogenin 2 alone is sufficient to induce differentiation of embryonic stem cells into mature neurons. *PLoS One* *7*, e38651
- Toyo-oka, K., Shionoya, A., Gambello, M.J., Cardoso, C., Leventer, R., Ward, H.L., Ayala, R., Tsai, L.H., Dobyns, W., Ledbetter, D., et al. (2003). 14-3-3epsilon is important for neuronal migration by binding to NUDEL: a molecular explanation for Miller-Dieker syndrome. *Nat. Genet.* *34*, 274–285
- Tsai, J.W., Chen, Y., Kriegstein, A.R., and Vallee, R.B. (2005). LIS1 RNA interference blocks neural stem cell division, morphogenesis, and motility at multiple stages. *J. Cell Biol.* *170*, 935–945
- Van Aelst, L., and D'Souza-Schorey, C. (1997). Rho GTPases and signaling networks. *Genes Dev.* *11*, 2295–2322
- Vasudevan, S., Tong, Y., Steitz, J.A. (2007). Switching from repression to activation: microRNAs can up-regulate translation. *Science* *318*(5858), 1931–1934
- Victor, M.B., Richner, M., Hermansteyne, T.O., Ransdell, J.L., Sobieski, C., Deng, P.Y., Klyachko, V.A., Nerbonne, J.M., and Yoo, A.S. (2014). Generation of human striatal neurons by microRNA-dependent direct conversion of fibroblasts. *Neuron* *84*, 311–323
- Vierbuchen, T., Ostermeier, A., Pang, Z.P., Kokubu, Y., Südhof, T.C., and Wernig, M. (2010). Direct conversion of fibroblasts to functional neurons by defined factors. *Nature* *463*, 1035–1041
- Visvanathan, J., Lee, S., Lee, B., Lee, J.W., and Lee, S.K. (2007). The microRNA miR-124 antagonizes the anti-neural REST/SCP1 pathway during embryonic CNS development. *Genes Dev.* *21*, 744–749
- Vo, N., Klein, M.E., Varlamova, O., Keller, D.M., Yamamoto, T., Goodman, R.H., Impey, S., (2005). A cAMP-response element binding protein-induced microRNA regulates neuronal morphogenesis. *Proc. Natl. Acad. Sci. U. S. A.* *102*, 16426–16431
- Volvvert, M.-L., Prévot, P.-P., Close, P., Laguesse, S., Pirotte, S., Hemphill, J., Rogister, F., Kruzy, N., Sacheli, R., Moonen, G. et al. (2014). MicroRNA targeting of CoREST controls polarization of migrating cortical neurons. *Cell Rep.* *7*, 1168–1183

- Wang, X., Liu, P., Zhu, H., Xu, Y., Ma, C., Dai, X. et al. (2009). miR-34a, a microRNA up-regulated in a double transgenic mouse model of Alzheimer's disease, inhibits bcl2 translation. *Brain Res Bull* *80*, 268–273
- Wayman, G. A., Davare, M., Ando, H., Fortin, D., Varlamova, O., Cheng, H. Y., et al. (2008). An activity-regulated microRNA controls dendritic plasticity by down-regulating p250GAP. *Proc. Natl. Acad. Sci. U.S.A.* *105*, 9093–9098
- Weintraub, H., Tapscott, S.J., Davis, R.L., Thayer, M.J., Adam, M.A., Lassar, A.B., Miller, A.D. (1989). Activation of muscle-specific genes in pigment, nerve, fat, liver, and fibroblast cell lines by forced expression of MyoD. *Proc Natl Acad Sci U S A.* *86*, 5434–5438
- Wen, Z., Nguyen, H.N., Guo, Z., Lalli, M.A., Wang, X., Su, Y., Kim, N.S., Yoon, K.J., Shin, J., Zhang, C., Makri, G., Nauen, D., Yu, H., Guzman, E., Chiang, C.H., Yoritomo, N., Kaibuchi, K., Zou, J., Christian, K.M., Cheng, L., Ross, C.A., Margolis, R.L., Chen, G., Kosik, K.S., Song, H., Ming, G.L. (2015). Synaptic dysregulation in a human iPS cell model of mental disorders. *Nature* *515(7527)*, 414-8
- Weissbein, U., Ben-David, U., and Benvenisty, N. (2014). Virtual karyotyping reveals greater chromosomal stability in neural cells derived by transdifferentiation than those from stem cells. *Cell Stem Cell* *15*, 687–691
- Wong, H.K., Veremeyko, T., Patel, N., Lemere, C.A., Walsh, D.M., Esau, C., Vanderburg, C., Krichevsky, A.M. (2013). De-repression of FOXO3a death axis by microRNA-132 and -212 causes neuronal apoptosis in Alzheimer's disease. *Human Molecular Genetics* *22(15)*, 3077–3092
- Wu, H., Xu, J., Pang, Z.P., Ge, W., Kim, K.J., Bianchi, B., Chen, C., Sudhof, T.C., and Sun, Y.E. (2007). Integrative genomic and functional analyses reveal neuronal subtype differentiation bias in human embryonic stem cell lines. *Proc. Natl. Acad. Sci.* *10* (4) , 13821– 13826
- Wynshaw-Boris, A. (2007). Lissencephaly and LIS1: Insights into the molecular mechanisms of neuronal migration and development. *Clin. Genet.* *72*, 296–304
- Xie, H., Ye, M., Feng, R., Graf, T. (2004). Stepwise reprogramming of B cells into macrophages. *Cell* *117*, 663–676
- Xie, W., Schultz, M.D., Lister, R., Hou, Z., Rajagopal, N., Ray, P., Whitaker, J.W., Tian, S., Hawkins, R.D., Leung, D., et al. (2013). Epigenomic analysis of multilineage differentiation of human embryonic stem cells. *Cell* *15* (3) , 1134–1148
- Xu, Z., Jiang, H., Zhong, P., Yan, Z., Chen, S., Feng, J. (2016). Direct conversion of human fibroblasts to induced serotonergic neurons. *Mol Psychiatry* *21(1)*, 62–70
- Xue, Y., Ouyang, K., Huang, J., Zhou, Y., Ouyang, H., Li, H., Wang, G., Wu, Q., Wei, C., Bi, Y., et al. (2013). Direct conversion of fibroblasts to neurons by reprogramming PTB-regulated microRNA circuits. *Cell* *152*, 82–96

- Xue, Y., Qian, H., Hu, J., Zhou, B., Zhou, Y., Hu, X., Karakhanyan, A., Pang, Z., and Fu, X.D. (2016). Sequential regulatory loops as key gatekeepers for neuronal reprogramming in human cells. *Nat. Neurosci.* *19*, 807–815
- Yamamizu, K., Piao, Y., Sharov, A.A., Zsiros, V., Yu, H., Nakazawa, K., Schlessinger, D., and Ko, M.S.H. (2013). Identification of transcription factors for lineage-specific ESC differentiation. *Stem Cell Reports* *1*, 545–559
- Ye, Z., Mostajo-Radji, M.A., Brown, J.R., Rouaux, C., Tomassy, G.S., Hensch, T.K., Arlotta, P. (2015). Instructing Perisomatic Inhibition by Direct Lineage Reprogramming of Neocortical Projection Neurons. *Neuron* *88*(3), 475-83
- Yingling, J., Toyo-oka, K., Wynshaw-Boris, A. (2003). Miller-Dieker Syndrome: Analysis of a Human Contiguous Gene Syndrome in the Mouse. *Am J Hum Genet.* *73*(3), 475-88
- Yingling, J., Youn, Y.H., Darling, D., Toyo-Oka, K., Pramparo, T., Hirotsune, S., & Wynshaw-Boris, A. (2008). Neuroepithelial stem cell proliferation requires LIS1 for precise spindle orientation and symmetric division. *Cell* *132*, 474–486
- Yoo, A.S., Staahl, B.T., Chen, L., Crabtree, G.R. (2009). MicroRNA-mediated switching of chromatin-remodelling complexes in neural development. *Nature* *460*, 642–646
- Youn, Y.H., Pramparo, T., Hirotsune, S., and Wynshaw-Boris, A. (2009). Distinct dose-dependent cortical neuronal migration and neurite extension defects in Lis1 and Ndel1 mutant mice. *J. Neurosci.* *29*, 15520–15530
- Yu, H., Wu, M., Zhao, P., Huang, Y., Wang, W., and Yin, W. (2015). Neuroprotective effects of viral overexpression of microRNA-22 in rat and cell models of cerebral ischemia-reperfusion injury. *J. Cell. Biochem.* *116*, 233–241
- Zhang, Y., Pak, C., Han, Y., Ahlenius, H., Zhang, Z., Chanda, S., Marro, S., Patzke, C., Acuna, C., Covy, J., et al., (2013). Rapid single-step induction of functional neurons from human pluripotent stem cells. *Neuron* *78*, 785–798
- Zhou, Q., Brown, J., Kanarek, A., Rajagopal, J., Melton, D.A. (2008). In vivo reprogramming of adult pancreatic exocrine cells to beta-cells. *Nature* *455*, 627–32
- Zhou, J., Parada, L.F. (2012). PTEN signaling in autism spectrum disorders. *Curr Opin Neurobiol.* *22*, 873– 879
- Zuccotti, A., Le Magueresse, C., Chen, M., Neitz, A., and Monyer, H. (2014). The transcription factor Fezf2 directs the differentiation of neural stem cells in the subventricular zone toward a cortical phenotype. *Proc. Natl. Acad. Sci. USA* *111*, 10726–10731

10. Danksagung

Zuerst möchte ich mich bei Prof. Dr. Oliver Brüstle für die Möglichkeit an seinem Institut unter hervorragenden Forschungsbedingungen promovieren zu können bedanken.

Dr. Julia Ladewig danke ich für die Möglichkeit an diesem interessanten Thema arbeiten zu dürfen und für die Beratung und Betreuung während meiner Doktorandenzeit.

Prof. Dr. Philipp Koch, Prof. Dr. Hubert Schorle, Prof. Dr. Gerhard von der Emde und Prof. Dr. Ulrich Kubitscheck danke ich für die Bereitschaft mein Prüfungskomitee zu bilden.

Jasmin Jatho-Gröger, Ruven Wilkens, Fabio Marsoner danke ich nicht nur für unsere fachlichen Diskussionen, sondern vor allem für die entstandenen Freundschaften, die trotz unserer nun getrennten Wege mein Privatleben immer noch bereichern.

Frederike Klaus und Marianna Tolve danke ich dafür, dass sie mich aufgefangen haben, als ich das einzige Mitglied meiner Gruppe geworden bin und in kurzer Zeit zu guten Freundinnen geworden sind.

Meinen ehemaligen Arbeitskollegen Ammar Jabali, Bettina Bohl, Karolina Kleinsimlinghaus, Vira Iefremova danke ich für viele spaßige Momente im Labor, weswegen ich immer gerne zur Arbeit gekommen bin.

Meiner Partnerin Yvonne Drücke kann ich nicht im Einzelnen für all die Dinge danken, die sie für mich tut, da diese Arbeit sonst doppelt so lang wäre. Aber ohne ihre Geduld und ihr Verständnis wäre diese Arbeit nicht zustande gekommen.

Meinen Eltern Iris und Thomas Weynans danke ich dafür, dass ich zu dem Menschen geworden bin, der ich jetzt bin, dass sie immer für mich da sind und immer an mich glauben.

11. Erklärung

Diese Dissertation wurde an dem Institut für Rekonstruktive Neurobiologie des Universitätsklinikums Bonn unter der Leitung von Frau Dr. Julia Ladewig angefertigt.

Hiermit versichere ich, dass die vorliegende Arbeit ohne unzulässige Hilfe Dritter und ohne die Benutzung anderer als angegebener Quellen angefertigt wurde. Die aus fremden Quellen direkt oder indirekt übernommenen Gedanken sind als solche kenntlich gemacht.

Die vorgelegte Arbeit ist außerdem nicht bereits anderweitig als Dissertation eingereicht worden und ich habe früher noch keinen Promotionsversuch unternommen.

Bonn, den

Kevin Weynans